การสังเคราะห์และการประยุกต์ด้านเซ็นเซอร์ของพอลิเมอร์บรัชที่มีหมู่คาร์บอกซิล

นางสาวปิยะพร อรรคฮาต

วิทยานิพนธ์นี้เป็นส่วนหนึ่งของการศึกษาตามหลักสูตรปริญญาวิทยาศาสตรดุษฎีบัณฑิต
สาขาวิชาปิโตรเคมี
คณะวิทยาศาสตร์ จุฬาลงกรณ์มหาวิทยาลัย
ปีการศึกษา 2553

SYNTHESIS AND SENSOR APPLICATION OF CARBOXYL-CONTAINING POLYMER BRUSHES

Miss Piyaporn Akkahat

A Thesis Submitted in Partial Fulfillment of the Requirements

for the Degree of Doctor of Philosophy Program in Petrochemistry

Faculty of Science

Chulalongkorn University

Academic Year 2010

Thesis Title	SYNTHESIS AND SENSOR APPLICATION OF CARBOXYL-CONTAINING POLYMER BRUSHES
By	Miss Piyaporn Akkahat
Field of Study	Petrochemistry
Thesis Advisor	Associate Professor Voravee P. Hoven, Ph.D.
Thesis Co-advisor	Professor Suda Kiatkamjornwong, Ph.D.
Thesis Co-advisor	Professor Yasuhiko Iwasaki, Ph.D.

Accepted by the Faculty of Science, Chulalongkorn University in Partial Fulfillment of the Requirements for the Doctoral Degree

……..Dean of the Faculty of Science
(Professor Supot Hannongbua, Dr.rer.nat.)

THESIS COMMITTEE

……Chairman
(Assistant Professor Warinthorn Chavasiri, Ph.D.)

……Thesis advisor
(Associate Professor Voravee P. Hoven, Ph.D.)

……Thesis Co-advisor
(Professor Suda Kiatkamjornwong, Ph.D.)

……Thesis Co-advisor
(Professor Yasuhiko Iwasaki, Ph.D.)

……Examiner
(Associate Professor Nuanphan Chantarasiri, Ph.D.)

……Examiner
(Associate Professor Wimonrat Trakarnpruk, Ph.D.)

……External Examiner
(Assistant Professor Toemsak Srikhirin, Ph.D.)

ปิยะพร อรรคฮาต: การสังเคราะห์และการประยุกต์ด้านเซ็นเซอร์ของพอลิเมอร์บรัชที่มีหมู่คาร์บอกซิล (SYNTHESIS AND SENSOR APPLICATION OF CARBOXYL-CONTAINING POLYMER BRUSHES) อ.ที่ปรึกษาวิทยานิพนธ์หลัก : รศ.ดร. วรวีร์ โฮเว่น, อ.ที่ปรึกษาวิทยานิพนธ์ร่วม : ศ.ดร. สุดา เกียรติกำจรวงศ์, Prof. Yasuhiko Iwasaki, Ph.D., 117 หน้า.

งานวิจัยนี้ได้พัฒนาวัสดุรองรับของเซ็นเซอร์จากพอลิเมอร์บรัชที่มีหมู่คาร์บอกซิลเป็นองค์ประกอบ ได้เตรียมพอลิเมอร์บรัชที่มีหมู่คาร์บอกซิลบนแผ่นเซอร์เฟซพลาสมอนเรโซแนนซ์ (เอสพีอาร์) ที่เคลือบด้วยทองโดยใช้ 2 แนวทางคือ (1) ปฏิกิริยาอะตอมทรานส์เฟอร์แรดิคัลพอลิเมอไรเซชันที่ริเริ่มจากพื้นผิว และ (2) การเกิดการเรียงตัวได้เองของโซ่พอลิเมอร์ที่มีหมู่ปลายเป็นไทออล โฮโมพอลิเมอร์บรัชของพอลิแอคริลิกแอซิด (พีเอเอ) ที่มีความหนาแน่นของการตรึงแตกต่างกันสามารถเตรียมได้ด้วยปฏิกิริยาอะตอมทรานส์เฟอร์แรดิคัลพอลิเมอไรเซชันที่ริเริ่มจากพื้นผิว จากการวิเคราะห์ด้วยเทคนิคเอสพีอาร์แสดงให้เห็นว่าความหนาแน่นของการตรึงโซ่พอลิเมอร์และความสามารถในการบวมตัวของพีเอเอส่งผลกระทบอย่างมีนัยสำคัญต่อปริมาณการตรึงโพรบและความสามารถในการตรวจวัดโมเลกุลเป้าหมาย โพรบที่ถูกตรึงบนพีเอเอบรัชไม่เพียงแต่แสดงการจับยึดโมเลกุลเป้าหมายอย่างจำเพาะเจาะจงแต่ยังป้องกันการดูดซับอย่างไม่จำเพาะเจาะจงของโปรตีนชนิดอื่น ส่งผลทำให้มีความเลือกจำเพาะในการตรวจวัดสูงกว่าเมื่อเปรียบเทียบกับโพรบที่ตรึงบนพื้นผิวโมเลกุลชั้นเดียวที่เกิดการเรียงตัวได้เองของสารประกอบไทออลที่มีปลายเป็นหมู่คาร์บอกซิล โคพอลิเมอร์บรัชของพอลิเมทาคริลิกแอซิดและพอลิ(2-เมทาคริโลอิลออกซีเอทิลฟอสโฟริลโคลีน (พีเอ็มเอเอ็มพีซี) ที่เตรียมโดยการตรึงโซ่พอลิเมอร์ลงบนพื้นผิวเป็นวัสดุรองรับของเซ็นเซอร์ที่มีประสิทธิภาพดีเยี่ยมสำหรับการตรวจวัดโมเลกุลเป้าหมายในพลาสมาของเลือด ผลการทดลองทั้งหมดแสดงให้เห็นถึงศักยภาพของพอลิเมอร์บรัชในการเป็นวัสดุรองรับของเอสพีอาร์สำหรับการประยุกต์ใช้งานด้านเซ็นเซอร์ชีวภาพ

สาขาวิชา ปิโตรเคมี ลายมือชื่อนิสิต .....

ปีการศึกษา 2553 ลายมือชื่ออ.ที่ปรึกษาวิทยานิพนธ์หลัก .....

ลายมือชื่ออ.ที่ปรึกษาวิทยานิพนธ์ร่วม .....

ลายมือชื่ออ.ที่ปรึกษาวิทยานิพนธ์ร่วม .....

4973832823 : MAJOR PETROCHEMISTRY
KEYWORDS: POLYMER BRUSHES / POLY(ACRYLIC ACID) / POLY(2-METHACRYLOYLOXYETHYL PHOSPHORYLCHOLINE) / SENSOR / SPR

PIYAPORN AKKAHAT: SYNTHESIS AND SENSOR APPLICATION OF CARBOXYL-CONTAINING POLYMER BRUSHES. ADVISOR: ASSOC. PROF. VORAVEE P. HOVEN, Ph.D., CO-ADVISOR: PROF. SUDA KIATKAMJORNWONG, Ph.D., PROF. YASUHIKO IWASAKI, Ph.D., 117 pp.

In this work, sensor platforms based on carboxyl-containing polymer brushes have been developed. The carboxyl-containing polymer brushes, were prepared on gold-coated surface plasmon resonance (SPR) disks by two approaches (1) “grafting from” *via* surface-initiated atom transfer radical polymerization (SI-ATRP) and (2) “grafting to” *via* self-assembly of thiol-terminated polymer. The homopolymer brushes of poly(acrylic acid) (PAA) with varied graft density were obtained by SI-ATRP. The result obtained from SPR technique indicated that the graft density and swellability of the PAA brushes had significant impact on the sensing probe immobilization and analyte detectability. The sensing probes immobilized on PAA brushes not only showed the specific binding with target molecules but also maintained high resistance to non-specific protein adsorption yielding the high *S/N* in comparison with those immobilized on the carboxyl-terminated self-assembled monolayer surface. The copolymer brushes of poly[(methacrylic acid)-*ran*-(2-methacryloyloxyethyl phosphorylcholine)] (PMAMPC) prepared by “grafting to” method was an excellent sensor platform for detecting the target molecules in blood plasma. All results have demonstrated the potential of the carboxyl-containing brushes as SPR-precursor layer for biosensing applications.

Field of Study : Petrochemistry Student’s Signature .....

Academic Year : 2010 Advisor’s Signature .....

Co-advisor’s Signature .....

Co-advisor’s Signature .....

ACKNOWLEDGEMENTS

I would like to thank and express my sincere and deep gratitude to my thesis advisors, Associate Professor Dr. Voravee Hoven and my co-advisor, Professor Dr. Suda Kiatkamjornwong, and Professor Dr. Yasuhiko Iwasaki for invaluable suggestion, guidance, encouragement and kindness throughout the course of this research. I am sincerely grateful to the members of the thesis committee: Assistant Professor Dr. Warinthorn Chavasiri, Associate Professor Dr. Nuanphan Chantarasiri, Associate Professor Dr. Wimonrat Trakarnpruk, and Assistant Professor Dr. Toemsak Srikhirin for reviewing my thesis and making valuable suggestions and critical comments. Financial supports for this work from Commission of Higher Education and Thailand Research Fund (RMU5080072), and Ph.D. scholarship from Strategic Scholarships Fellowships Frontier Research Networks, are greatly acknowledged. The authors are grateful to the Scientific and Technological Research Equipment Center, Chulalongkorn University, for providing the SPR facility and Department of Chemistry and Materials Engineering Faculty of Chemistry, Materials and Bioengineering, Kansai University, for providing the XPS and other laboratory facilities. Special thanks go to Mrs. Wanwimon Mekboonsonglarp from Scientific and Technological Research Equipment Centre, Chulalongkorn University for the assistance with surface plasmon resonance operation.

Moreover, I wish to thank all members of Organic Synthesis Research Unit (OSRU) of Chulalongkorn University and biomaterials laboratory of Kansai University for their friendship, assistance and suggestions concerning experimental techniques during my thesis work. Finally, I also wish to especially thank my family members for their love, inspiration and support throughout my entire study.

CONTENTS

Page

Page

Page

Page

LIST OF TABLES

LIST OF FIGURES

Figure Page

Figure Page

Figure Page

Figure Page

Figure Page

Figure Page

Figure Page

LIST OF ABBREVIATIONS

ACVA	: 4,4′-Azobis(4-cyanovaleric acid)
AFM	: Atomic force microscopy
AIBN	: Azobisisobutyronitrile
Ar	: Argon
ATRP	: Atom transfer radical polymerization
AVD	: Avidin
BSA	: Bovine serum albumin
^{o}C	: Degree celcius
$CDCl_3$	: Deuterated chloroform
DNA	: Deoxyribonucleic acid
COO-	: Carboxylate groups
COOH	: Carboxyl group
CPD	: 4-Cyanopentanoic acid dithiobenzoate
CRP	: C-reactive protein
CTA	: Chain transfer reagent
2D	: 2-Dimensional
3D	: 3-Dimensional
DNA	: Deoxyribonucleic acid
D_2O	: Deuterium monoxide
DP	: Degree of polymerization
EBiB	: Ethyl 2-bromoisobutyrate
EDC	: 1-(3-Dimethylaminopropyl)-3-ethylcarbodiimide hydrochloride
EtOH	: Ethanol
FBS	: Fetal bovine serum

FIB	:	Fibrinogen
FITC	:	Fluorescein isothiocyanate
FT-IR	:	Fourier transform infrared
g	:	Gram
GMA	:	Glycidyl methacrylate
GPC	:	Gel permeation chromatography
h	:	Hour
H	:	proton
IgG	:	Immunoglobulin G
kD	:	Kilodalton
KHz	:	Kilohertz
LODs	:	Limit of detection
LYS	:	Lysozyme
m°	:	Millidegree
MA	:	Methacrylic acid
Me_6TREN	:	Tris(2-(dimethylamino)ethyl)amine
Mg	:	Milligram
MHz	:	Megahertz
Min	:	Minute
mL	:	Milliliter
mmol	:	Millimole
mM	:	Millimolar
$\overline{M}_n$	:	Number average molecular weight
MPC	:	2-Methacryloyloxyethyl phosphorylcholine
MUA	:	11-Mercaptoundecanoic acid
MUD	:	11-Mercaptoundecanol

MW : Molecular weight

MWD : Molecular weight distribution

N_A : Avogadro's number

ng : Nanogram

NHS : *N*-Hydroxysuccinimide

nm : Nanometer

NMR : Nuclear magnetic resonance

NTA : Nitrilotriacetate

OEG : Oligo(ethylene glycol)

PAA : Poly(acrylic acid)

PBS : Phosphate buffered saline

PC : Phosphorylcholine

PCBMA : Poly(carboxybetaine methacrylate)

PDI : Polydispersity index

PEG : Poly(ethylene glycol)

PGAMA : Poly(D-gluconamidoethyl methacrylate)

PGMA : Poly(glycidyl methacrylate)

PHEMA : Poly(2-hydroxyethyl methacrylate)

PHEMA-*b*-PDMAEMA : Poly(2-hydroxyethyl methacrylate) and poly(2-(dimethylamino)ethyl methacrylate)

pI : Isoelectric point

pKa : Acid dissociation constant

PMA : Poly(methacrylic acid)

PMAMPC : Poly[(methacrylic acid)-*ran*-(2-methacryloyloxyethyl phosphorylcholine)]

PMAMPC-SH : Thiol-terminated poly[(methacrylic acid)-*ran*-(2-methacryloyloxyethyl phosphorylcholine)]

PMDETA : *N*,*N*,*N*′,*N*″,*N*″-Pentamethyldiethylenetriamine

PMMA : Poly(methyl methacrylate)

pmol : Picomole

PMPC : Poly(2-methacryloyloxyethyl phosphorylcholine)

PMPC-*b*-PGMA : Poly(2-methacryloyloxyethyl phosphorylcholine)-*block*-poly(glycidyl methacrylate)

*p*OEGMA : Poly(oligo(ethylene glycol) methacrylate)

PPP : Platelet-poor plasma

PS : Poly(styrene)

P*t*-BA : Poly(*tert*-butyl acrylate)

QCM : Quartz crystal microbalance

RAFT : Reversible addition-fragmentation chain transfer

RI : Refractive index

rms : Root mean square

RX : Organic halide

SA : Streptavidin

SAM : Self-assembled monolayer

SI-ATRP : Surface-initiated atom transfer radical polymerization

SIP : Surface-initiate polymerization

S/N : Signal-to-noise ratio

SPR : Surface plasmon resonance

t : Dry film thickness

t-BA : *t*-Butyl acrylate

TBO	:	Toluidine Blue O
THF	:	Tetrahydrofuran
UV	:	Ultraviolet
v/v	:	Volume per volume
w/v	:	Weight per volume
XPS	:	X-ray photoelectron spectroscopy
μL	:	Microliter
μmol	:	Micromole
θ_A	:	Dynamic advancing
θ_R	:	Dynamic receding
σ	:	Grafting densities
ρ	:	Mass density
Δθ	:	Angle shift

CHAPTER I

INTRODUCTION

1.1 Statement of problem

Selectivity of sensor or measurement platforms for target molecules plays an important role for successful biosensor development. In order to achieve specific recognition for target molecules, the covalent attachment of active biomolecules, a so-called sensing probe, such as protein, antibody, enzyme, and DNA has been immobilized to sensor surface. However, the resistance of non-specific adsorption of sensor surface is also important. Non-specific adsorption leads to undesirable features such as high background noise or low signal-to-noise ratio (*S/N*), especially in the complex matrices such as blood plasma and clinical samples. Thus, the excellent sensor platform should not only allow for covalent immobilization of sensing probe but also resist non-specific adsorption.

To date, there are many strategies to create functionalized layer onto sensor surface to be a platform for immobilizing probes such as self-assembled monolayer (SAM) of end-functionalized alkanethiol, and polymeric thin film. In particular, it has been demonstrated previously that the surface-tethered polymer brushes could be used for enhancement of sensor response by increasing the number of bioactive site due to high concentration of functional groups at the brush interface in comparison with the SAM system. Most of strategies to establish functionalized polymer brushes onto surface have been achieved by either “grafting to” or “grafting from” methods. Although “grafting to” method is easy to be performed, it should be noted that it inherently processes a low grafting density on the surface. Surface-initiated polymerization (SIP), or so-called “grafting from” has attracted much interest in recent years due to the ability to provide a better control over the characteristic of the polymer films, such as polymer chain length, grafting density, and thickness. In other words, the number of binding sites for immobilizing biomolecules could also be controlled.

In our previous work, we have generated densely packed poly(acrylic acid) (PAA) brushes (0.21 - 0.32 chain/nm^2) on SPR sensor chip by acid hydrolysis of poly(*tert*-butyl acrylate) (P*t*-BA) brushes, formerly prepared by SI-ATRP of *tert*-butyl acrylate (*t*-BA). The biotin probes, a model of sensing probe, were immobilized on the carboxyl groups of the PAA brushes. The biotinylated PAA brushes showed a high specific binding with target molecule, streptavidin (SA), and a low non-specific adsorption of non-target proteins (bovine serum albumin and fibrinogen) in comparison with a self-assembled monolayer (SAM) of carboxyl-terminated alkanethiol as determined by SPR technique. However, the densely packed PAA brushes suffer from the limited accessability of the SA molecule to the immobilized biotin situated inside the polymer layer. It is, therefore, important to lower the packing density as well as to enhance the swellability of the PAA brushes, the two parameters that should help improve the performance of the PAA brushes as a sensor platform for biosensors.

To the best of our knowledge, no studies have reported about the effect of graft density of the polymer brushes-based sensing platform on the detection of analyte. Most of researches have been mainly focused on generating surfaces having a high density of sensing probes in order to achieve a superior analyte detectability. Therefore, this research aims to further explore the applicability of PAA brushes as a sensor platform by focusing on the variation of the the PAA brushes graft density on the SPR sensor chip. The determination of whether the extent of the carboxyl group activation would have any impact on the swellability of the sensing layer based on PAA brushes after probe immobilization and analyte detectability was also investigated.

In addition, this research also introduces “grating to” method an alternative way to prepare the sensor platform of carboxyl-containing polymer brushes on SPR sensor chip. The thiol-terminated poly[(methacrylic acid)-*ran*-(2-methacryloyloxyethyl phosphorylcholine)] (PMA-*ran*-MPC-SH, PMAMPC-SH) was grafted to gold surface of the SPR sensor chip *via* S atom. Parameters that may affect the sensitivity and specificity in term of *S/N* of sensors for detecting target molecules in complex sample were investigated. These issues are likely to be equally important for the optimization and development of sensor platform for biosensing applications.

1.2 Objectives

The objective was to evaluate the use of carboxyl-containing polymer brushes obtained from either “grafting from” or “grafting to” as a sensor platform for biosensing applications.

1.3 Scope of investigation

The stepwise investigation was carried out as follows:

1. Literature survey for related research work.
2. Preparation and characterization of carboxyl-containing polymer brushes obtained from either “grafting from” or “grafting to” method
3. Protein adsorption study.
4. Immobilization of sensing probe onto carboxyl groups of carboxyl-containing polymer brushes.
5. Investigation on the specific interactions of sensing probe immobilized on the sensor platform with target molecule.

CHAPTER II

THEORY AND LITERATURE REVIEW

2.1 Biosensor

A biosensor is analytical devices consisting of bio-recognition systems, typically enzymes or binding proteins, such as antibodies, immobilized onto the surface of transducers. Specific interactions between the target analyte and the complementary bio-recognition molecule produce a biochemical signal which was converted to a detectable signal by the transducer. The common transducer systems are electrochemical, optical, mass and thermal. The immobilization of the biological molecule is a particularly important aspect of the fabrication of biosensors. The immobilization procedure must reproducibly keep the biological molecule close to the surface of transducer while maintaining its biological activity.

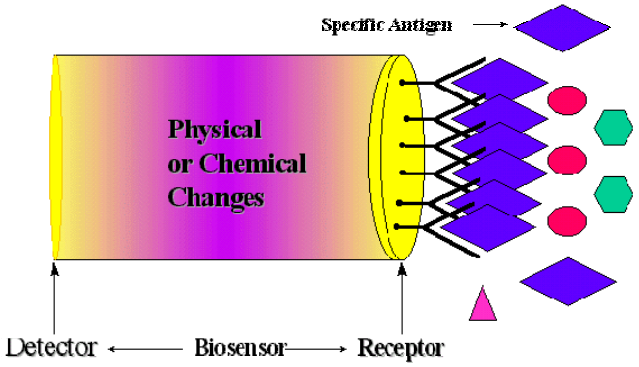

Figure 2.1 Schematic diagram of a biosensor device.

The development of biosensors largely relies on the immobilization of bioactive molecules such as protein, antibody, enzyme, and DNA [1-3] to a sensor surface or measurement platform. The density of the immobilized bioactive species, as well as the distance between the surface of sensor and the bioactive species, should, in principle,

affect the sensitivity, detection limit and signal-to-noise ratio of the biosensor. However, the resistance of non-specific adsorption of sensor surface is also important. Non-specific adsorption leads to undesirable features such as high background noise or “false positives” [4-5]. Thus, excellent sensor platform should not only allow for covalent immobilization of bioactive species but also resist non-specific adsorption.

To date, there are many strategies to create the precursor layer onto which the bioactive molecules (probes) are immobilized. One of these is a self-assembled monolayer (SAM) of end-functionalized alkanethiol, especially for gold-coated substrates, but the density of bioactive molecules cannot be greatly enhanced [2, 6-7]. Moreover, the use of SAM does not expressly reduce non-specific adsorption. One common approach to reduce this non-specific adsorption background is to functionalize the SAM with highly hydrophilic terminal groups such as oligo(ethylene glycol) (OEG) [8-10] and phosphorylcholine (PC) [11]. But this approach is not always as effective in more complex samples such as blood plasma [12-13]. This often causes an adverse effect on the biosensor efficiency.

Polymeric thin film, especially polymer brushes, has recently been recognized as an alternative precursor layer for the covalent attachment of biomolecules [2, 4, 14]. It has been demonstrated previously that polymer brushes, of which the number of binding sites for bioactive molecules can be controlled, effectively enhance the sensor response in consequence of high concentration of functional groups at the brush interface providing more bioactive site or binding site in comparison with SAM [15-18] and provides a better environment for the preservation of immobilized molecules during prolonged storage [19]. Moreover, polymer brushes exhibit much lower protein adsorption not only from single-protein solution but also from human blood plasma than SAM having the same functional group [20]. In recent years, there are many reports showing that the polymer brushes such as poly(oligo(ethylene glycol)methacrylate) (*p*OEGMA) [15], poly(2-methacryloyloxyethyl phosphorylcholine)-*b*-poly(glycidyl methacrylate) [21], poly(carboxybetaine methacrylate) [22], and poly(acrylic acid) brushes [23] provide desirable platforms in terms of functional group availability and the ability to resist non-specific binding. As shown by Lee and coworkers [15], *p*OEGMA brushes, having hydroxyl groups along the polymer chain, were grown form gold and Si/SiO_2 surfaces. The hydroxyl groups

were utilized for the immobilization of biotin having biospecific binding with streptavidin, while ethylene glycol part presents a resistance to non-specific binding of lysozyme. As monitored by SPR, the enhanced binding specificity/capacity of biotin-SA can be achieved about a 10-fold higher signal-to-noise ratio as compared with that obtained with the SAM-based system.

Poly(acrylic acid) (PAA) brushes containing carboxyl groups, are commonly used for immobilization of biomolecules and widely employed as matrices for binding a number of proteins, namely bovine serum albumin (BSA), myoglobin, anti-IgG antibodies [24] and ribonuclease A [25]. Their high-protein binding capacity has made the surface-tethered PAA brushes a potential candidate for the development of affinity-based chromatography media for protein purification and protein microarrays. For example, the frequency response, monitored by quartz crystal microbalance (QCM), between anti-C-reactive protein (CRP) antibodies attached to PAA brushes that was prepared via atom transfer radical polymerization (ATRP) from a plasma-polymerized allyl alcohol film that was functionalized with a bromoester inititator, and CPR in solution was shown to be 10 times higher than that immobilized on SAM of cysteamine [18]. PAA brushes synthesized by surface-initiated ATRP from SPR sensor chip exhibited an 11-fold higher biotin density and revealed a 2-fold higher specific binding with SA as compared with the MUA system, and also prevented non-specific adsorption of BSA and fibrinogen [26].

2.2 Polymer brushes

Polymer brushes refer to the polymer chains tethered on a surface or interface by one end of polymer chain. By a sufficient dense polymer chain, a high grafting density, the polymer chains are crowded and forced to stretch away from the surface or interface to avoid overlapping [27]. Generally, there are two ways to fabricate polymer brushes: physisorption and covalent attachment (Figure 2.2). For polymer physisorption, block copolymers adsorb onto a suitable substrate with one block interacting strongly with the surface and the other block interacting weakly with the substrate. The disadvantages of physisorption include thermal and solvolytic instabilities due to the non-covalent nature of the grafting, poor control over polymer chain density and complications in synthesis of suitable block copolymers. Tethering of

the polymer chains to the surface is one way to surmount some of these disadvantages. Covalent attachment of polymer chains to the surface, a much stronger bonding between polymer chains and substrate, can be accomplished by either “grafting to” or “grafting from” approaches. In a “grafting to” approach, preformed end-functionalized polymer molecules react with an appropriate substrate to form polymer brushes. The “grafting from” approach involves immobilization of initiators onto the substrate followed by surface-initiated polymerization to generate polymer brushes on the surface.

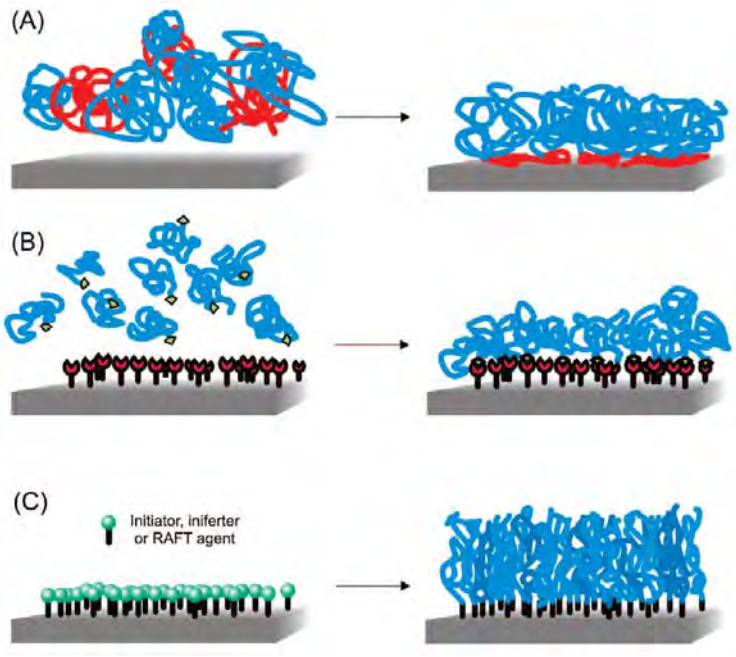

Figure 2.2 Preparation of polymer brushes by (a) “physisorption”, (b) “grafting to” and (c) “grafting from” [28].

2.2.1 “Grafting to” approach

In a “grafting to” approach, preformed end-functionalized polymer molecules react with an appropriate substrate to form polymer brushes. Although the brushes layer exhibits thermal and solvolytic stability, this technique often leads to low grafting density and low film thickness, as the polymer molecules must diffuse through the existing polymer film to reach the reactive sites on the surface that are sterically hindered by surrounding bounded chains. The steric hindrance for surface attachment

increases as the tethered polymer film thickness increases. Although the “grafting to” approach is reported to provide low packed polymer brush surfaces, the modification can be applied to versatile surfaces by several interactions such as adsorption, electrostatic interaction, and covalent conjugations.

The synthesis of polymer chains has been performed using several techniques such as anionic, cationic, and living free radical. These techniques allow for the facile conversion of the chain ends to any number of desired functionalities such as hydroxyl, carboxyl, amino, and thiol. In recent years, reversible addition-fragmentation chain transfer (RAFT) free radical polymerization is attractive to synthesize the end-functionalized polymer molecules because after the polymerization was completed, the thiocarbonylthio end-capped polymers such as dithioester group were easily converted to thiol functionalities by aminolysis reaction of either primary or secondary amine [29-32] and by $NaBH_4$ [33-34]. Subsequently, thiol-terminated polymer chains can be readily grafted on metal surface by the formation of metal–sulfur bonds, especially gold surfaces [35] that have been widely used in various bioanalytical devices [30, 36].

As described above, the grafting density of polymer brushes produced by “grafting to” method is low that tends to allow for adsorption of protein. However, many research groups have published the high graft density and the non-fouling property of polymer brushes prepared by a “grafting to” method using a thiol-terminated polymer chain. For example:

In 2007, Uhida *et al.* [37] have reported the preparation of mixed PEG brushes constructed on a SPR gold-sensor chip from thiol-PEG. The preconstructed longer PEG brushes (5k) were filled with a short chain thiol-PEG (2k). The mixed polymer brushes of PEG5k and PEG2k significantly reduced the nonspecific adsorption not only of high molecular weight proteins, BSA, but also of small-molecular weight peptides. Moreover, they reported that the increase in the amount of PEG density on the SPR chip decreased the non-specific adsorption of BSA.

In 2009, Yoshimoto *et al.* [38] prepared poly(2-(methacryloyloxy)ethyl phosphorylcholine) (PMPC) and PEG modified gold surfaces by “grafting to” method using a thiol-terminated polymer chain. PEG densities of 0.15–0.43 chain/nm^2 and PMPC density of less than 0.1 chains/nm^2 were obtained. The adsorption of BSA was suppressed in both PMPC and PEG brushes. Moreover, the extent of BSA adsorption

on PMPC modified surfaces was systematically reduced for thicker PMPC layers, thus the number of MPC units on the gold surface appears to be an important factor for the excellent protein resistance while PEG 5k provided the highest resistance toward BSA adsorption as a result of the balance between their steric repulsion and high surface chain density.

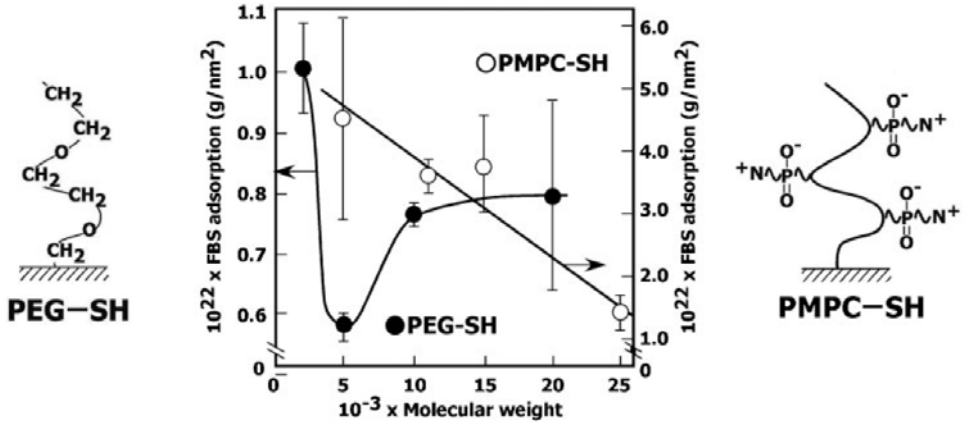

Figure 2.3 The extent of protein adsorption on PEG (2k, 5k, 10k, 20k) (closed circles) and PMPC (5k, 11k, 15k, 25k) (open circles) modified gold surfaces observed after injection of 10% Fetal bovine serum (FBS) solution [38].

2.2.2 "Grafting from" approach

The "grafting from" approach or so-called surface-initiated polymerization (SIP) holds advantages over the "grafting to" method of which the process suffers from the entropic barrier due to the crowding of the initial grafting polymer chains that prevent further insertion of the polymer onto the surface and so leads to a relatively low graft density. The "grafting from" approach, on the other hand, involves a stepwise growth of the polymer chain from the surface immobilized initiators by insertion of monomer, which allows a better control over the polymer chain length, graft density and thickness. SIP coupled with "living radical polymerization" such as atom transfer radical polymerization (ATRP) has proven to be the most popular method for creating surface-tethered polymer brushes [28, 39-42].

In 2002, Jones *et al.* [42] prepared poly(methyl methacrylate) (PMMA) and poly(glycidyl methacrylate) (PGMA) brushes on gold surface by surface-initiated atom

transfer radical polymerization (SI-ATRP). The density of surface initiator was varied, and it was found that the thickness of both PMMA and PGMA increased as a function of initiator density and polymerization time.

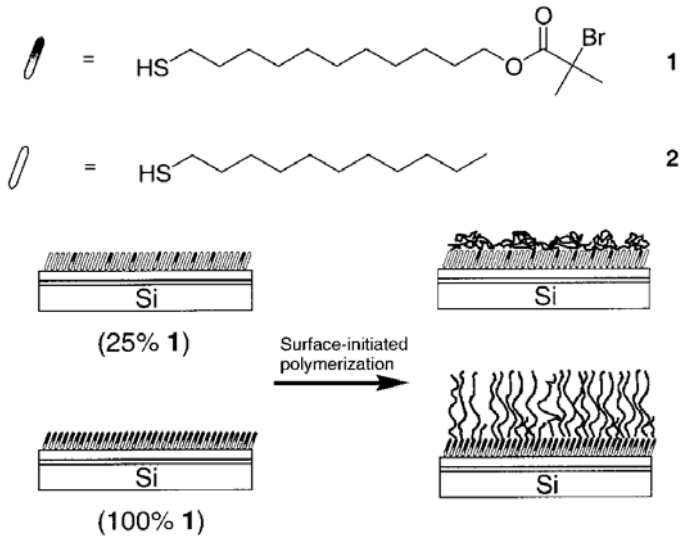

Figure 2.4 Schematic diagram of the polymer brushes formed from monolayers composed of 25% initiator (1) and 100% initiator; undecanethiol (2) [42].

SI-ATRP has attracted much interest in recent years it can provide well-defined polymer brushes for biosensor application as the number of functional groups or binding sites for immobilizing biomolecules could also be controlled [15, 21, 43]. For example:

In 2006, Dai *et al.* [24] showed that PAA brushes, that was prepared on gold surface by SI-ATRP of *tert*-butyl acrylate and subsequently hydrolysis, exhibited high binding capacity of many proteins, such as bovine serum albumin (BSA), myoglobin, anti-IgG, and lysozyme, obtained by both covalent binding and nitrilotriacetate (NTA)-Cu^{2+} complexes. The amount of protein binding depends upon the immobilization method and the type of protein.

In 2008, Iwata *et al.* [21] prepared polymer brushes and block copolymer brushes consisting of 2-methacryloyloxyethyl phosphorylcholine (MPC) and glycidyl methacrylate (GMA) by SI-ATPR on silicon wafer. Antibody fragments, Fab' fragments, were immobilized on GMA units and were utilized for binding with antigent. The amount of immobilized antibody increased with increasing GMA unit as a

consequence of the increase in epoxy group. Moreover, the activity of the antibodies immobilized on the block copolymer brushes (PMPC-*block*-PGMA) having biocompatible PMPC was greater than that in the absence of PMPC.

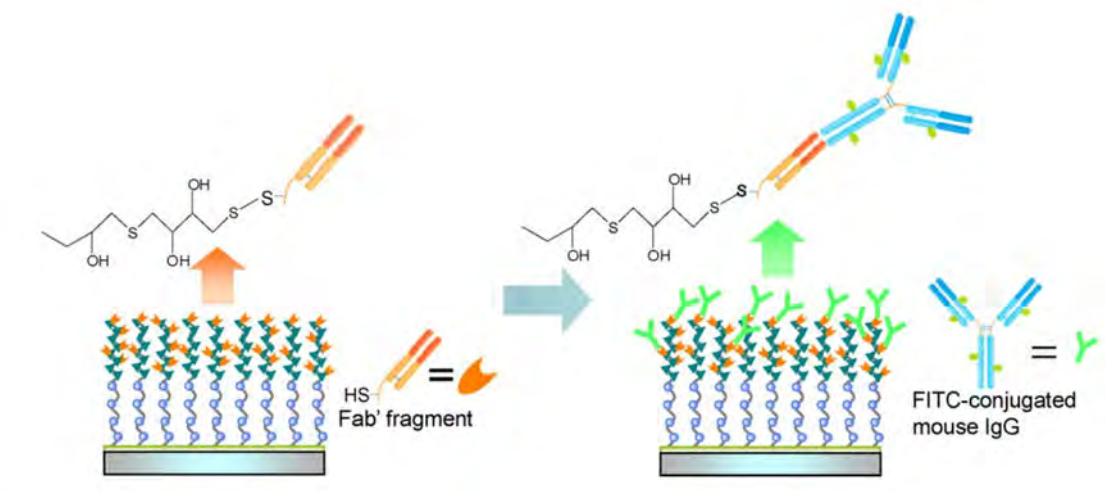

Figure 2.5 Scheme showing antibody immobilized on PMPC-*block*-PGMA and reaction with FITC-labeled IgG [21].

2.3 Atom transfer radical polymerization (ATRP)

Atom transfer radical polymerization (ATRP) is one kind of controlled radical polymerization, and was originally reported by Matyjaszewski et al. in 1995 [44]. This mechanism is an efficient method for carbon-carbon bond formation in organic synthesis. In some of these reactions, a transition-metal catalyst acts as a carrier of the halogen atom in a reversible redox process (Figure 2.6). Initially, the transition-metal species, M_t^n, abstracts halogen atom X from the organic halide, RX, to form the oxidized species, $M_t^{n+1}X$, and the carbon-centered radical $R^\bullet$. In the subsequent step, the radical $R^\bullet$ participates in an inter- or intramolecular radical addition to alkene, Y, with the formation of the intermediate radical species, $RY^\bullet$. The reaction between $M_t^{n+1}X$ and $RY^\bullet$ results in a target product, RYX, and regenerates the reduced transition-metal species, M_t^n, which further promotes a new redox process. The fast reaction between $RY^\bullet$ and $M_t^{n+1}X$ apparently suppresses bimolecular termination between alkyl radicals and efficiently introduces a halogen functional group X into the final product in good to excellent yields.

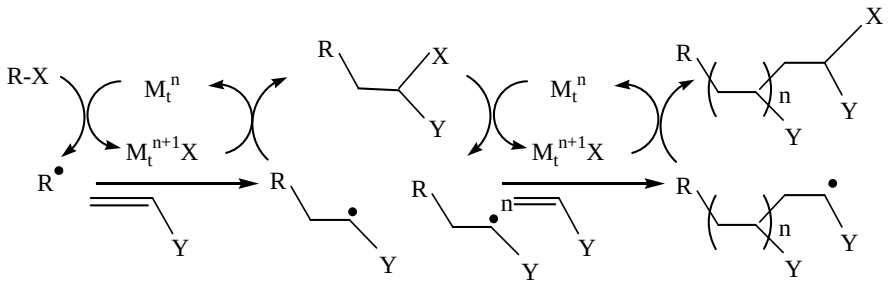

Figure 2.6 Mechanism of ATRP.

The ATRP system relies on one equilibrium reaction in addition to the classical free-radical polymerization scheme (Figure 2.7). In this equilibrium, a dormant species, RX, reacts with the activator, M_t^n, to form a radical $R^\bullet$ and deactivating species, $M_t^{n+1}X$. The activation and deactivation rate parameters are k_{act} and k_{deact}, respectively. Since deactivation of growing radicals is reversible, control over the molecular weight distribution and, in the case of copolymers, over chemical composition can be obtained if the equilibrium meets several requirements [45].

1. The equilibrium constant, k_{act}/k_{deact}, must be low in order to maintain a low stationary concentration of radicals. A high value would result in a high stationary radical concentration, and as a result, termination would prevail over reversible deactivation.

2. The dynamics of the equilibrium must be fast; i.e. deactivation must be fast compared to propagation in order to ensure fast interchange of radicals in order to maintain a narrow molecular weight distribution.

$$R\text{-}X + M_t^n \underset{k_{deact}}{\overset{k_{act}}{\rightleftharpoons}} R^\bullet + M_t^{n+1}X$$

Figure 2.7 Equilibrium reaction in ATRP [46].

ATRP has been widely explored as a method for grafting polymer chains from many solid surfaces such as silicon [47], membrane [48], cellulose [49], and gold [50]. The first step in SI-ATRP an ATRP initiator is attached to the substrate for subsequent

polymerization. There are many possible methods of initiator attachment depending on type of surface including silanization of silane compound on alumina or silica surface, and adsorption of thiol compound on gold surface. Huang et al. [51] prepared diblock copolymer brushes poly(2-hydroxyethyl methacrylate) and poly(2-(dimethylamino) ethyl methacrylate) (PHEMA-*b*-PDMAEMA) via SI-ATRP from 2-bromoisobutyrate-functional thiol SAMs on gold surfaces.

From the drawback of ATRP method is that direct polymerization of acidic monomer such as (meth)acrylic acid is challenging. Thus, there are many reports utilizing protected monomers, followed by a polymer-analogous deprotection, e.g. hydrolysis of protecting ester groups [48, 52-53]. Dai *et al.* [24] have also successfully synthesized PAA brushes on gold surface through the growth of poly(*tert*-butyl acrylate) (P*t*-BA) polymers from surfaces and then hydrolyze the *tert*-butyl ester to form poly(acrylic acid). By using a highly active ATRP catalyst, P*t*-BA brushes can be formed at room temperature.

2.4 Reversible addition-fragmentation chain transfer (RAFT) polymerization

In recent years, reversible addition-fragmentation chain Transfer or RAFT polymerization, one kind of controlled radical polymerization, is attractive for development of living radical polymerization. RAFT polymerization has successfully synthesized a wide range of polymers with controlled molecular weight and low polydispersity index (PDI) [30, 34, 54]. Some monomers capable of polymerizing by RAFT include styrenes, acrylates, acrylamides as well as a range of other vinyl monomers. In addition, the RAFT process allows the synthesis of variety macromolecular architectures such as block, gradient, statistical, comb/brush, star, hyperbranched, and network copolymers as well as ATRP system.

RAFT is a type of living polymerization involving a conventional radical polymerization in the presence of a reversible chain transfer reagent (CTA). The CTA or RAFT agents such as dithioesters, thiocarbamates, and dithiocarbonates (xanthates), are used to be intermediate in the polymerization via a reversible chain-transfer process. The general structure of CTA is shown in Figure 2.8. The Z group serves to activate or deactivate the reactivity of the C=S bond towards addition. The R group, a homolytic leaving group, must form a stable free radical. Like other living

polymerizations, there is no termination step in the RAFT process. It is a very versatile method to form low polydispersity polymer from monomers capable of radical polymerization. The reaction is usually done with a dithioester. There are four steps in RAFT polymerization: initiation, addition-fragmentation, reinitiation and equilibration (Figure 2.9).

(1) Initiation: The reaction is started by radical initators such as AIBN. In this step, the initiator (I) reacts with a monomer unit to create a radical species which starts an active polymerizing chain.

(2) Addition-Fragmentation: The active chain (P_n) reacts with the dithioester, which kicks out the homolytic leaving group (R). This is a reversible step, with an intermediate species capable of losing either the leaving group (R) or the active species (P_n).

(3) Reinitiation: The leaving group radical then reacts with another monomer species, starting another active polymer chain. This active chain (P_m) is then able to go through the addition-fragmentation or equilibration steps.

(4) Equilibration: This is the fundamental step in the RAFT process which traps the majority of the active propagating species into the dormant thiocarbonyl compound. This limits the possibility of chain termination through. Active polymer chains (P_m and P_n) are in an equilibrium between the active and dormant stages. While one polymer chain is in the dormant stage (bound to the thiocarbonyl compound), the other is active in polymerization.

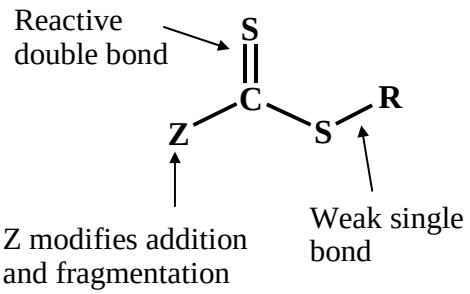

Figure 2.8 General form of RAFT chain transfer agents.

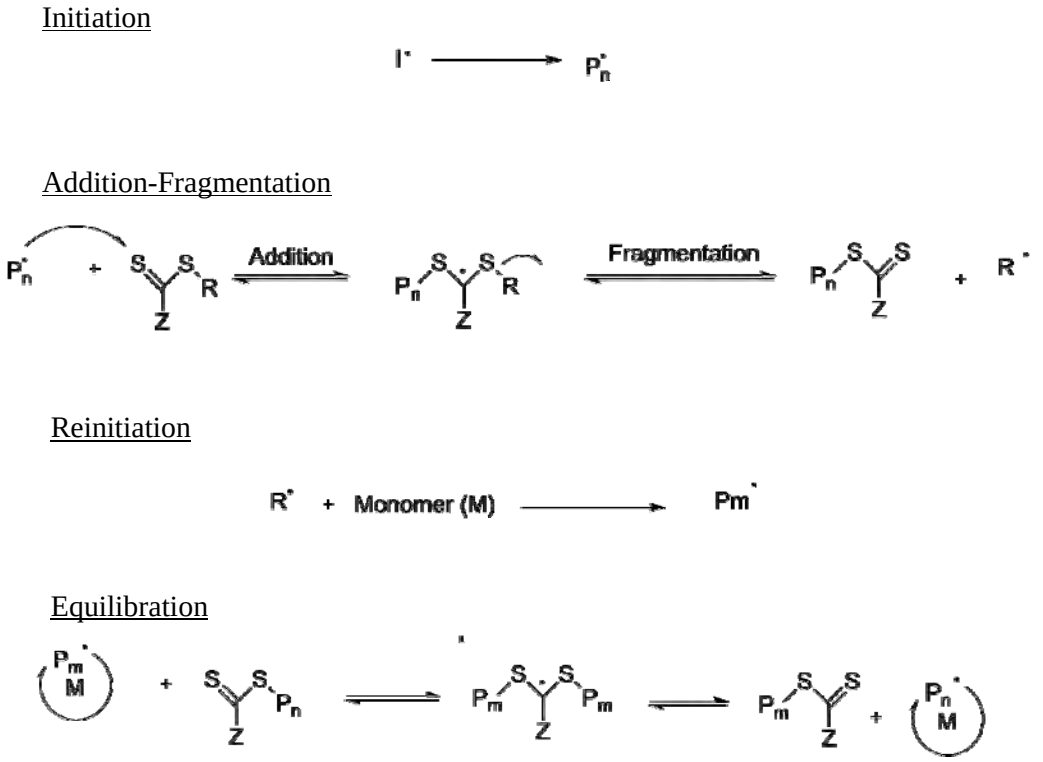

Figure 2.9 Mechanism of RAFT.

By controlling the concentration of initiator and CTA, it is possible to produce controlled molecular weight with low polydispersities. In RAFT polymerization, the concentration on the active species is kept low relative to the dormant species by controlling the amount of initiator and capping agent. This in turn will limit termination steps such as radical combination and disproportionation, increasing the polymer length.

Due to the inertness of the process to protic solvents such as water, RAFT can potentially address the limitations that other radical polymerizations encounter in direct polymerizations of acidic monomer in aqueous media. In recent years, there are many publications have reported a well-controlled polymerization of acidic monomer using RAFT [55-56]. For example, a well-defined and high molecular weight of poly(methacrylaic acid) (PMA) (113,900) with narrow PDI (~1.13) was achieved by the direct polymerization of methacylic acid in methanol or water/1,4-dioxane by RAFT polymerization [57].

CHAPTER III

METHODS AND MATERIALS

3.1 Materials

Chemicals were purchased from Fluka (Switzerland), Merck (Germany), Aldrich Chemical Co., Ltd. (USA), or Wako (Japan) and were purified as appropriate. Solvents for reactions are reagent grade and used without purification, otherwise specified. Dichloromethane was dried over CaH_2 under reflux and nitrogen atmosphere. Nitrogen gas was obtained from TIG and Naniwa Sanso Co., Ltd. (Japan) with 99.5 % purity while argon was obtained from Yamazaki Sangyo Co., Ltd. (Japan) with 99.5 % purity. *t*-Butyl acrylate (*t*-BA) was extracted three times with 5% aqueous NaOH and then washed with distilled water. After drying over $MgSO_4$ and filtering off the drying agent, *t*-BA was distilled under reduced pressure (60°C/60 mmHg). Tris(2-(dimethylamino)ethyl)amine (Me_6TREN) [58], and ω–mercaptoundecyl bromoisobutyrate ($BrC(CH_3)_2COO(CH_2)_{11}SH$) [42] were prepared following the methods described in the literature. CuBr (95% purity), ethyl 2-bromoisobutyrate (EBiB, 98% purity), Toluidine Blue O (TBO, 98% purity), 1-(3-dimethylaminopropyl)-3-ethylcarbodiimide hydrochloride (EDC, 98% purity), *N*-hydroxysuccinimide (NHS, 98% purity) were used as received. Methacrylic acid was distilled under reduced pressure with added *p*-methoxyphenol (59°C/13.5mmHg). 2-Methacryloyloxyethyl phosphorylcholine (MPC) was purchased from NOF Corporation (Japan). Gold-coated SPR disk was purchased from AutoLab ESPR (Eco Chemie, The Netherlands) and SPR-670M Moritex Co. (Kanagawa, Japan)

The (+)-biotinyl-3,6,9-trioxaundecanediamine (biotin-NH_2) and streptavidin (SA) were purchased from Bio-active Co., Ltd. (Thailand) and Thermo Scientific Co., Ltd. (USA). Bovine serum albumin (BSA), fibrinogen (FIB), lysozyme (LYS), avidin (AVD, from egg white), and anti-bovine serum albumin (anti-BSA, developed in

rabbit) were purchased from Aldrich Chemical Co., Ltd. (USA). Human platelet-poor plasma (PPP) was donated from healthy volunteer. Phosphate buffered saline (PBS) pH 7.4 (10 mM PBS consisting of 10 mM phosphate buffer, 137 mM NaCl, and 2.7 mM KCl) were purchased from Sigma (USA). Solutions were made with MilliQ water purified by ultrapure water systems with a Millipak® 40 filter unit (0.22 μm, Millipore, USA) and Millipore Milli-Q system that involves reverse osmosis, ion exchange, and filtration steps (18.2 MΩ).

3.2 Equipments

The dynamic advancing (θ_A) and receding (θ_R) water contact angles were measured using a contact angle goniometer (Ramé-Hart, Inc., USA, model 100-00 or a First Ten Angstroms FTÅ125 goniometer, USA), equipped with a Gilmont syringe and a 24-gauge flat-tipped needle. All of the measurements were carried out in air at ambient temperature. The reported angle is an average of 5 measurements on different area of each sample. The molecular weight and the molecular weight distribution of the Pt-BA homopolymer were determined by a Water GPC system (USA) with a Water E600 column connected to a refractive index (RI) detector. The column was eluted with THF at a flow rate of 1 mL/min. Narrow PS standards were used for generating a calibration curve. The molecular weight and the molecular weight distribution of the PMA, PMPC and their copolymer were measured with a Tosoh GPC system with a RI detector and size-exclusion columns, Shodex, SB-804 HQ and SB-806 HQ. The column was eluted with distilled water containing 10 mM LiBr at a flow rate of 0.75 mL/min. A poly(ethylene glycol) (PEG, Tosoh standard sample) standard were used for generating a calibration curve. ^{1}H NMR spectra were recorded in $CDCl_3$ or D_2O using a NMR spectrophotometer (Varian, model Mercury-400, USA or JEOL, model ECA-400, Japan) operating at 400 MHz.

The morphology and thickness of samples were analyzed by AFM recorded with Scanning Probe Microscope model NanoScope®IV, Veeco, USA. Measurements were performed in air using tapping mode. Silicon nitride tips with a resonance frequency of 267-295 KHz and a spring constant 20-80 N/m were used. The FT-IR spectra of polymer prepared as KBr pellets were recorded with a FT-IR spectrometer

(JASCO), model system FT-500, with 32 scans at a resolution of 4 cm^{-1} using a TGS detector. The surface composition was characterized by x-ray photoelectron spectroscopy (XPS) on a Scienta ESCA 200 spectrometer (Uppsala, Sweden) with Al Kα x-rays. All the XPS data were collected at takeoff angles of 15° and 90°. SPR measurements were conducted using a double channel, AutoLab ESPR (Eco Chemie, The Netherlands) at Scientific and Technological Research Equipment Centre, Chulalongkorn University (Thailand) and a double channel surface plasmon resonance (SPR; Moritex, Kanagawa, Japan) sensor at Department of Chemistry and Materials Engineering, Kansai University (Japan).

3.3 Experimental procedure

3.3.1 Preparation of surface-tethered poly(acrylic acid) (PAA) brushes by "grafting from" method

3.3.1.1 Synthesis of tris(2-(dimethylamino)ethyl)amine (Me_6TREN)

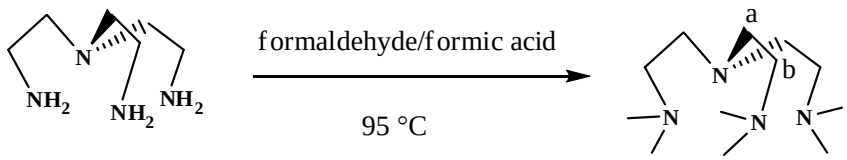

The synthetic method was modified from the previously reported procedure [58]. A mixture of 35%(w/v) formaldehyde (12.0 mL, 0.4 mole) and 98%(w/v) formic acid (36.0 mL, 0.95 mole) was stirred at 0 ^{o}C under nitrogen atmosphere. After 1 h, 0.05 mole of tris(2-(aminoethyl)amine) or TREN was added dropwise via cannula, followed by an addition of deionized water via syringe. A mixture was refluxed for 24 h at 95 ^{o}C. After cooling to room temperature, a red-brown mixture was treated with saturated NaOH until pH reached 12. The resulting brown oil layer was extracted with dichloromethane and washed with saturated NaOH (aq). The organic phase was dried over sodium sulfate before solvent removal under reduced pressure over 3 h to give yellow oil as a product in 88% yield.

^{1}H-NMR (400 MHz, $CDCl_3$): δ 2.2 (6H, s, $N(C\underline{H}_3)_2$), 2.4 (6H, dd, $b(C\underline{H}_2N\text{-})_3$), 2.6 (6H, dd, $a(C\underline{H}_2N)_3$).

3.3.1.2 Synthesis of ω–mercaptoundecyl bromoisobutyrate ($BrC(CH_3)_2COO\ (CH_2)_{11}SH$, ATRP surface initiator) (1)

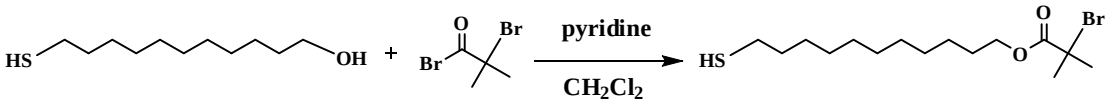

The synthetic procedure was done following the method described in the literatute [42]. Briefly, bromoisobutyryl bromide (0.41 mL, 3.34 mmol) was added dropwise to a stirred solution of mercaptoundecanol (0.75 g, 3.67 mmol) and pyridine (0.27 mL, 3.34 mmol) in dry dichloromethane (15 mL) at 0 °C. The reaction mixture was stirred at 0 °C for 1 h and then at ambient temperature for 16 h. Deionized water was added, and the product was extracted with toluene, which was later removed under reduced pressure by a rotary evaporator. The extract was dissolved in diethyl ether, washed with saturated ammonium chloride, and dried over $MgSO_4$, and volatiles were removed under reduced pressure by a rotary evaporator. The product was purified by column chromatography (Al_2O_3, hexane) to give a colorless oil product (68% yield).

^{1}H NMR (400 MHz, $CDCl_3$): δ 4.14 (2H, t, *J* = 6.6 Hz, OCH_2), 2.51 (2H, q, *J* = 7.5 Hz, SCH_2), 1.91 (6H, s, CH_3), 1.57-1.68 (4H, m, CH_2), 1.24-1.36 (16H, m, CH_2).

3.3.1.3 Preparation of mixed self-assembled monolayer (SAMs) of ATRP initiator

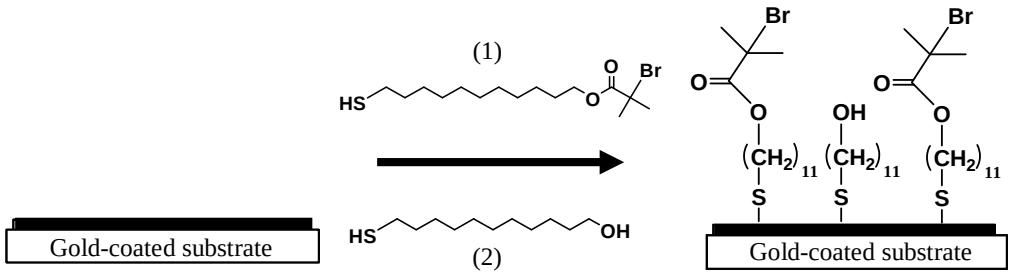

The gold-coated glass slide and SPR disk was clean in piranha solution (7:3 mixtures of H_2SO_4 and H_2O_2) at ambient temperature for 15 min, washed with water and ethanol, and dried in a stream of nitrogen. A freshly cleaned substrates were then immersed in 1 mM ethanolic mixed solutions of $BrC(CH_3)_2COO(CH_2)_{11}SH$ (ATRP initiator, 1) and $HO(CH_2)_{11}SH$ (MUD, 2) for 24 h at ambient temperature. The molar fraction of ATRP initiator and MUD ranged from 10% to 100% (v/v). After this treatment, the gold-coated substrates were rinsed with ethanol and dried in a stream of nitrogen.

3.3.1.4 Surface-initiated polymerization of *tert*-butyl acrylate by ATRP

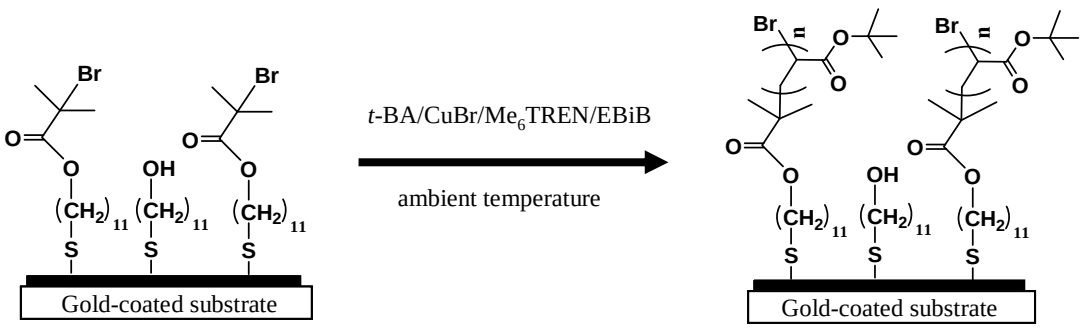

The substrates having surface grafted initiators, $BrC(CH_3)_2COO(CH_2)_{11}S$-Au (obtained from section 3.3.1.3), were placed in a Schlenk flask and sealed with a rubber septum. The flask was evacuated and back-filled with nitrogen three times and then left under a nitrogen atmosphere. *t*-BA and acetone was bubbled by nitrogen gas for 1 h before use. CuBr (49.3 mg, 0.34 mmol), *t*-BA (10 mL, 68 mmol) and acetone (15 mL) were added to a separate Schlenk flask with a magnetic bar, sealed with a rubber septum, and degassed by purging with nitrogen for 1 h. Me_6TREN (88 μL, 0.34 mmol) was added to the mixture via a syringe, and the solution was stirred at ambient temperature until it became homogeneous. The solution was then transferred to the flask containing the substrates via a cannula, followed by an addition of the sacrificial initiator, ethyl 2-bromoisobutyrate (EBiB) (54.6 μL, 0.34 mmol). The polymerization

was allowed to proceed for a set reaction time (0 - 24 h) at ambient temperature. The substrates were removed from the solution, rinsed by acetone and THF, and constantly agitated in THF for 24 h, and then dried with nitrogen stream. The substrates bearing P*t*-BA brushes were then characterized by water contact angle and AFM analyses. Free polymer from the polymerization solution was isolated by first evaporating the residual monomer and solvent under reduced pressure, dissolving in THF, and then passing the polymer solution in THF through a short column of silica to remove any residual catalyst and analyzed by gel permeation chromatography (GPC).

3.3.1.5 Hydrolysis of surface-tethered poly(*tert*-butyl acrylate) brushes [24]

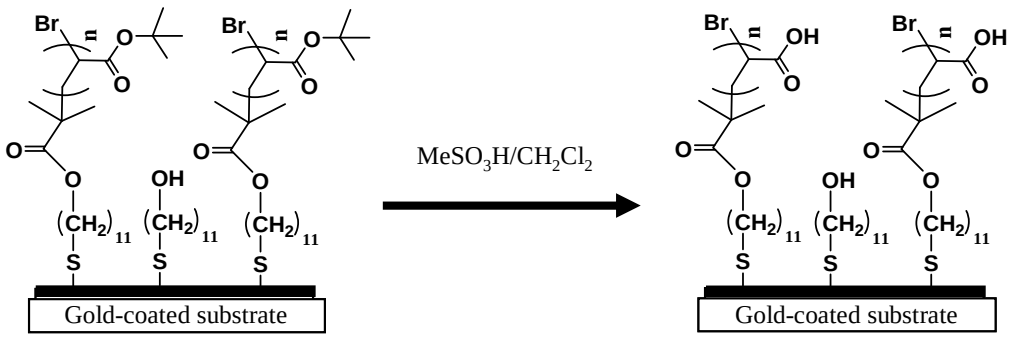

The mixture of methanesulfonic acid (0.1 mL) and dichloromethane (10 mL) were added to a Schlenk flask containing the substrates having P*t*-BA brushes (obtained from section 3.3.1.4*)*. After stirring at ambient temperature for 15 min, the substrates were removed and rinsed thoroughly with dichloromethane and ethanol, and then dried in a stream of nitrogen. The substrates bearing PAA brushes obtained were then characterized by water contact angle and AFM measurements.

3.3.1.6 Determination of carboxyl groups of PAA brushes grafted on gold surface

The toluidine blue O (TBO) staining method was employed to determine the amount of carboxyl groups on PAA brushes [59]. A 0.5 mM TBO aqueous solution was

prepared at pH 10 and the substrates bearing PAA brushes (obtained from section 3.3.1.5) were immersed in the dye solution for 6 h at 30°C. The substrates were then removed and thoroughly rinsed with a 0.4 mM NaOH (aq) (pH 9) for 2 h to remove any noncomplexed dye adhering to the substrates. The dye complexed with carboxyl groups was then desorbed from the surface by soaking the substrates in a 50% (v/v) acetic acid solution for 16 h and the desorbed dye content was obtained by measuring the optical density of the solution at 633 nm with an UV-vis spectrophotometer (Model Techne Specgene, UK). The PAA content was determined from a predetermined calibration curve (0.001-0.05 mM) of the optical density versus dye concentration assuming one carboxyl group reacted with one dye molecule.

3.3.2 Preparation of surface-tethered poly[(methacrylic acid)-*ran*-(2-methacryloyloxyethyl phosphorylcholine)] (PMAMPC) brushes by "grafting to" method

3.3.2.1 Synthesis of poly[(methacrylic acid)-*ran*-(2-methacryloyloxyethyl phosphorylcholine)] (PMAMPC) by RAFT polymerization

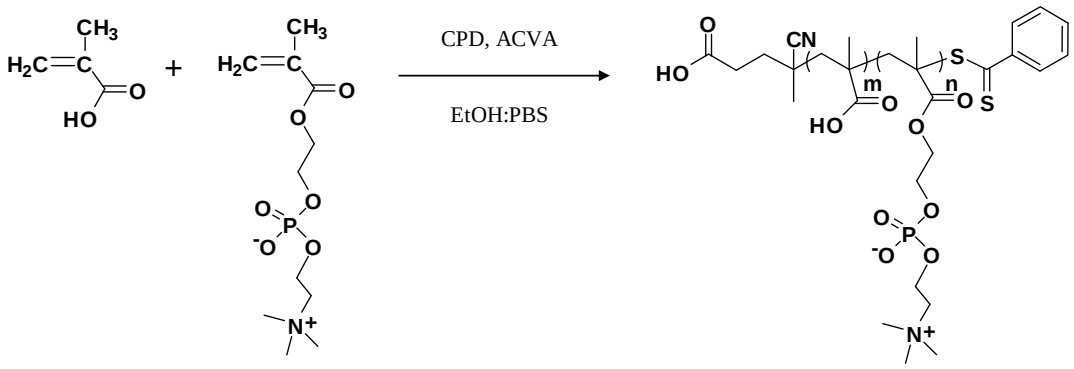

MPC monomer (1.5 g, 5 mmol) was dissolved in 20 mL of mixed solvent (1:1, EtOH:PBS). After MPC monomer was completely dissolved, MA monomer (0.43 g, 5mmol), 4,4'-azobis(4-cyanovaleric acid) (ACVA, 18.78 mg, 0.067mmol), and 4-cyanopentanoic acid dithiobenzoate (CPD, 55.87 mg, 0.2 mmol) were added to

monomer solution. The solution was bubbled with Ar gas for 30 min and then put in an oil bath at 70°C for a set reaction time. The samples were withdrawn from the solution periodically to monitor the average molecular weight and molecular weight distribution (MWD) by GPC. The reaction was terminated by cooling reaction mixture with an ice bath. The polymer solution was then purified by dialysis in DI water for 3 days and then lyophilized. In order to vary composition and molecular weight of the copolymer, the mole ratio of MA and MPC monomer in feed and the ratio of monomer to CTA were varied, respectively. The composition of the copolymer was determined by ^{1}H NMR. Homopolymers of poly(2-methacryloyloxyethyl phosphorylcholine) (PMPC) and poly(methacrylic acid) (PMA) were prepared and purified using the same method as described above. The (co)polymers were characterized by ^{1}H NMR and FT-IR.

3.3.2.2 Preparation of thiol-terminated PMAMPC (PMAMPC-SH)

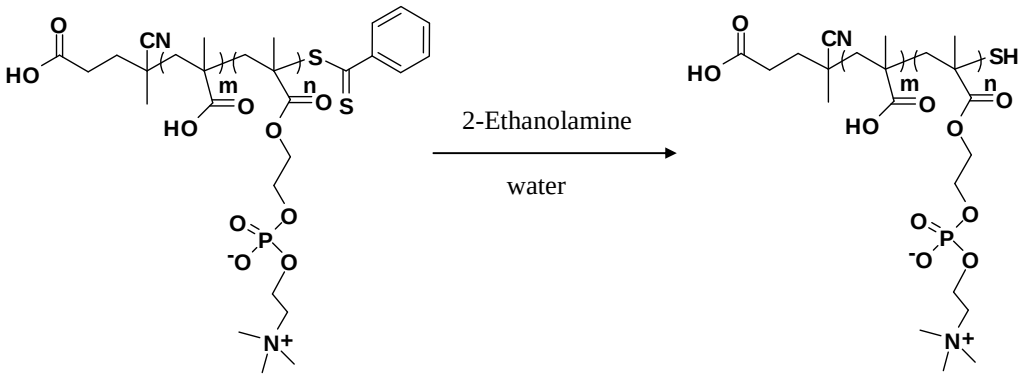

A 0.5 g (10 μmol) of PMAMPC was dissolved in 5 mL DI water. After the polymer completely dissolved in water, a trace of (tris(2-carboxyethyl)phosphine (TCEP) was added to the solution, and then 12 μL (0.2 mmol) of ethanolamine was added. The solution was stirred at ambient temperature for 1 h or until the color of the polymer solution changed to colorless. For homopolymer of PMPC-SH and PMA-SH, a 0.5 g (85 μmol) of PMPC or 0.5 g (58 μmol) of PMA in 5 mL DI water were added by 51 μL (0.85 mmol) and 105 μL (1.74 mmol) of ethanolamine, respectively. The product

was obtained after purification by dialysis in DI water for 3 days and lyophilization and then characterized by ^{1}H NMR, FT-IR, GPC, and UV.

3.3.2.3 Immobilization of PMAMPC-SH on gold-coated SPR disk by "grafting to" method

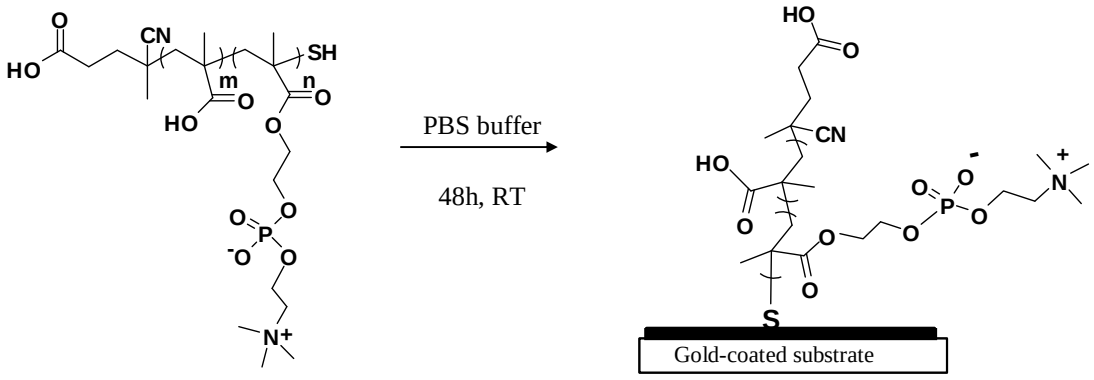

The SPR disk was cleaned by oxygen plasma treatment for 2 min, immersed in Milli-Q water for 2 min, dried under a nitrogen stream, and finally immersed in a 0.2 mM of PMAMPC-SH solution in PBS buffer (10 mM, pH 7.4) for 48 h. The substrates were then removed from the solution, rinsed by constant agitation in 1% SDS, PBS buffer, and Milli-Q water for 2, 20, and 2 h, respectively, and dried under a nitrogen stream. Immobilization of the homopolymer brushes, PMPC-SH and PMA-SH were also prepared by using the same procedure as described above. The modified gold-coated SPR chip was characterized by XPS, water contact angle, and AFM.

3.3.3 SPR measurements

The SPR measurements were conducted using a double channel AutoLab ESPR (Eco Chemie, The Netherlands) and SPR-670M (Moritex, Kanagawa, Japan) at room temperature. The instrument uses a laser diode at a wavelength of 670 nm and a vibrating mirror to modulate the angle of incidence of the p-polarized light beam on the SPR substrate. In a kinetic measurement mode, the angle values were monitored over time, and the measured SPR angle shifts which correspond to the amount of adsorbed

molecules were converted into mass uptakes, using a sensitivity factor of 120 mDegrees per 100 ng/cm^2 [60].

For comparison, a gold-coated SPR disk bearing a monolayer of carboxyl terminated thiol, 11-mercatoundecanoic acid (MUA), as a so-called 2D substrate, was prepared by immersing the cleaned disk in an ethanolic solution of MUA (1 mM) at ambient temperature for 24 h. The disk was then rinsed thoroughly with ethanol and dried in a stream of nitrogen.

The gold-coated SPR disk bearing PAA brushes, PMAMPC, or MUA was first seated in the SPR cell before being stabilized with a running solution of sodium acetate buffer (10 mM, pH 4.5), NaOH (10 mM), and PBS buffer (10 mM, pH 7.4) until the equilibrium SPR angle frequency value in buffer solution was obtained, the obtained sensor was ready to be used.

3.3.4 Swelling behavior of the PAA brushes grafted on on gold-coated SPR disk

The pH response of PAA brushes in aqueous solution was measured by SPR. After SPR disk grafted with PAA was seated in the SPR cell, the cycle of aqueous solutions under different pH values (sodium acetate pH 4.5 and 6.5, and sodium hydroxide pH 9.5) were flowed over the surface. The change of SPR angle corresponding to the change in reflective index and thickness of polymer layer was monitored in real time.

3.3.5 Determination of protein adsorption of the PAA brushes grafted on gold-coated SPR disk

The SPR measurements were conducted using a double channel AutoLab ESPR (Eco Chemie, The Netherlands) at a flow rate of 15 μL/min and held at ambient temperature (24-25 ^{o}C). The protein adsorption on the surface-tethered PAA brushes and MUA monolayer grafted on gold surfaces was tested with four proteins, SA, BSA, FIB, and LYS, in a PBS buffer (10 mM, pH 7.4). After the gold-coated SPR disk

bearing PAA brushes or MUA was seated in the SPR cella 0.2 mg/mL protein solution of was flowed over the substrate for 15 min and then rinsed with PBS buffer for 5 min.

3.3.6 Determination of protein adsorption of the PMAMPC brushes grafted on gold-coated SPR disk

The SPR measurements were conducted using a double channel SPR-670M (Moritex, Kanagawa, Japan) at a flow rate of 15 μL/min and held at a constant temperature of 30 °C. The protein adsorption on the surface-tethered PMAMPC brushes was tested with 3 proteins, BSA, AVD, and blood plasma in PBS buffer (10 mM, pH 7.4). After the SPR disk bearing PMAMPA was seated in the SPR cell, the 0.1 mg/mL of BSA and AVD solution was injected over the substrate and left for a period of 10 min, followed by a 5 min rinse with PBS. In the case of blood plasma, whole blood plasma carrying about 70 mg of proteins per milliliter of plasma was diluted by PBS buffer at a plasma to PBS ratio of 1:700, 1:100, 1:10, 1:5, and 1:0 to a obtain blood plasma protein with concentration in a range of 0.1-70 mg/mL or equivalent to0.14-100% blood plasma in PBS. The blood plasma solution was flowed over the substrate for 15 min and then washed with PBS buffer for 5 min.

3.3.7 Immobilization of probes on the gold-coated SPR disks bearing PAA brushes and MUA

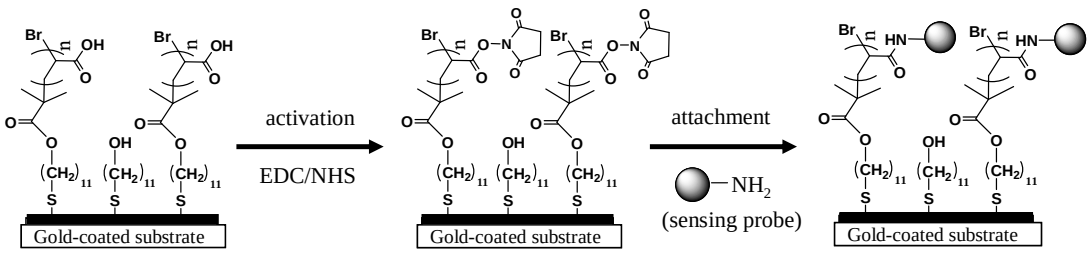

For immobilization of sensing probe, NH_2-biotin or BSA, via amine coupling, the gold-coated SPR disks bearing PAA brushes and MUA were first seated in the SPR

cell before being rinsed with a running solution of sodium acetate buffer (10 mM, pH 4.5). After a baseline SPR response was established, the activation by a mixture of 0.05 M EDC and 0.05 M NHS in aqueous solution, the attachment of NH_2-biotin (1 mg/mL) or BSA (0.1 mg/mL) solution in sodium acetate buffer, pH 4.5, and the subsequent blocking by ethanolamine (pH 8.5, 1 M in water) were all carried out sequentially *in situ* in a running solution of sodium acetate buffer for 5, 15, and 5 min, respectively. At the end of each step, the substrate was rinsed with a running solution of sodium acetate buffer to remove unbound molecules. The obtained sensor was ready to detect the specific binding with target analyte (SA or anti-BSA) and non-specific binding with BSA and FIB.

3.3.8 Immobilization of biotin probes on the gold-coated SPR disks bearing PMAMPC brushes and MUA

The immobilization of biotin was done outside the SPR instrument. The carboxyl groups were firstly activated by immersing the gold-coated SPR disk bearing PMAMPC brushes, PMA brushes, and MUA in an aqueous solution of 0.2 M EDC and 0.05 M NHS for 15 min. The substrates were rinsed immediately with Milli-Q water before immersed in a solution of biotin-NH_2 (1 mg/mL) in PBS buffer for 2 h at ambient temperature and washed thoroughly with PBS solution. The unreacted activated carboxyl groups (having NHS groups attached) were deactivated by immersing in PBS buffer (10 mM, pH 7.4) overnight.

3.3.9 Specific interactions of the probes immobilized on the gold-coated SPR disks bearing PAA brushes and MUA with target analytes

Upon probe immobilization, each sensor platform was subjected to specific target molecules, SA for biotin-immobilized platform and anti-BSA for BSA-immobilized platform. After a baseline SPR response was recorded in running buffer (10 mM PBS), 50 μL of target molecule in PBS at selected concentration was then applied and left for 15 min. The unbound molecule was removed by washing with PBS for 5 min. Non-specific interactions of each sensor platform was tested against non-target proteins; BSA and FIB for biotin-immobilized platform, SA and FIB for BSA-

immobilized platform by passing each protein solution of 0.1 mg/mL over the disks for 15 min. The shift of the SPR angle at the end-point of the washing step and after baseline subtraction ("angle shift") was used to calculate the amount of the target molecules bound onto the surface, using a sensitivity factor of 120 mDegrees equals to 100 ng/cm^2 and its molecular weight.

To quantify the binding efficiency of the sensor platform, a signal-to-noise (*S/N*) ratio was calculated using the following equation.

$$S/N = \frac{amount\ of\ bound\ target\ molecule}{amount\ of\ bound\ non-target\ molecule} \tag{3.1}$$

3.3.10 Specific interactions of biotin immobilized on the gold-coated SPR disks bearing PMAMPC brushes and MUA with avidin in complex sample

The specific binding of biotin immobilized on the gold-coated SPR disks bearing PMAMPC brushes with avidin in blood plasma solution was conducted using a double channel SPR-670M (Moritex, Kanagawa, Japan). The gold-coated SPR disks bearing PAA brushes and MUA immobilized with biotin were first seated in the SPR cell before being rinsed with a running solution of PBS buffer. After a baseline SPR response was established, the solution of AVD (10 μg/mL equivalent to 0.15 μM) in blood plasma solution (0.14% in PBS buffer) was applied and left for 10 min. The unbound AVD was removed by washing with PBS for 5 min. The amount of specific binding of AVD was quantified by the shift of the SPR response angle at the end-point of the washing step and after baseline subtraction. The non-specific binding (binding in the absence of AVD in blood plasma solution) was also determined in order to quantify the specific binding of AVD in blood plasma in term of the signal-to-noise (*S/N*) ratio. The signal-to-noise (*S/N*) ratio was calculated by the following equation.

$$S/N = \frac{SPR\ angle\ shift\ after\ exposed\ to\ blood\ plasma\ with\ ADV}{SPR\ angle\ shift\ after\ exposed\ to\ blood\ plasma\ without\ ADV} \tag{3.2}$$

CHAPTER IV

RESULTS AND DISCUSSION

In this chapter, the results are divided into two sections. The first section mainly focuses on the synthesis and biosensing applications of surface-tethered poly(acrylic acid) (PAA) brushes. The PAA brushes having varied graft density were prepared by surface-initiated atom transfer radical polymerization (ATRP) of *tert*-butyl acrylate (*t*-BA) from gold-coated SPR disk supported with 2-bromoisobutyrate monolayer followed by acid hydrolysis. Effects of graft density, degree of activation, extent of probe immobilization on the ability to prevent non-specific adsorption and to detect analyte were evaluated in comparison with the conventional 2D monolayer of MUA using surface plasmon resonance (SPR) technique. The second section explains the synthesis and biosensing applications of surface-tethered copolymer brushes of poly[(methacrylic acid)-*ran*-(2-methacryloyloxyethyl phosphorylcholine)] (poly(MA-*ran*-MPC), PMAMPC). The immobilization of the copolymer brushes was performed by "grafting to" approach via by self-assembly formation of thiol-terminated polymer chain (PMAMPC-SH) on gold-coated SPR disk. Effects of copolymer composition and molecular weight on the ability to prevent non-specific adsorption and to detect analyte were evaluated in comparison with the conventional 2D monolayer of MUA using SPR.

4.1 Preparation of surface-tethered poly(acrylic acid) (PAA) brushes by "grafting from" method

4.1.1 Preparation of mixed self-assembled monolayer (SAMs) of ATRP initiator

Controlling the surface coverage of the immobilized initiator is a prerequisite for tailoring the grafting density of polymer brushes prepared by surface-initiated

polymerization. Water contact angle measurements were used to follow the extent of the initiator immobilization. According to Figure 4.2, the water contact angle increased with increasing ATRP initiator (molecule 1 in Figure 4.1) in the mixed thiol solution from 0% to 100%. This trend was expected considering that the bromoester-terminated initiator is hydrophobic, and the SAM of 100% ATRP initiator exhibited a water contact angle in a range similar to those reported in the literatures [42,61]. Moreover, a difference between the advancing (θ_A) and the receding (θ_R) contact angle or contact angle hysteresis (θ_A - θ_R) can be used as a measure of the SAM surface roughness and heterogeneity. Slight greater hysteresis values (~24°) of the substrates prepared from the mixed thiol containing 10 and 50% ATRP initiator suggested that they are more chemically heterogeneous in comparison with those having no and 100% ATRP initiator (~15°).

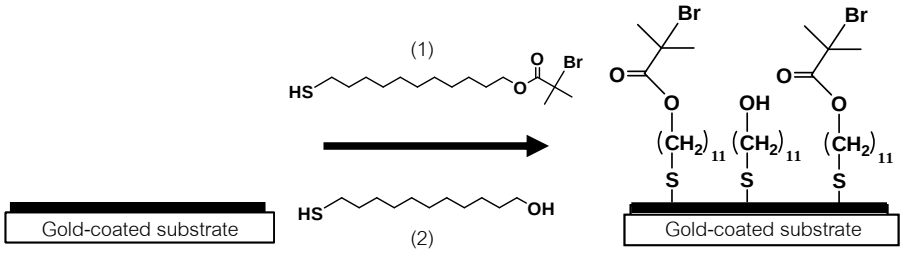

Figure 4.1 Formation of mixed self-assembled monolayer of ATRP initiator on gold-coated SPR disk.

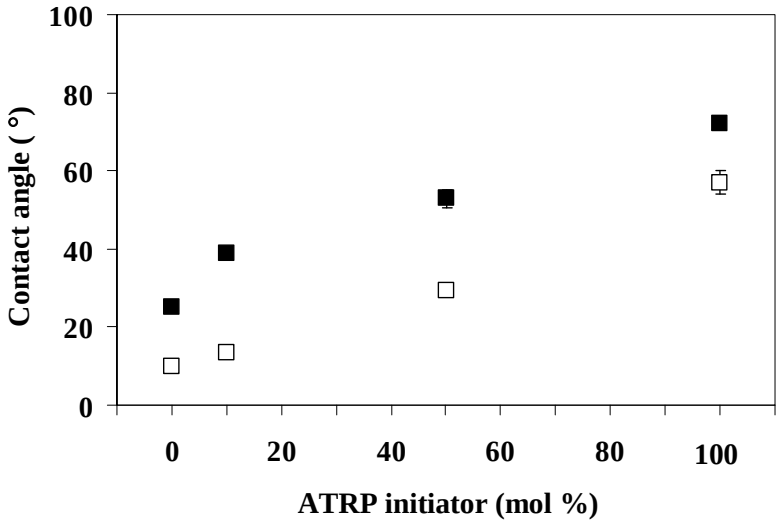

Figure 4.2 Advancing (θ_A) and receding (θ_R) contact angles of mixed SAM layers with different ATRP initiator content.

In addition, the values of observed contact angle (θ_{obs}) or the advancing contact angle (θ_A) in this case can be used for calculating surface coverage of initiator (f_1). The equilibrium contact angle of a chemically heterogeneous surface, θ_{obs}, can be related to the fraction of different chemical groups via Cassie-Baxter equation and the modified related equations [53,62].

$$[1+\cos(\theta_{obs})]^2 = f_1[1+\cos(\theta_1)]^2 + f_2[1+\cos(\theta_2)]^2 \qquad (4.1)$$
$$f_1 + f_2 = 1$$

Where θ_1 is advancing water contact angle of 100% ATRP-initiator (72°), and θ_2 is advancing water contact angle of 100% MUD (25°).

The initiator surface coverage (f_1) calculated from the water contact angle according to eq 4.1 is shown in Table 4.1. The results imply that the amount of initiator in monolayer is at least similar to the ratio in mixed solution. It has been well studied and generally accepted that alkanethiols with different end groups, produce well-mixed SAMs [63-64]. Therefore, a SAM with randomly mixed ATRP initiator was successfully prepared on the gold-coated SPR disk and the density of the ATRP initiator can be controlled by the mole fraction of ATRP initiator in the thiol mixture.

Table 4.1 Water contact angle (θ_A) and initiator surface coverage (f_1) on gold surface obtained for different mole fraction of ATRP initiator in the mixed thiol solution.

ATRP initiator (mol% in mixed thiol solution)	θ_A (deg)	f_1 (%)
0	25 ± 1.2	0
10	39 ± 1.3	24
50	53 ± 2.3	55
100	72 ± 0.5	100

4.1.2 Surface-initiated polymerization of *tert*-butyl acrylate by ATRP

The SPR disks having ATRP initiator were then allowed to react with *t*-BA monomer in the presence of an ATRP catalyst system (CuBr/ Me_6TREN/EBiB) at ambient temperature to grow polymer brushes by surface-initiated polymerization (SIP) as shown in Figure 4.3. As shown in our previous study [26] the molecular weight and thickness of the P*t*-BA brushes can be controlled by reaction time as well as the monomer to initiator ratio (the targeted DP) in the solution. Unlike the previous work, the more active ligand, Me_6TREN, was used in this research instead of PMDETA, so that the polymerization could be performed at ambient temperature without thermal treatment. This was done in order to avoid the gold detachment from the substrate upon elevating the temperature.

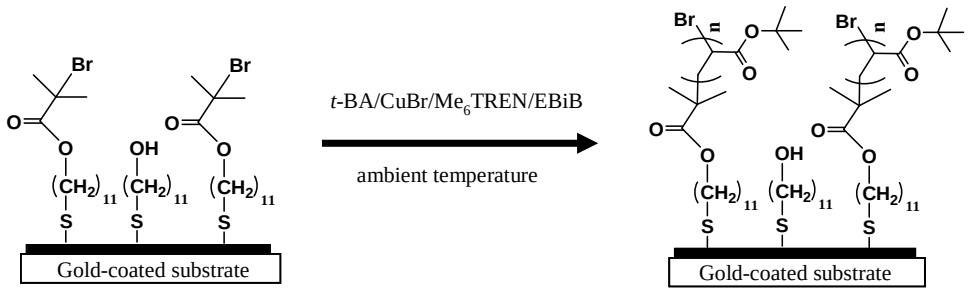

Figure 4.3 SI-ATRP of *t*-BA monomer on gold-coated SPR disk.

Figure 4.4 clearly shows that the change in the molecular weight ($\overline{M}_n$) of the free P*t*-BA generated in the solution from the sacrificial initiator (EBiB) increased as the polymerization time increased (over the tested range of 0 – 24 h) for the P*t*-BA made from targeted DPs of 200. The fact that the molecular weight distribution is close to 1 suggests that the polymerization is living and can be well controlled. Therefore, it can be concluded that P*t*-BA can be performed at ambient temperature.

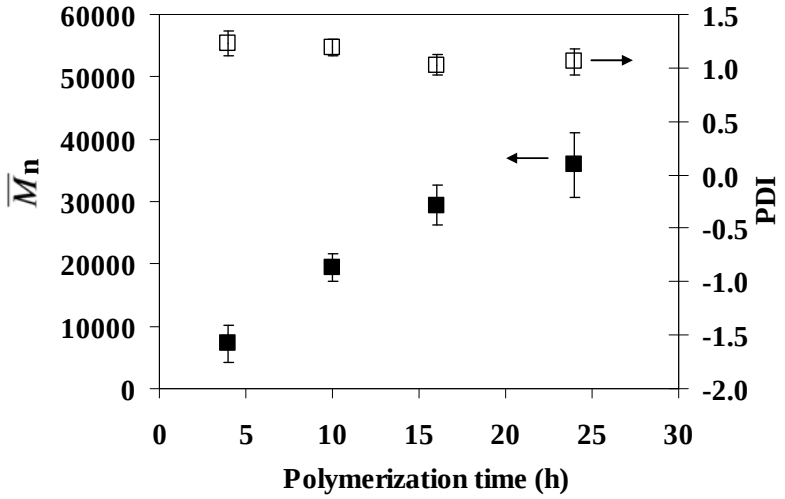

Figure 4.4 The molecular weight ($\overline{M}_n$) (■) and PDI (□) of the P*t*-BA in solution as a function of the polymerization time for targeted DP of 200. Data are shown as the mean ± SD and are derived from 3 repeats.

It should be emphasized it is not practically possible to directly determine the molecular weight of the grafted polymer in this particular case since the amount of the removed polymer brushes was too low to be characterized by GPC. However, it has previously been demonstrated that the molecular weight of this free polymer closely resembled that of the grafted polymer brushes cleaved from the surface [65]. In this study, the molecular weight of the P*t*-BA brushes on surface was determined by measuring the molecular weight of a free polymer simultaneously formed in the solution from the "sacrificial" or "added" initiator (Figure 4.4). Moreover, the controlled growth of the polymer in solution was found to be independent of the surface initiator density [62]. Therefore, it is assumed that the molecular weights of the free and grafted polymer chains are similar in our study despite the variation in surface-grafted initiator.

The growth of P*t*-BA brushes on the gold-coated SPR disk can also be monitored by water contact angle measurement. Figure 4.5 illustrates θ_A and θ_R of the P*t*-BA brushes grown from the surface having 100% coverage of surface initiator as a function of polymerization time. Both θ_A and θ_R rapidly increased from $76^o/55^o$ of the

gold-supported initiator monolayer to ~ $88^o/70^o$ - $95^o/76^o$ after the polymerization was conducted for 4 - 24 h. This result indicated that more hydrophobic surface has been formed as a consequence of P*t*-BA brushes formation. Moreover, the contact angle hysteresis (θ_A - θ_R) being less than 20^o also implies that the surface bearing linear P*t*-BA brushes is quite homogeneous and smooth.

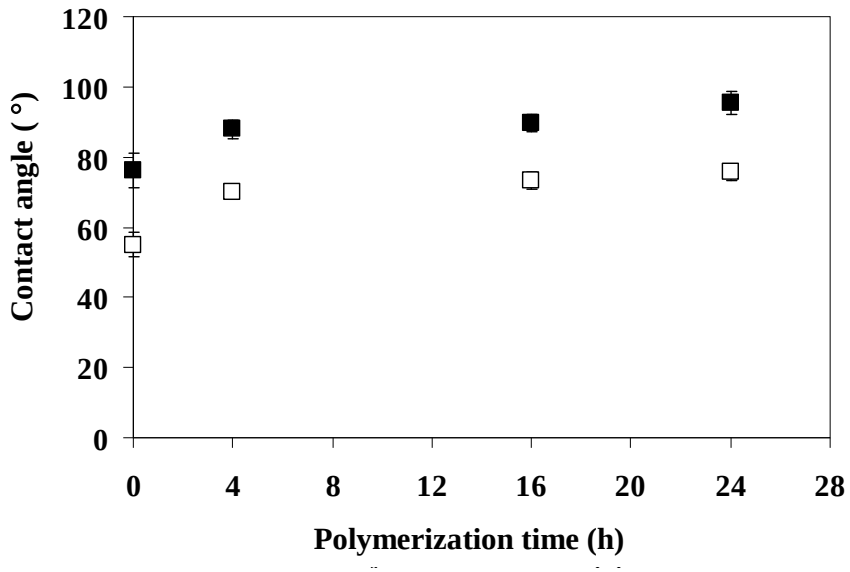

Figure 4.5 Water contact angle data of P*t*-BA brushes grown from the surface having 100% coverage of surface initiator as a function of polymerization time for targeted DP = 200 (θ_A (■),θ_R (□)).

The thickness of dry polymer layer made from the surface having 100% coverage of surface initiator was obtained by measuring the surface profile after being scraped by AFM tip using AFM technique (Figure A-3 in Appendix A). The thickness of the P*t*-BA brushes layer obtained after polymerization for 4 h of which $\overline{M}_n$ of the free polymer is 8 kD is 3.8 ± 0.3 nm, while that obtained after polymerization for 16 h of which $\overline{M}_n$ of the free polymer is 30 kD is 9.5 ± 0.6 nm. It is evident that the thickness of P*t*-BA brushes can be increased with polymerization time. The data also shows a good correlation between the polymer film thickness and the molecular weight of the free polymer in solution.

The grafting densities (σ) of the grafted P*t*-BA can be calculated from the molecular weight of the free polymer ($\overline{M}_n$) and from the dry film thickness (*t*) determined by AFM according to eq 4.2.

$$\sigma = \frac{t\rho N_A}{Mn} = \frac{1}{A_X} \tag{4.2}$$

Where ρ is the mass density (1.1 g/cm^3 for P*t*-BA) and N_A is Avogadro's number. The calculated grafting density of P*t*-BA brushes grown from the surface having 100% coverage of surface initiator varied between 0.21 and 0.31 chains/nm^2.

Figure 4.6 shows the advancing water contact angle (θ_A) of the gold-coated SPR disks after stepwise modification (initiator immobilization and P*t*-BA brushes formation) as a function of ATRP initiator content. As mentioned above, the contact angle of the gold-supported initiator increased with the ATRP initiator content. SI-ATRP led to an increase in contact angle for all surfaces except that containing 0% grafted ATRP initiator. These results clearly indicated that the polymer chains can only grow on the surface having ATRP initiator. However, the contact angle of P*t*-BA brushes obtained from the surface having 10% grafted ATRP initiator is relatively low (70 ± 1.7°) because polymer chains, at relatively low graft density, were not able to completely cover the surface. Whereas, the contact angles of P*t*-BA brushes obtained from the surfaces having 50 and 100% grafted ATRP initiator became considerably high, 87 ± 3.4° and 91 ± 4.0°, respectively, indicating more thorough surface coverage.

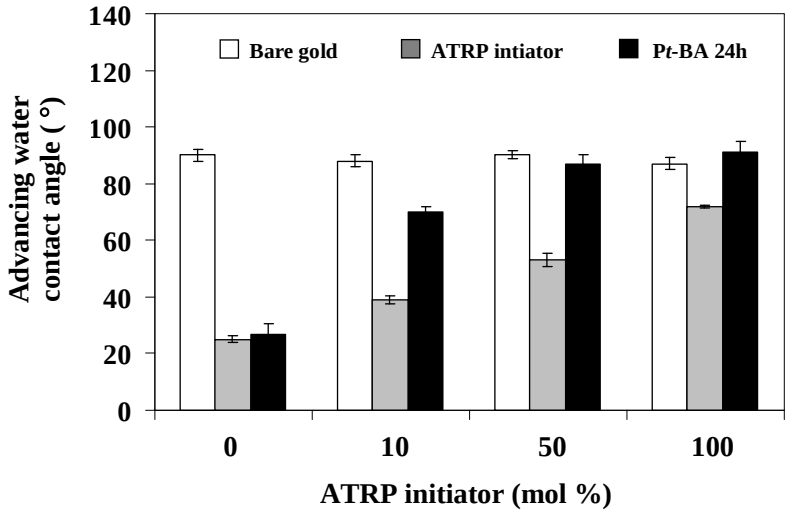

Figure 4.6 Advancing water contact angle data of the gold-coated SPR disk having different ATRP initiator content before and after self-assembly of ATRP initiator, and after polymerization for 24 h.

The variation in surface coverage of the P*t*-BA brushes could also be monitored by AFM. At low and medium surface coverage, the hydrophobic chains of Pt-BA brushes grown from the surface having 10 and 50% surface-grafted ATRP initiator tried to minimize their interactions with the hydrophilic surrounding area covered with hydroxyl-terminated thiol by forming aggregates which appear as protrusions (Figure 4.7b-c) and yielding the surfaces with relatively higher roughness (rms) of 2.9 and 2.1 nm, respectively in comparison with the bare gold surface (rms = 1.2 nm). For high surface coverage, the surface having 100% grafted Pt-BA brushes (Figure 4.7d) appear smoother implying that the polymer chains were closely and homogeneously packed with roughness of 1.9 nm. Therefore, these data indicated that the surface coverage or grafting density of P*t*-BA brushes could be controlled by varying surface coverage of ATRP initiator.

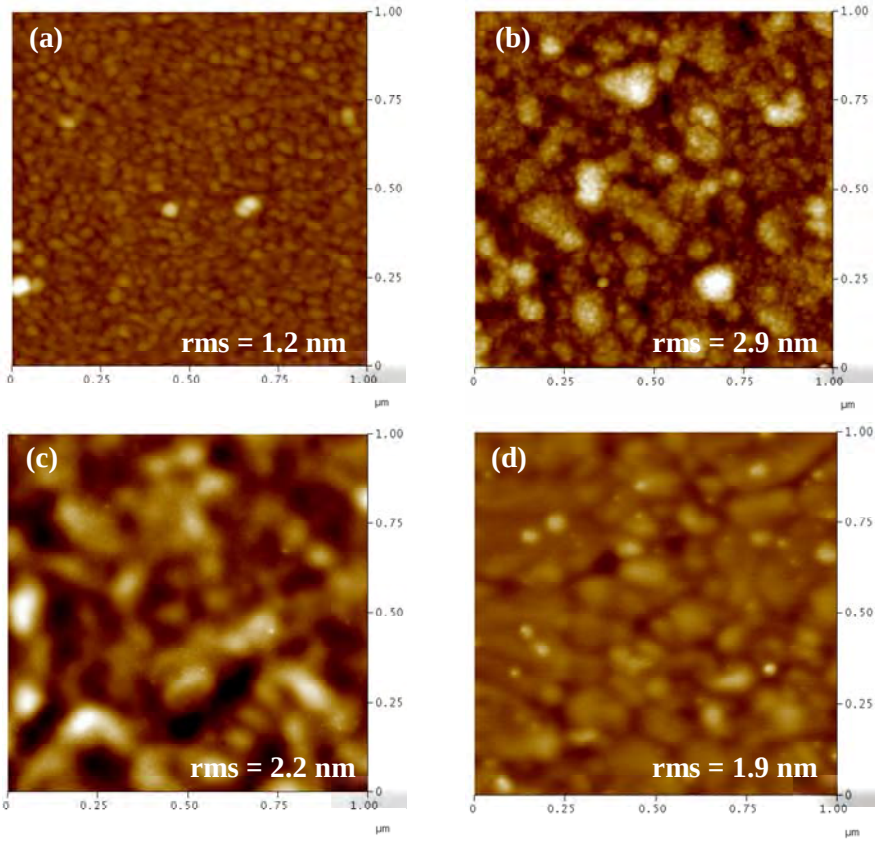

Figure 4.7 AFM images of (a) bare gold surface and dry films of P*t*-BA brushes prepared by SI-ATRP for 24 h from the gold-coated SPR disk having different surface-grafted ATRP initiator content: (b) 10%, (c) 50%, and (d) 100%.

For further investigations, we assume, in agreement with previous studies by other research groups [42,66] that the increase of ATRP initiator density should lead to an increased surface coverage or grafting density of the P*t*-BA brushes. It should be noted that absolute graft density cannot be determined because the incomplete coverage of the surface-immobilized ATRP initiator [41-42] together with the unfortunate fact that the direct analysis of the grafted polymer brushes on the planar substrates is practically impossible because the amount of the removed polymer brushes would be too low to be characterized by GPC.

4.1.3 Hydrolysis of poly(*tert*-butyl acrylate) brushes

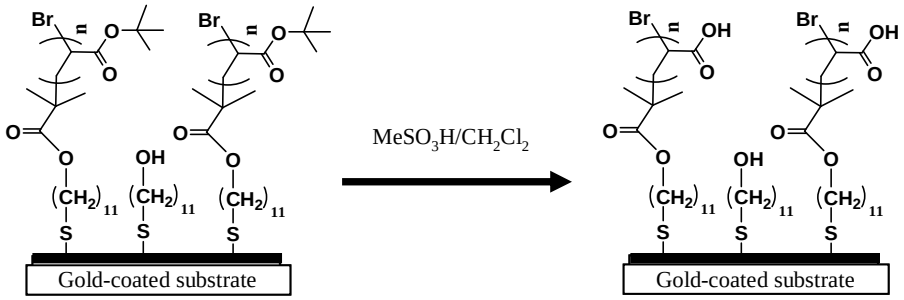

Figure 4.8 Acid hydrolysis of poly(*tert*-butyl acrylate) (P*t*-BA) brushes.

Poly(*tert*-butyl acrylate) (P*t*-BA) brushes was converted to poly(acrylic acid) (PAA) brushes by immersing the surface in 0.1 mL of methanesulfonic acid ($MeSO_3H$) in 10 mL of dichloromethane at room temperature for 15 min [24]. After hydrolysis, the θ_A decreased drastically from the hydrophobic P*t*-BA brushes to the hydrophilic PAA brushes (Figure 4.9). These data suggest that the hydrophobic *tert*-butyl groups of the P*t*-BA brushes were converted to the hydrophilic carboxyl groups of PAA brushes. As anticipated, the lowest θ_A was obtained from the surface having PAA brushes with 100% graft density implying its greatest hydrophilicity.

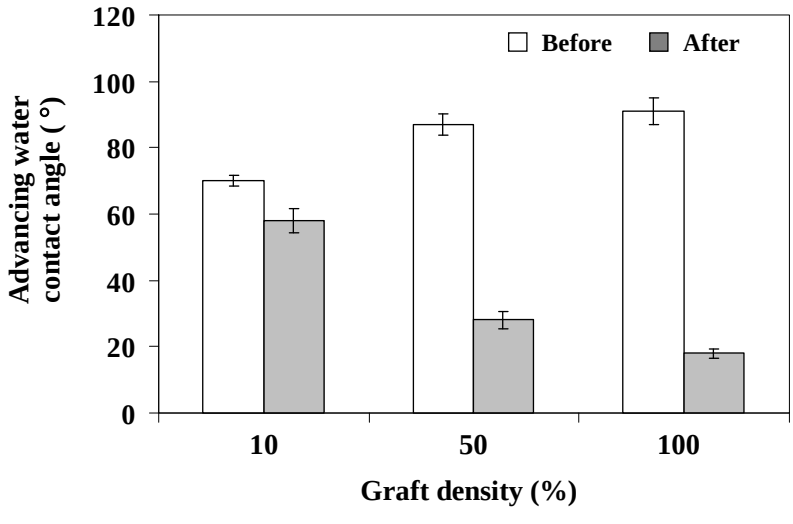

Figure 4.9 Advancing water contact angle (θ_A) data of the gold-coated SPR disk grafted with different graft density of P*t*-BA brushes before and after hydrolysis.

AFM was also used as a tool to determine the surface topography and roughness of the PAA brushes obtained after hydrolysis. As demonstrated in Figure 4.10, the change in topography and roughness after hydrolysis is clearly evident for the polymer brushes having low graft density with a decrease in the film roughness from 2.9 to 2.1 nm. However, the film roughness was not much changed for the polymer brushes having medium and high graft density.

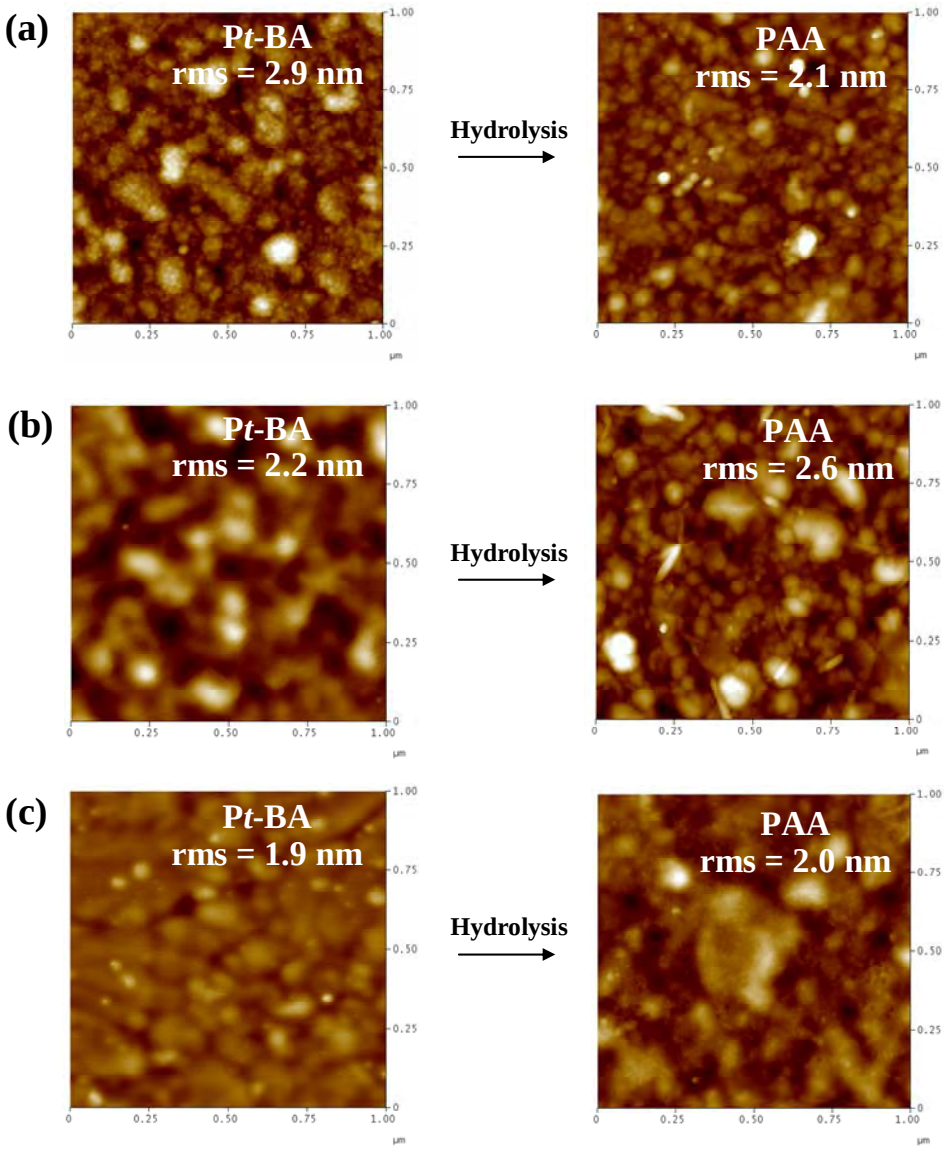

Figure 4.10 AFM images of polymer films before (P*t*-BA brushes) and after hydrolysis (PAA brushes) having different graft density: (a) 10%, (b) 50%, and (c) 100%.

The carboxyl group density of the PAA brushes on gold-coated substrate was quantitatively determined by using Toluidine blue O (TBO) assay. The carboxyl groups of PAA brushes can form a complex with Toluidine blue O. The absorbance of the solution containing the desorbed complex was measured at 633 nm. The carboxyl group content was obtained from a calibration plot of the optical density versus dye concentration which is displayed in Appendix C. Our previous study showed that the carboxyl group density of PAA brushes can be varied as a function of $\overline{M}_n$ or polymer chain length [26]. In this study, the relation of carboxyl group density and graft density of the polymer brushes was investigated. As determined by TBO assay, the carboxyl group density of the PAA brushes increased as a function of graft density of the polymer brushes which can be varied as a function of surface-grafted ATRP initiator content (Figure 4.11). The graft density dependent carboxyl group density values are in good agreement with the water contact angle data. The higher the carboxyl group density is the lower water contact angle and the more hydrophilic of surface becomes.

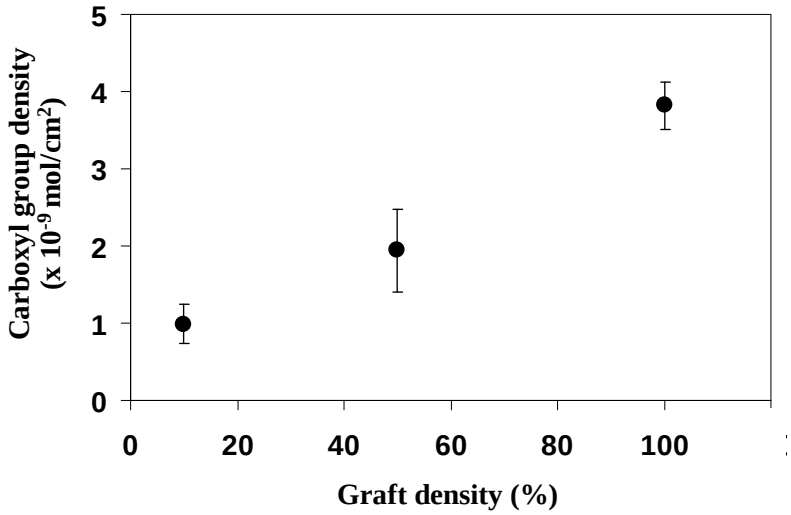

Figure 4.11 Carboxyl group densities of the PAA brushes as a function of graft density.

4.1.4 Swelling behavior of the surface-grafted PAA brushes

In principle, PAA brushes having stretched or coiled conformations should be sensitive to pH variation of aqueous medium, resulting in the change of the thickness

and refractive index of polymer layer [67-68]. In this study, the swelling behavior of the PAA brushes was determined by SPR measurement. It was assumed that the SPR angle shift would be changed as a function of thickness and refractive index variation. Figure 4.12 showed the angle shift of the 100% surface-grafted PAA brushes having two different $\overline{M}_n$ (13 and 30 kD) in response to pH variation. The reversible change of the angle shift upon pH alternation was observed for both samples. The magnitude of angle shift variation of the MUA monolayer (Figure A-4 in Appendix A) was less than those observed here suggesting that the change of SPR angle shift should be a consequence of PAA conformational changes which could be attributed to the ionization of the carboxyl (COOH) groups. Upon pH raise to 9.5, all of COOH groups should be deprotonated and existed in the form of carboxylate groups (COO^-). The negatively charged ions should cause electrostatic repulsion among the adjacent PAA chains. As a result, the polymer chains became more stretched resulting in increasing thickness of the polymer layer. On the other contrary, when pH was lowered down to 6.5 and 4.5 (pKa of PAA = 6.5-6.6 [69]), not all of COOH groups were deprotonated. The surface-grafted PAA chains became less stretched with lower thickness. Moreover, it was found that the magnitude of angle shift in response to pH variation increased with increasing molecular weight of the polymer brushes: ~80 m° for $\overline{M}_n$ of 13 kD to ~300 m° for 30 kD (Figure 4.12).

In the case of PAA brushes having $\overline{M}_n$ of 30 kD, the SPR angle shift first dropped down as a consequence of the decrease in thickness upon pH lowering from 9.5 to 6.5. The angle then gradually increased to a certain value. This subsequent angle shift increase may be explained as a result of elevated refractive index. The effect should be much more pronounced for the polymer with high molecular weight. This is the reason why the same behavior was not observed in the case of PAA brushes having $\overline{M}_n$ of 13 kD of which the change in refractive index was not significant enough to offset the effect of thickness variation.

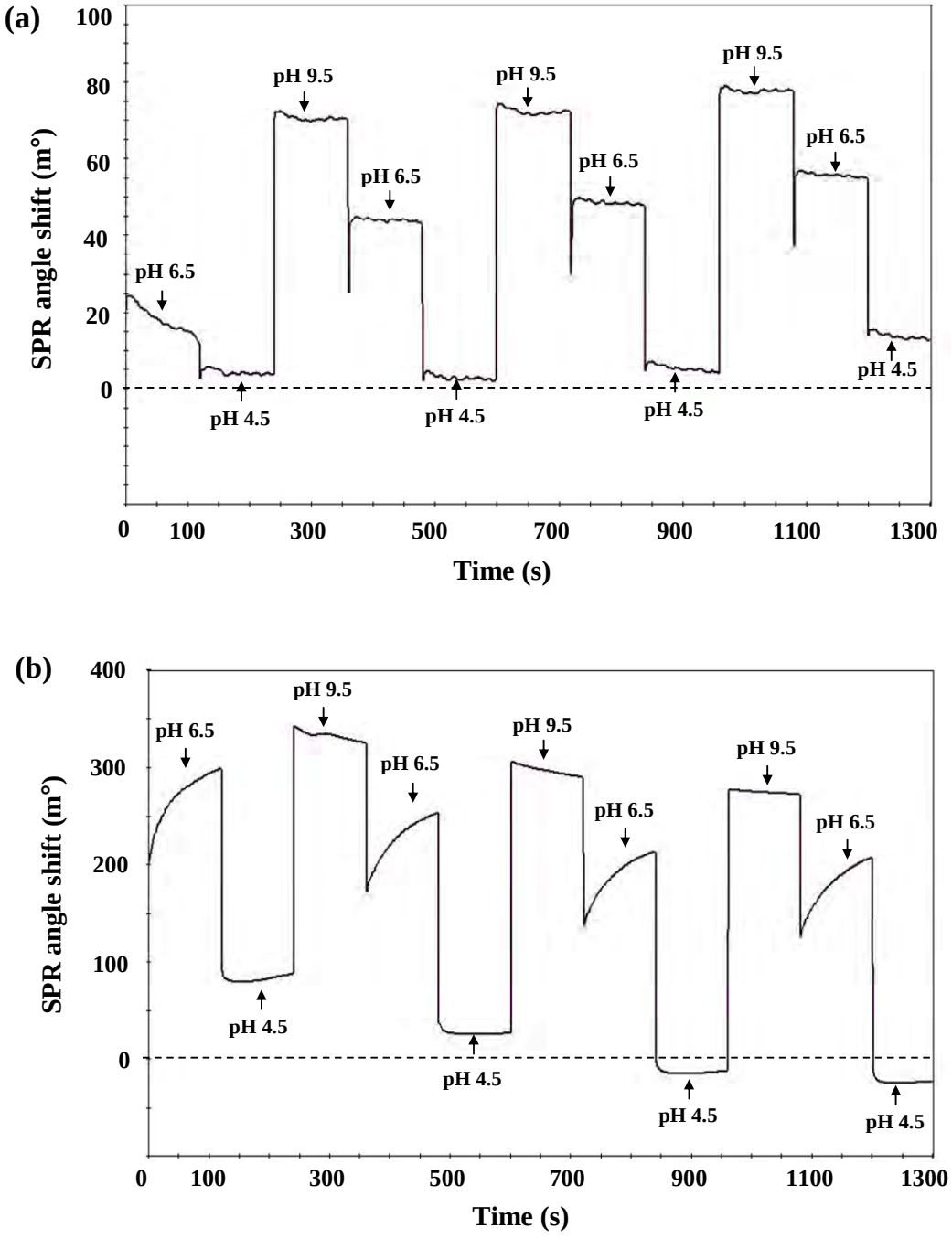

Figure 4.12 SPR angle shift of 100% surface-grafted PAA brushes having $\overline{M}_n$ of (a) 13 kD and (b) 30 kD upon pH alternation.

As shown by Chu and coworkers [68], the thickness of the PAA layer in PBS buffer solution after immobilizing galactose ligand was lower than that of the original

PAA layer. They have explained this as a result of suppressed swellability. In this study, the swelling of the surface-grafted PAA brushes before and after biotin immobilization was also investigated. Figure 4.13 shows the SPR angle shift of the 100% surface-grafted PAA brushes and $\overline{M}_n$ of 30 kD before (solid line) and after (dashed line) biotin immobilization in response to pH switching. It was found that the pH response of PAA brushes after biotin immobilization (changing range ~100 m°) was lower than that of those before immobilization (changing range ~300 m°). This lower degree of pH response so as the swellability can be explained as a consequence of the COOH group being replaced by non-ionizable and more hydrophobic biotin.

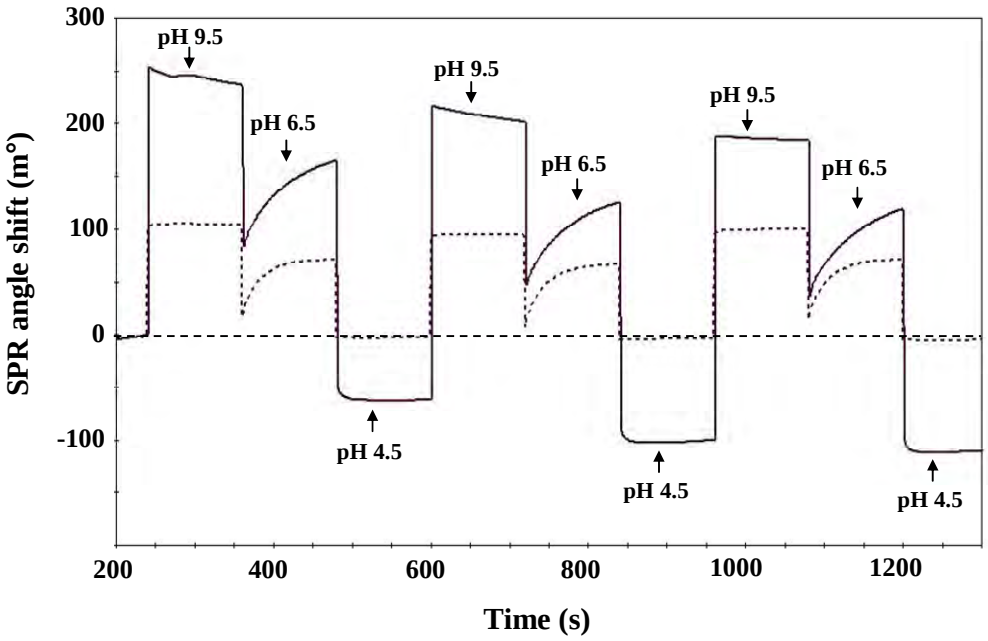

Figure 4.13 SPR angle shift of 100% surface-grafted PAA brushes having $\overline{M}_n$ of 30 kD before (solid line) and after (dashed line) biotin immobilization upon pH alternation using degree of COOH activation of 4.42 ± 0.92 nmol/cm^2.

In order to prove the assumption that the swelling of PAA brushes was restricted by the replacement of COOH group by biotin, the amount of biotin immobilization was reduced to lower than that of those obtained in Figure 4.13 so that a higher amount of the COOH groups was still remained in the polymer chain. The

reduction of biotin immobilization was done by decreasing degree of COOH activation by EDC/NHS that will be discussed in subsection *4.1.6.1*. Figure 4.14 illustrates that the magnitude of SPR angle shift change in response to pH variation of the PAA brushes having degree of COOH activation of 2.14 ± 0.21 nmol/cm^2 before and after biotin immobilization (changing range decreased from ~250 m° to ~150 m°) was less than those observed in Figure 4.13 (changing range decrease from ~300 m° to ~100 m°), in which a higher amount of biotin immobilization (degree of COOH activation of 4.42 ± 0.92 nmol/cm^2) was obtained. This result verified that the greater content of remaining ionizable COOH groups that were not bound to biotin can definitely help maintaining the swellability of the polymer brushes. It can then be concluded that the swelling of the PAA brushes strongly depends on the number of carboxyl groups along the chains of PAA.

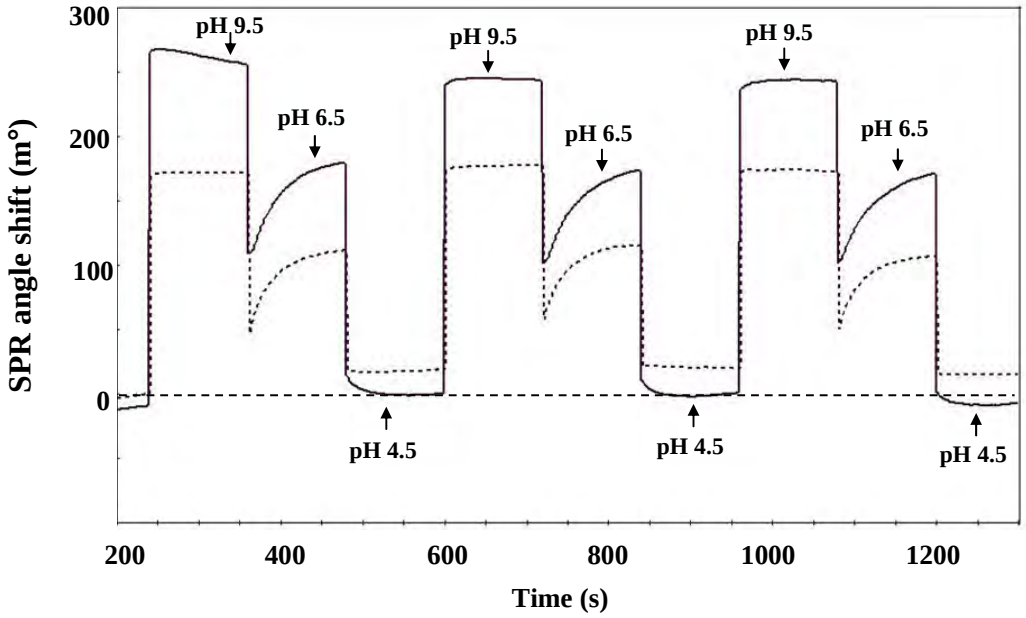

Figure 4.14 SPR angle shift of 100% surface-grafted PAA brushes having $\overline{M}_n$ of 30 kD before (solid line) and after (dashed line) biotin immobilization upon pH alternation using degree of COOH activation of 2.14 ± 0.21 nmol/cm^2.

4.1.5 Protein adsorption of the surface-grafted PAA brushes

The protein adsorption on the PAA brushes having different surface graft density was tested with four proteins, SA, BSA, FIB, and LYS in comparison with the conventional sensing layer based on carboxyl-terminated thiol, 11-mercaptoundecanoic acid (MUA). Figure 4.15 shows the amount of adsorbed proteins on PAA brushes and MUA after soaking with protein solution in PBS (pH 7.4) as measured by SPR. For the PAA brushes with low graft density (10%) adsorbed all of the negatively charged proteins: SA (60 kDa, pI = 5), BSA (69 kDa, pI = 4.8), and FIB (340 kDa, pI = 5.5). Whereas the PAA brushes with medium (50%) and high (100%) graft density adsorbed much less proteins as opposed to the MUA layer. The relative adsorbed amount of protein on PAA brushes having varied graft density in comparison with the MUA are also expressed in Table 4.2.

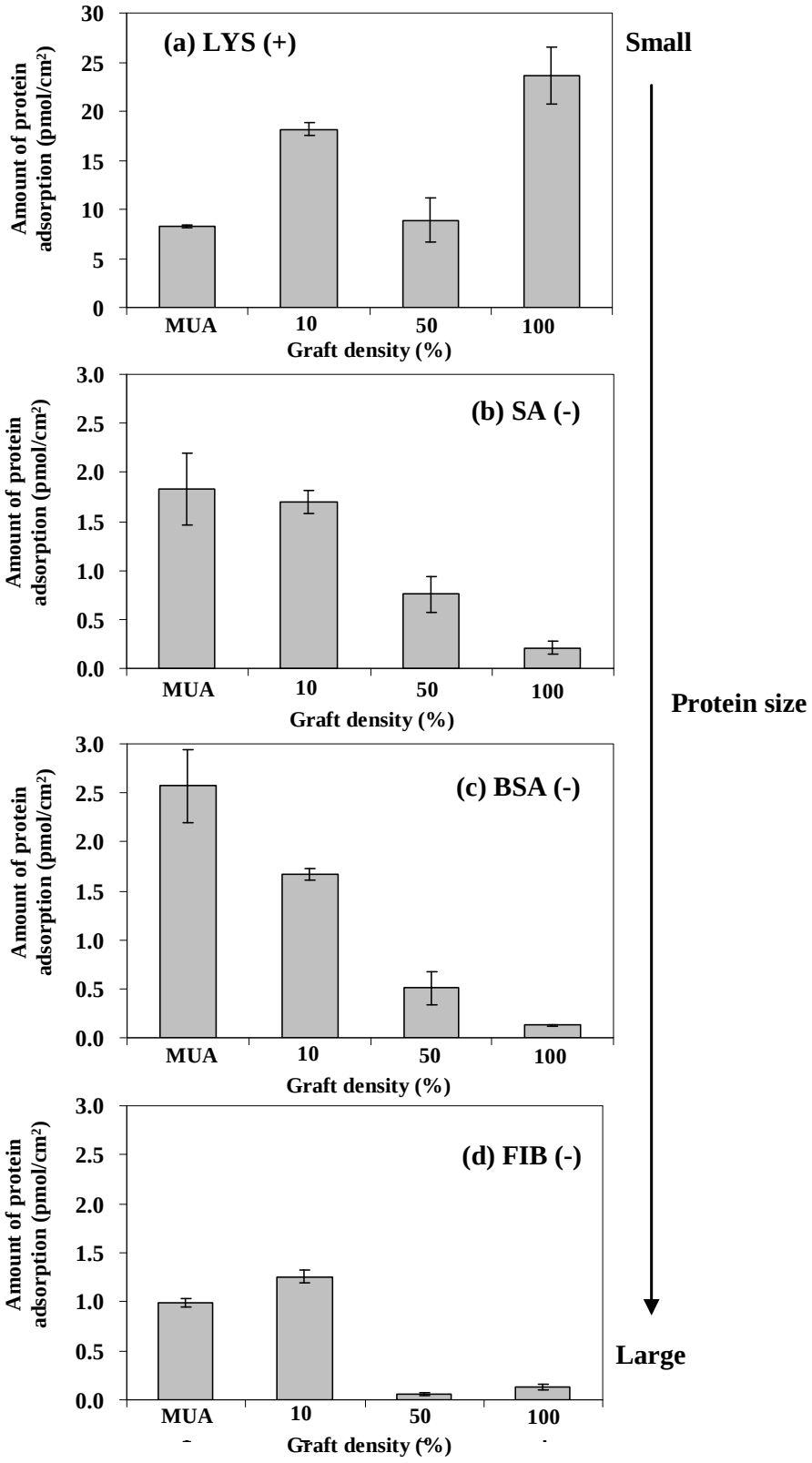

Figure 4.15 Amount of adsorbed protein on the surface-grafted PAA brushes having varied graft density as compared with MUA: (a) LYS, (b) SA, (c) BSA, and (c) FIB.

Table 4.2 Amount of adsorbed protein and the relative protein adsorption of the PAA brushes having varied graft density in comparison with MUA.

	Adsorbed amount (pmol/cm^2)			% Adsorption with respect to MUA		
	SA	BSA	FIB	SA	BSA	FIB
MUA	1.83 ± 0.37	2.57 ± 0.37	0.99 ± 0.05	100	100	100
10	1.75 ± 0.19	1.66 ± 0.06	1.26 ± 0.06	95.6	64.6	127
50	0.75 ± 0.18	0.51 ± 0.47	0.06 ± 0.02	40.9	19.8	6.1
100	0.21 ± 0.06	0.13 ± 0.01	0.12 ± 0.03	11.5	5.1	12

These results can be described by the fact that, at low graft density of the PAA brushes, the proteins may be able to penetrate into the polymer layer and adsorb on the gold surface that was not covered by the polymer, resulting in high level of non-specific protein adsorption. However, proteins are difficult to diffuse into the swollen layer of the PAA brushes having medium and high graft density, on which low extent of protein adsorption was observed. This observation is in good agreement with the work previously reported by others based on different system of polymer brushes. As shown by Yoshikawa and co-workers, the adsorption of protein can be greatly suppressed by a densely graft of poly(2-hydroxyethyl methacrylate) brushes [70]. Yang and coworkers also reported that the protein adsorption on poly(D-gluconamidoethyl methacrylate) (PGAMA) can be reduced by increasing the polymer chain density [61].

Unlike other proteins, LYS, the smallest protein tested (14 kD) which is positive in charge (pI = 12) was capable of adsorbing on the PAA brushes especially that having 100% graft density. It is believed that the negative charges of the COO- of the PAA brushes at pH 7.4 in PBS solution (pKa = 6.5-6.6) [69] can electrostatically attract the negatively charged LYS. Since LYS is small, its accessability is no longer limited by the highly grafted polymer brushes. Being suffered from the non-specific adsorption of the positively charged proteins, the surface-grafted PAA brushes are not suitable to be used in the system having positively charged components.

Apparently, the amount of adsorbed protein having negative charges (SA, BSA, FIB) was in proportion to the size of the protein. This verified the previous speculation that the penetration of the protein was restricted by the extended chains of the polymer brushes. The surface-grafted PAA brushes having 50% and 100% graft density exhibit protein adsorption of ≤ 45 ng/cm^2 (0.75 pmol/cm^2) for SA, ≤ 35 ng/cm^2 (0.51 pmol/cm^2) for BSA, and ≤ 43 ng/cm^2 (0.12 pmol/cm^2) for FIB. These surfaces are considered to be low fouling surfaces. Therefore, both of them are effective in resisting non-specific adsorption of proteins and should be able to act as good biosensing platform. Figure 4.16 shows the schematic illustration of the potential adsorption behavior of the three negatively charge proteins on PAA brushes surfaces with different grafting density.

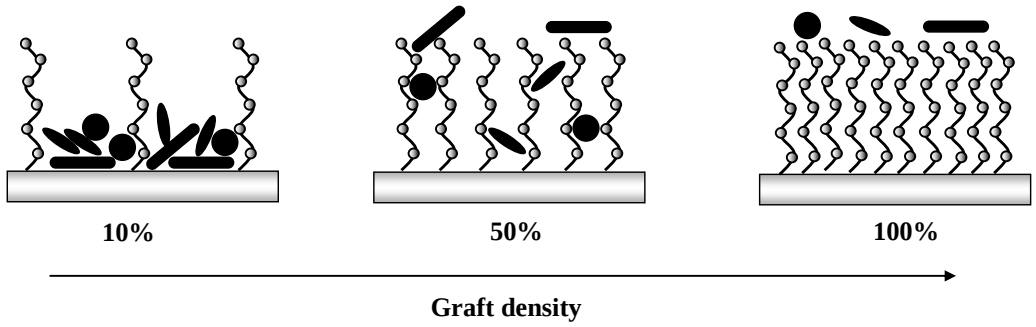

Figure 4.16 Schematic illustration of adsorption behavior of negatively charge proteins having different size on the PAA brushes with different graft density.

4.1.6 Sensing probe immobilization of the surface-grafted PAA brushes

In general, biomolecules or sensing probe is often immobilized on polymer surfaces via an amide bond formation between the amino group of biomolecule and the carboxyl group of polymer. In this study, biotin and BSA were chosen as model sensing probes, to be attached to the carboxyl groups of the surface-grafted PAA brushes via covalent bonds. The carboxyl groups of PAA brushes were first activated by a water-soluble carbodiimide, 1-(3-dimethylaminopropyl)-3-ethylcarbodiimide hydrochloride

(EDC) and *N*-hydroxysuccinimide (NHS) to form NHS group. The NHS group was then coupled with amine-terminated sensing probe, leading to amide bond formation as shown in Figure 4.17. SPR measurement was used to determine binding capacity of the sensing probe.

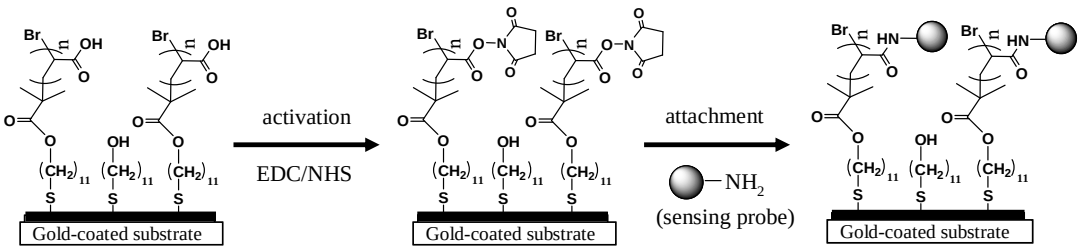

Figure 4.17 Attachment of sensing probes on the surface-grafted PAA brushes.

SPR is a surface-sensitive technique based on the detection of change in the refractive index (RI) that is known to provide quantitative information and can be used for the detection of the desired analyte with a high specificity and sensitivity. The changes in the SPR angle (angle shift, expressed as $\Delta\theta$), can be determined from the difference in the SPR angle at the baseline and after the washing, and is proportional to the quantity of molecules on the gold-coated SPR disks. Figure 4.18 and 4.19 show a typical SPR sensorgrams of sensing probe immobilization on PAA brushes and MUA, including three steps: activation, immobilization, and washing step, respectively. The SPR response in Figure 4.18 indicates that the $\Delta\theta$ values of the substrates bearing PAA brushes (100% graft density, 30 kD) after biotin attachment is 851 m°, which is equivalent to a biotin density of 709.2 ng/cm^2 or 1,896 pmol/cm^2 (based on a sensitivity factor of 120 m°/100 ng/cm^2 and a MW of 374 g/mol for biotin). The calculated immobilized biotin density was 171 pmol/cm^2 ($\Delta\theta$ = 77 m°) for the MUA. The results, therefore, suggest that the layer of PAA brushes possessed an 11- fold higher biotin density as compared to the MUA system.

The SPR response in Figure 4.19 shows the amount of BSA immobilized on the PAA brushes (100% graft density, 30 kD) as compared with MUA. The MW of BSA, 69,000 g/mol, was used to calculate the immobilized BSA density which was found to

be 16.28 ($\Delta\theta$ = 1348 m°) and 5.94 pmol/cm^2 ($\Delta\theta$ = 492 m°) for the PAA brushes and the MUA, respectively. The results imply that the substrates bearing PAA brushes possessed a 2.74- fold higher BSA density as compared to the MUA system. The results of both biotin and BSA immobilization are in good agreement with the fact that the layer of PAA brushes should provide a high binding capacity of sensing probe due to a higher concentration of COOH group at the brush interface than that of the monolayer of MUA.

Considering the effect of sensing probe size on binding capacity of, it was found that the binding capacity of BSA, the larger sensing probe, was lower (16.28 pmol/cm^2) than that of biotin (1,896 pmol/cm^2) whose size is a lot smaller (MW = 374 g/mol) , on both surface-grafted PAA brushes and MUA. These results also indicate a string impact of steric hindrance on the binding capacity of sensing probe.

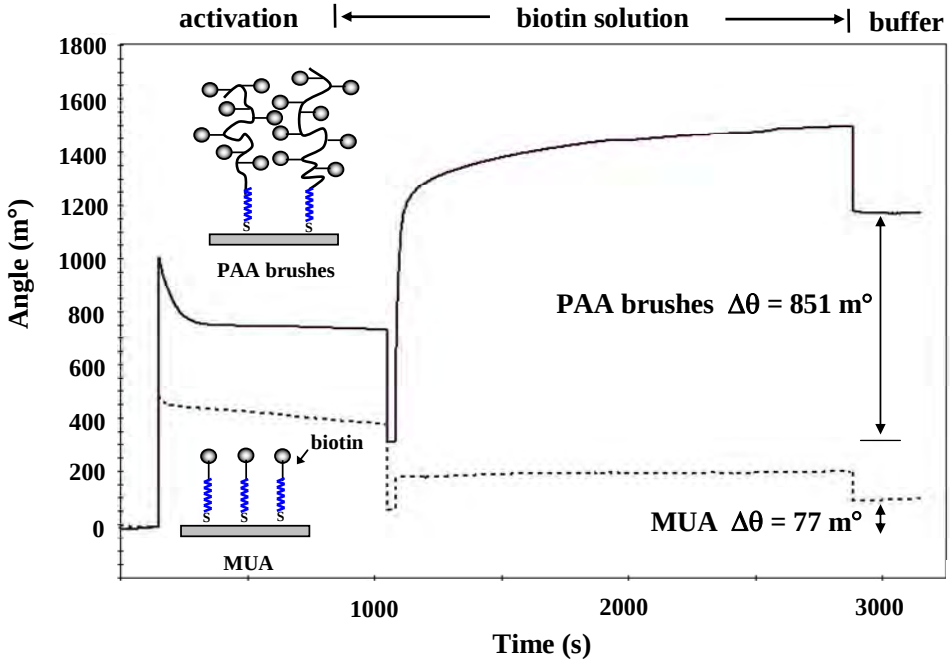

Figure 4.18 Typical SPR sensorgrams of the surface-grafted PAA brushes and MUA during biotin immobilization.

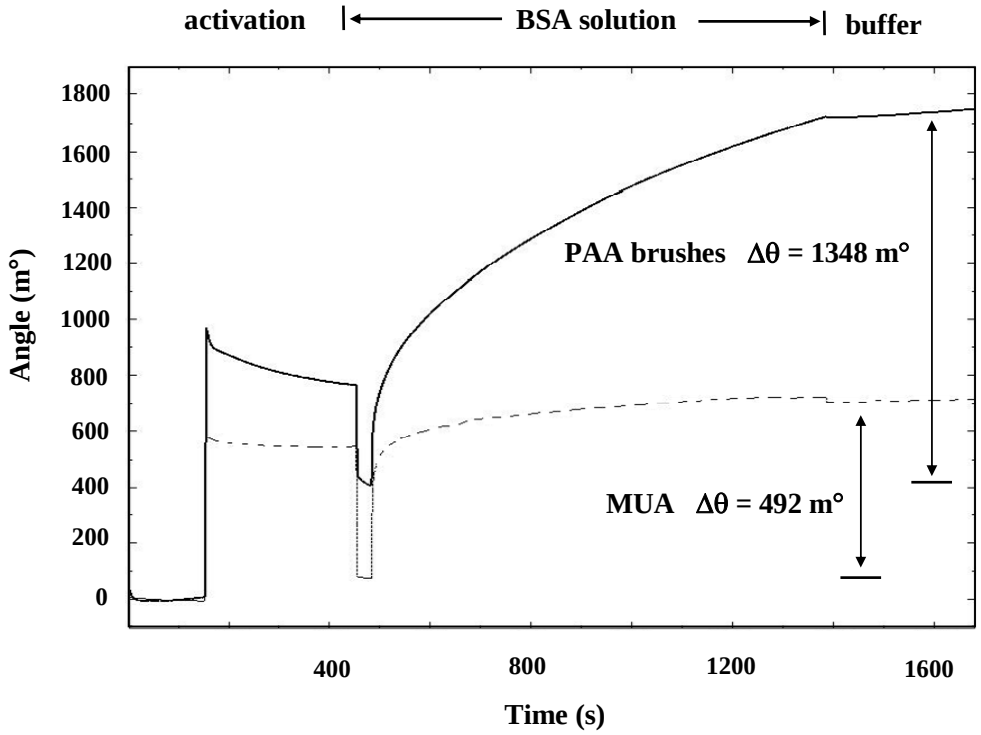

Figure 4.19 Typical SPR sensorgrams of the surface-grafted PAA brushes and MUA during BSA immobilization.

4.1.6.1 Effect of degree of carboxyl group activation

The degree of COOH activation was controlled by varying the molar ratio between EDC and NHS and the activation time. Figures 4.20 and 4.21 illustrate the amount of immobilized biotin and BSA, respectively, on PAA brushes having 100% graft density and $\overline{M}_n$ of 30 kD as a function of degree of COOH activation. The degree of activation shown in X-axis was calculated by the SPR angle shift in the activation step using a sensitivity factor of 120 m°/100 ng/cm^2 and a MW of 115 g/mol for NHS). The data in Figure 4.20 shows that the amount of immobilized biotin increased with the increase of degree of activation, indicating the dependence of biotin binding capacity on the amount of activated COOH group. On the contrary, BSA binding capacity decreased with increasing degree of activation (Figure 4.21). Not only can the increase of COOH group activation provide a high density of active group, NHS group (hydrophobic group), for immobilizing sensing probe but it also reduces the swelling of

PAA brushes resulting in the collapse of polymer chain. Thus, the diffusion of the large molecules into the collapse layer should be more difficult than that of those into the swollen layer. As demonstrated by Gautrot and coworkers [71], the swelling of the polymer brushes facilitates the penetration of proteins, histidine-tagged proteins, and subsequently provide the high protein loading levels. On the other hand, a low propensity to swell does not favor protein infiltration into the inner polymer layer. These results indicated that the swelling of PAA brushes has significant influence on the immobilization of large molecule. The degree of COOH group activation should be optimized in order to achieve the maximum amount of immobilized sensing probe.

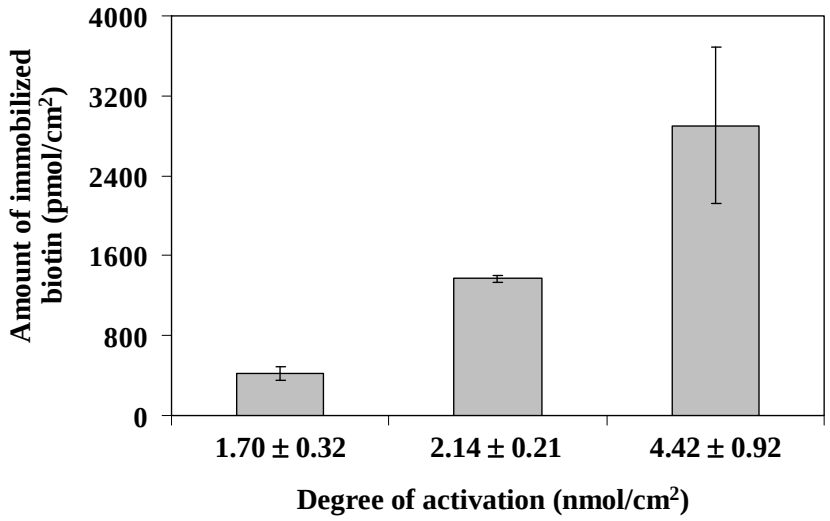

Figure 4.20 Amount of immobilized biotin on the surface-grafted PAA brushes having 100% graft density and $\overline{M}_n$ of 30 kD as a function of degree of COOH activation.

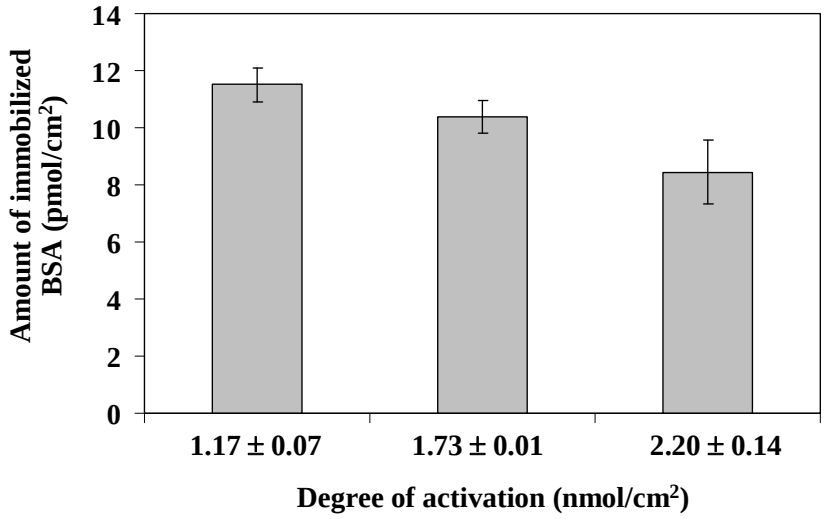

Figure 4.21 Amount of immobilized BSA on the surface-grafted PAA brushes having 100% graft density and $\overline{M}_n$ of 30 kD as a function of degree of COOH activation.

4.1.6.2 Effect of polymer chain length

Taking advantage of the ability to fine tune the carboxyl group density as a function of the molecular weight or polymer chain length of the polymer brushes, the effect of varying the carboxyl group density as a function of the $\overline{M}_n$ on the binding capacity of sensing probe was evaluated. Biotin was used as a sensing probe to investigate this effect in order to reduce the steric hindrance effects of large size sensing probe. Evidently in Figure 4.22, the amount of attached biotin increased with increasing $\overline{M}_n$ or polymer chain length. The increase of biotin binding capacity could be explained by the increased number of carboxyl groups of polymer side chains.

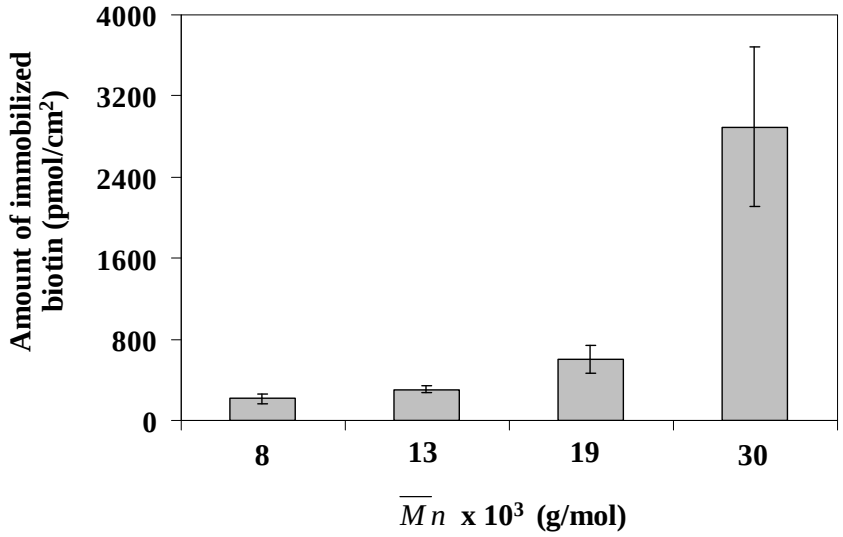

Figure 4.22 Amount of immobilized biotin on the surface-grafted PAA brushes having 100% graft density as a function of their $\overline{M}_n$.

4.1.6.3 Effect of graft density

In order to demonstrate the effect of graft density on a binding capacity of sensing probe, the PAA brushes obtained from the $\overline{M}_n$ of 30 kD with different graft density were used for immobilizing sensing probe. As expected, with the increase in graft density or the amount of carboxyl group, the immobilizing capacity of biotin probe also increased (Figure 4.23). In the case of BSA which is a larger probe in comparison with biotin, the immobilization of BSA was limited for the surface-tethered PAA brushes having high graft density (Figure 4.24). When the graft density is high, the space between polymer chains becomes much narrow, densely packed, and it is more hindered for the large molecule to reach inside the inner layer to react with the inner carboxyl groups of the PAA brushes, resulting in low binding capacity of BSA at 100% graft density despite its high amount of carboxyl group . As shown by Yang and coworkers [61], the penetration of the large proteins, BSA and especially fibrinogen into poly(D-gluconamidoethyl methacrylate (PGAMA) brushes was reduced by increasing graft density. Yoshikawa and coworker s [70] also reported the effect of grafting density of poly(2-hydroxyethyl methacrylate) (PHEMA) brushes on the

diffusion of large protein into the inner layer of polymer brushes. The grafting density at 0.06 and 0.7 chain/cm^2 showed exclusion effect to BSA and IgG.

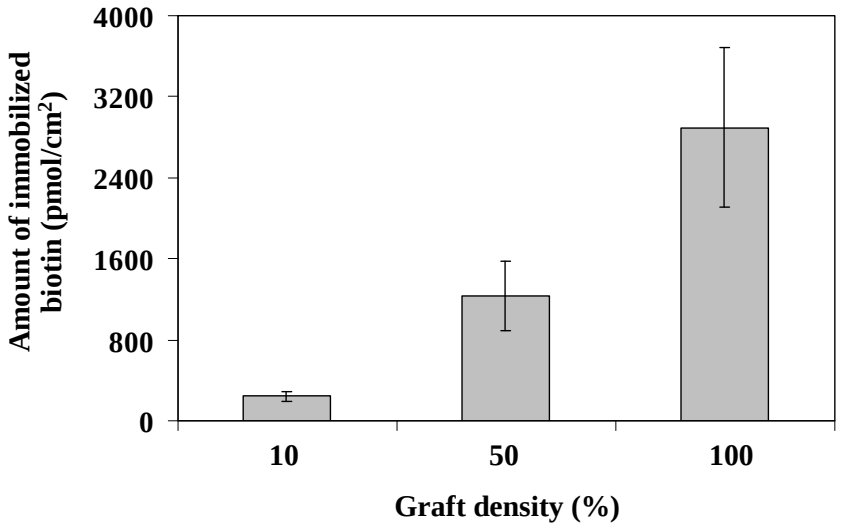

Figure 4.23 Amount of immobilized biotin on the surface-grafted PAA brushes having $\overline{M}_n$ of 30 kD as a function of graft density.

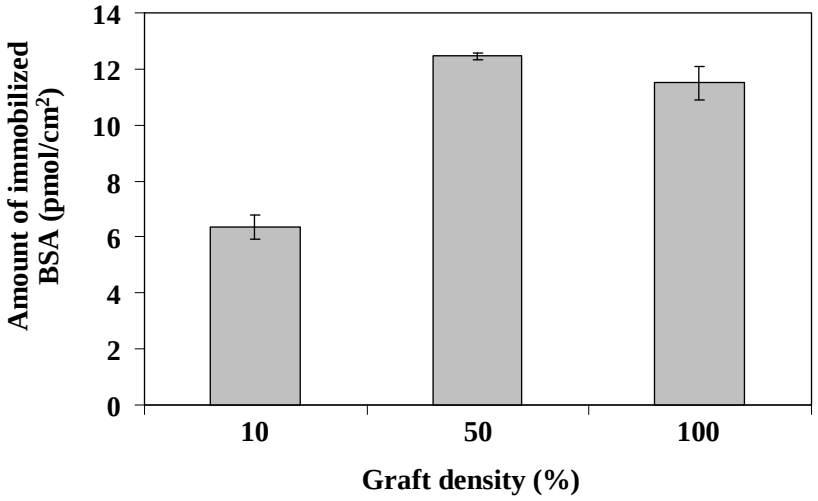

Figure 4.24 Amount of immobilized BSA on the surface-grafted PAA brushes having $\overline{M}_n$ of 30 kD as a function of graft density.

4.1.7 Specific interactions of of the probes immobilized on the gold-coated SPR disks bearing PAA brushes with target analytes

The SPR measurement was used to determine the specific binding of the sensing probes with target molecules. The changes of SPR angle is proportional to the quantity of target molecule bound with the sensing probe immobilized on sensor platform. After immobilizing sensing probe, biotin and BSA, each sensor platforms, biotinylated sensor platform and BSA sensor platform, were subjected to each specific target molecules, SA and anti-BSA, respectively. The efficiency of the sensor platforms developed from PAA brushes was compared to those based on the MUA.

4.1.7.1 Biotin- streptavidin system

A typical SPR response of streptavidin (SA) bound to biotinylated surface is shown in Figure 4.25. The binding capacity of SA was measured to be 881 m° (734.2 ng/cm^2 or 12.2 pmol/cm^2) and 428 m° (356.7 ng/cm^2 or 5.9 pmol/cm^2) for the PAA brushes-biotin and the MUA-biotin, respectively. Using a MW of 60,000 g/mol for SA, the PAA brushes exhibited just over a 2.1-fold higher SA binding density as compared to the MUA (12.2 and 5.9 pmol/cm^2). The result thereby suggested that the layer of the PAA brushes possessed greater biotin densities and greater binding capacity towards SA detection than the monolayer of MUA. This is in good agreement with the work reported by Lee and coworkers [15], who found that the binding capacity of SA to the biotinylated layer prepared on poly(oligo(ethylene glycol) methacrylate) brushes was some 2.5-fold higher than that on the carboxylic acid terminated SAM (648.5 ng/cm^2 and 255.6 ng/cm^2, respectively)

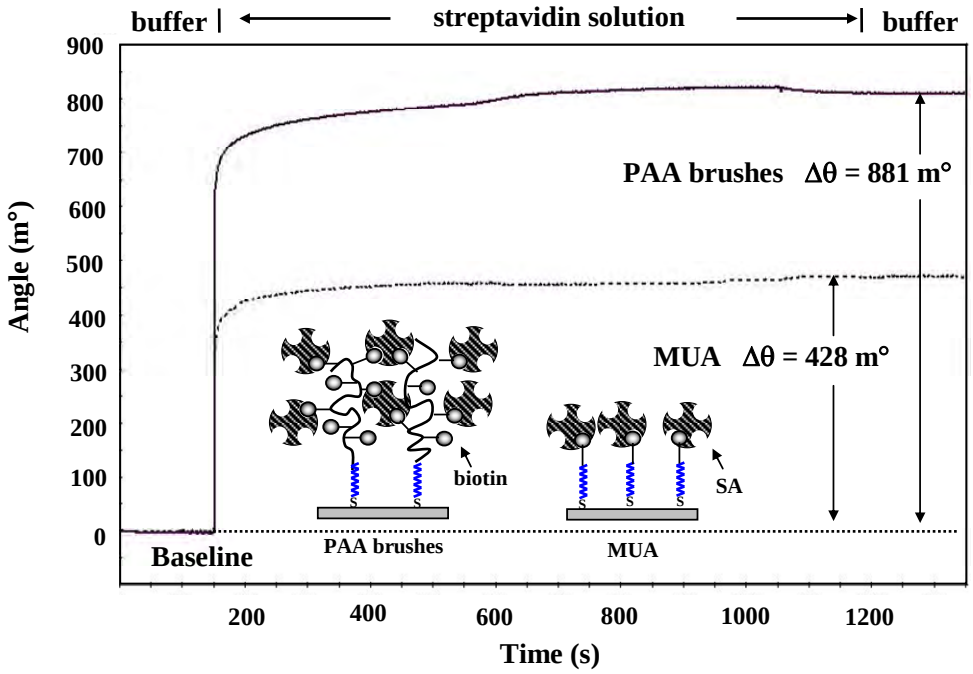

Figure 4.25 Typical SPR sensorgrams of SA binding to biotin immobilized on the PAA brushes having 100% graft density and $\overline{M}_n$ of 30 kD in comparison with that immobilized on MUA.

4.1.7.1.1 Effect of degree of COOH activation

As mentioned in subsection *4.1.6.1*, the increase in degree of COOH group activation yielded a high density of immobilized biotin probe. In the case of PAA brushes, after immobilized sensing probe onto carboxyl group through covalent bond, the polymer chains became less ionizable and not charged due to the replacement of COOH group with the sensing probe. Therefore, the polymer film in the aqueous environment was less swellable upon sensing probe immobilization (shown in Figure 4.13). To determine whether the extent of the carboxyl group activation have any impact on the detectability of target analytes, the biotinylated surfaces based on the PAA brushes having different degree of COOH group activation were used to detect SA molecules. As shown in Figure 4.26, the amount of immobilized biotin apparently increased with the degree of activation. However, the binding capacity of SA to the immobilized biotin was limited at high degree of activation. In principle, the binding

ratio between biotin and SA should be four if all of biotin molecules were bound to SA. The number written above each set of bar graphs in Figure 4.25 indicates the biotin/SA binding ratio. It was found that the biotin/SA binding ratios were significantly greater than the theoretical value indicating that most of the immobilized biotin was not bound to the SA. The biotin/SA binding was found to increase with increasing degree of activation. This may be explained as a result of the limited accessibility of the SA to the immobilized biotin that was embedded inside the inner layer of the polymer brushes**.** Therefore, this result indicated that the extent of the COOH group activation had a strong influence on diffusion of large molecule into the inner of polymer film as a consequence of low swellability of the sensor platform.

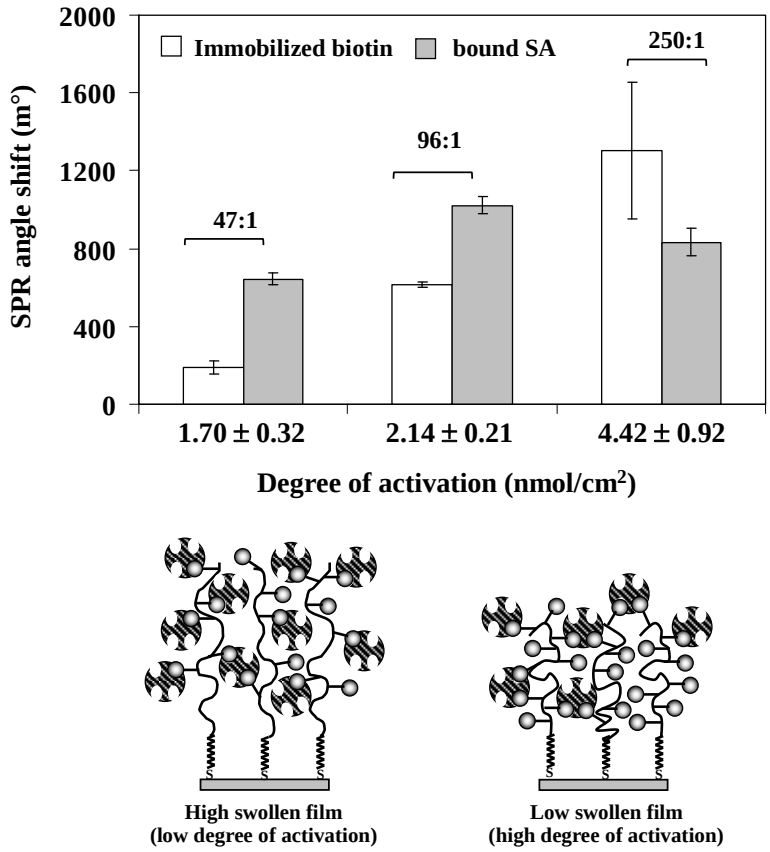

Figure 4.26 SPR angle shift corresponding to the biotin immobilization and subsequent SA binding capacity of the PAA brushes having 100% graft density and $\overline{M}_n$ of 30 kD as a function of degree of COOH activation.

4.1.7.1.2 Effect of polymer chain length

In this section, the relation between the polymer chain length and SA binding capacity was investigated. As demonstrated in the subsection *4.1.6.2*, the amount of attached biotin increased as a function of $\overline{M}_n$. The biotinylated sensor platform developed from the PAA brushes having varied $\overline{M}_n$ of were used to determine the effect of $\overline{M}_n$ on SA binding capacity. As shown in Figure 4.27, the binding capacity of SA increases linearly with increasing molecular weight of the PAA brushes. The increase of SA binding capacity could be rationalized by the increase of biotin density as a consequence of the increase in carboxyl group density along the chain of PAA brushes. These results could represent the nature of 3D in which the target molecules do not just bind to the sensing probe on the surfaces of PAA brushes but can also penetrate and interact with the sensing probe inside the brushes. The saturation of SA binding was reached at $\overline{M}_n$ of 19 KDa suggesting that the access of SA to the immobilized biotin that was embedded inside the inner layer would be sterically screened when the polymer chain is excessively long. The longer brushes may become so crowded that interior biotin is less accessible for SA binding. Similar outcome has also been reported by Lee and coworkers [15], As determined by QCM, they demonstrated that the binding capacity of SA to the biotinylated layer prepared on poly(oligo(ethylene glycol) methacrylate) (*p*OEGMA) brushes was maximized and saturated at the polymer thickness of about 20 nm whereas the binding capacity of biotin was saturated at the polymer thickness of about 110 nm. These results suggested that the amount of biotin probe increased as the increase of the *p*OEGMA film thickness, but the access of SA to some of biotin probes would be sterically screened for the thick polymer film. Therefore, the thickness of polymer film should be optimized in order to achieve the maximum binding specificity/capacity of target molecules. Nevertheless, the effect of steric hindrance at high $\overline{M}_n$ or long chain of polymer brushes can be suppressed by increasing the swelling of polymer brushes in a consequence of the decrease in degree of activation (shown in subsection *4.1.7.1.1*).

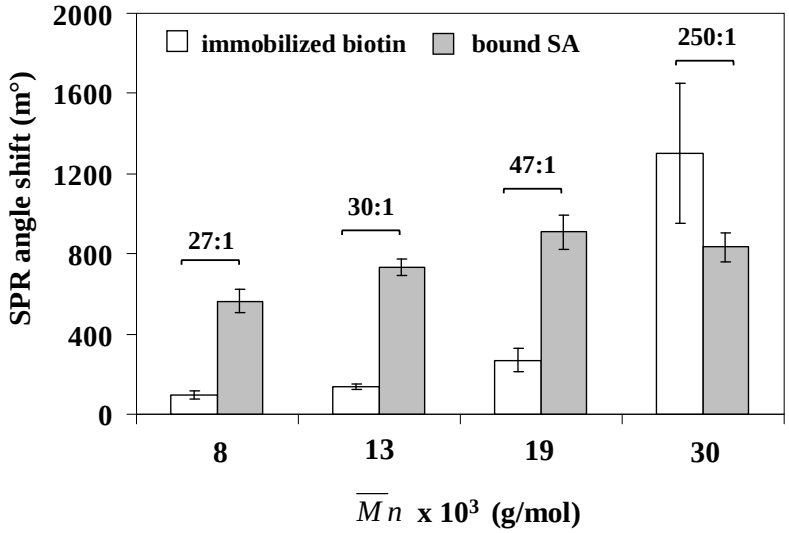

Figure 4.27 SPR angle shift corresponding to the biotin immobilization and subsequent SA binding capacity of the PAA brushes having 100% graft density as a function of their $\overline{M}_n$.

4.1.7.1.3 Effect of graft density

In order to demonstrate the effect of graft density on the analyte detectability, the biotinylated PAA brushes having varied graft density were used to investigate the SA binding capacity as a funtion of graft density. As shown in Figure 4.28, the amount of immobilized biotin increased with the increase in graft density or the amount of carboxyl group. However, the accessibility of SA, which is a large protein, was limited at high graft density of polymer brushes even though more biotin molecules were immobilized. This result implied that most of the immobilized biotin was not bound to SA. Again, this may be caused by steric hindrance effect of SA to some of immobilized biotin in densely packed polymer brushes. Moreover, it is believed that the multiple binding sites of SA for biotin can induce the inter-chain crosslinking of the polymer brushes resulting in low swellability of the polymer layer and limit the accessibility of SA to the immobilized biotin that was embedded inside the inner layer of the polymer brushes. Therefore, the decrease of graft density of polymer chains provided a wider distance of neighboring polymer chains, giving less chance for the crosslinking to occur. This result indicates that the steric hindrance and the tendency to be crosslinked

of the closely packed polymer chains can also be suppressed by reducing the grafting density of the polymer brushes.

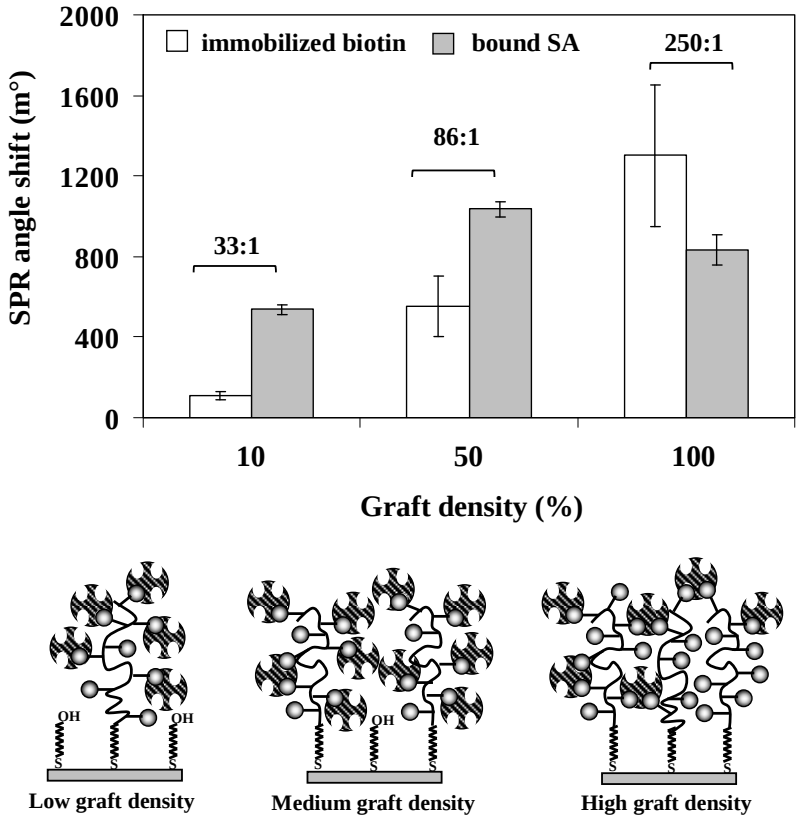

Figure 4.28 SPR angle shift corresponding to the biotin immobilization and subsequent SA binding capacity of the PAA brushes having $\overline{M}_n$ of 30 kD as a function of graft density.

4.1.7.1.4 Specificity of biotinylated surface

The success of a sensor platform cannot be judged only from the biospecific detection of the expected analyte, but it also depends upon the ability to resist adsorption of nonspecific components. Here, the two model proteins, BSA and FIB, that have a similar isoelectric point (pI) to that of the target analyte, SA, were evaluated for non-specific binding of biotinylated surface. The pI of SA, BSA and FIB is 5.0, 4.8 and 5.5, respectively, and so these three proteins should be negatively charged in PBS at pH 7.4. The results shown in Figure 4.29 indicated that the biotinylated surface

obtained from PAA brushes not only have excellent specific binding with SA but also prevent the adsorption of other non-specific proteins. Apparently, the non-specific adsorption of BSA and FIB was much more suppressed on the PAA brushes-biotin than that on the MUA-biotin. This may stem from the hydrophilic nature of the PAA brushes as opposed to the hydrophobic hydrocarbon linker of the MUA. This is a desirable characteristic of the sensing platform. The best performance was found on the PAA brushes having 50% graft density, of which the amount of bound SA was the highest with essentially no non-specific adsorption of other proteins. These results also suggested that the 3D layer of PAA brushes possessed greater binding capacity towards streptavidin (SA) detection as compared with the 2D monolayer of MUA. To quantify the binding specificity of the biotinylated surface, the signal-to-noise (*S*/*N*) ratio determined from the ratio between the amount of bound SA that of the model non-target protein was calculated and shown in Table 4.3. Considering the *S*/*N* ratio, the biotinylated sensor platform developed from the surface-grafted PAA brushes having 50% graft density provided about 33-fold (for BSA) and 29-fold (for FIB) enhancement of *S*/*N* ratio as compared with the biotinylated sensor platform based on MUA.

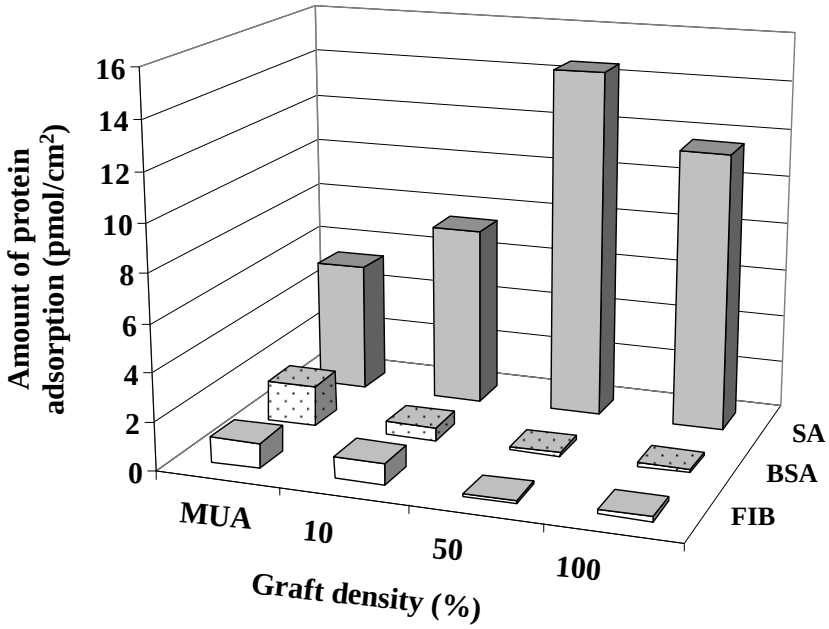

Figure 4.29 Adsorption of proteins at pH 7.4 on biotinylated PAA brushes having $\overline{M}_n$ of 30 kD as a function on graft density in comparison with biotinylated MUA.

Table 4.3 The protein adsorption amount and the signal-to-noise (*S*/*N*) ratio for SA and model protein.

	Substrate							
	MUA		10% PAA		50% PAA		100% PAA	
	pmol/cm^2	*S/N*	pmol/cm^2	*S/N*	pmol/cm^2	*S/N*	pmol/cm^2	*S/N*
SA	5.39±0.20		7.45±0.03		14.55±0.37		11.59±1.02	
BSA	1.70±0.22	3.2	0.56±0.08	16.3	0.14±0.04	103.9	0.13±0.11	89.2
FIB	1.06±0.01	5.1	0.91±0.06	8.2	0.10±0.05	145.5	0.17±0.02	68.2

4.1.7.2 BSA- anti BSA system

The sensor platforms based on BSA immobilized on PAA brushes and MUA surface were subjected for testing the interactions with the BSA-specific counterpart, anti-BSA and with its non-specific proteins, SA and FIB. Figure 4.30 shows a typical SPR response of anti-BSA bound to BSA immobilized sensor surface. As soon as anti-BSA was injected to the sensor surface having BSA molecules, the SPR response dramatically increased representing the specific binding between BSA and anti-BSA. In addition, after treatment with 10 mM NaOH for five minutes and rinsing with PBS, the SPR angle returned to the original baseline, indicating the bound anti-BSA was entirely removed and the regeneration of the sensor platform based on immobilized BSA was successful. In other words, only the bound anti-BSA molecules were removed from the surface, while the immobilized BSA remained intact. The remained BSA immobilized on the SPR disk was capable of rebinding with anti-BSA for the next cycle of anti-BSA detection. The binding capacity of anti-BSA (100 μg/mL) in Figure 4.30 was measured to be 1191 m° (992.5 ng/cm2 or 6.62 pmol/cm2) and 625 m° (520.8 ng/cm2 or 3.47 pmol/cm2) for the PAA brushes-BSA and the MUA-BSA platform, respectively. The calculation is based on MW of 150,000 g/mol for anti-BSA. The results thereby suggested that the layer of PAA brushes possessed greater BSA densities and greater binding capacity towards anti-BSA detection than the monolayer of MUA. This result is in good agreement with the biotin-SA system that PAA brushes possess high functional group density allowing for the great amount of immobilized sensing probe and lead to increased target molecules binding.

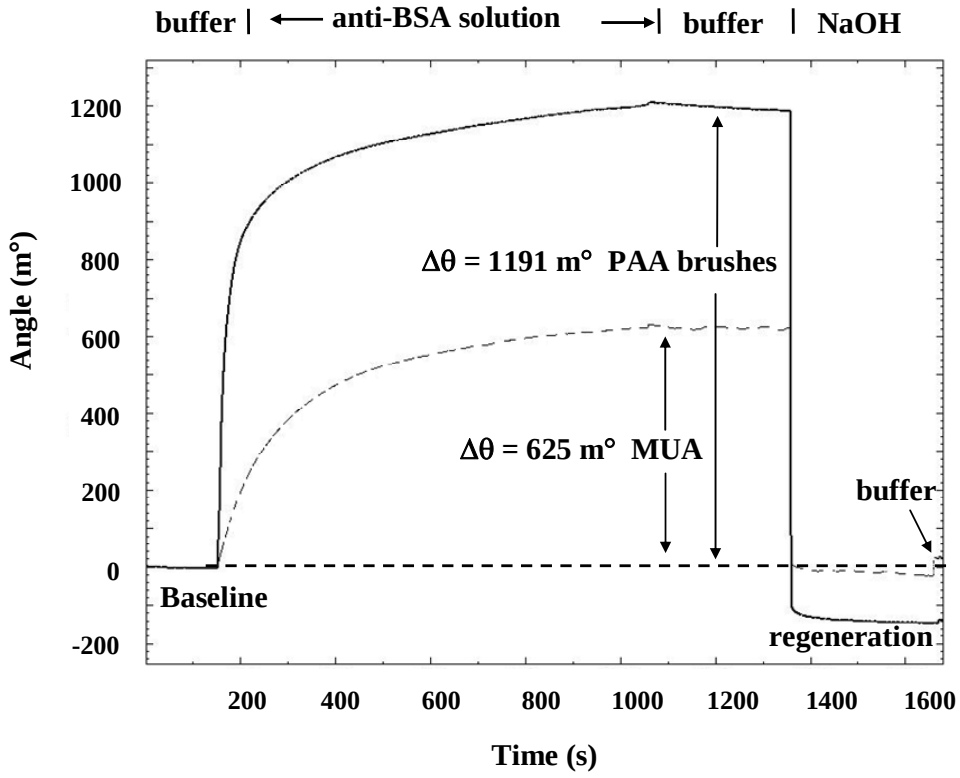

Figure 4.30 Typical SPR sensorgrams of anti-BSA (100 μg/mL) binding to BSA immobilized on the PAA brushes having 100% graft density and $\overline{M}_n$ of 30 kD in comparison with that immobilized on MUA.

4.1.7.2.1 Effect of degree of COOH activation

In this subsection, the determination of whether the extent of the carboxyl group activation would have any impact on the analyte detectability was also investigated. Figure 4.33 shows the comparison of SPR response between immobilized BSA and anti-BSA binding on the surface-tethered PAA brushes having 100% graft density with different degree of activation. It was found that the amount of immobilized BSA and anti-BSA binding decreased with the increase of degree of activation. The binding efficiency of the immobilized BSA with anti BSA is shown in term of the binding ratio between BSA and anti-BSA written above each set of bar graphs in Figure 4.31. In principle, the BSA/anti-BSA binding ratio should be two if all of BSA molecules were bound to anti-BSA. It was found that the BSA/anti-BSA binding ratios were

significantly greater than the theoretical value indicating that most of the immobilized BSA was not bound to the anti-BSA. In addition, the BSA/anti-BSA binding ratio was found to increase with increasing degree of activation. This may be explained as a result of the limited accessibility of a large protein, especially anti-BSA (150 kDa) to the immobilized BSA (69 kDa) that was embedded inside the inner layer of the polymer brushes. This observation follows the same trend as previously described for the system of biotin-SA. The effect was, however, less dramatic considering the size difference between BSA and anti-BSA (69 kDa vs 150 kDa) is much less than that between biotin and SA (0.374 kDa vs 60 kDa).

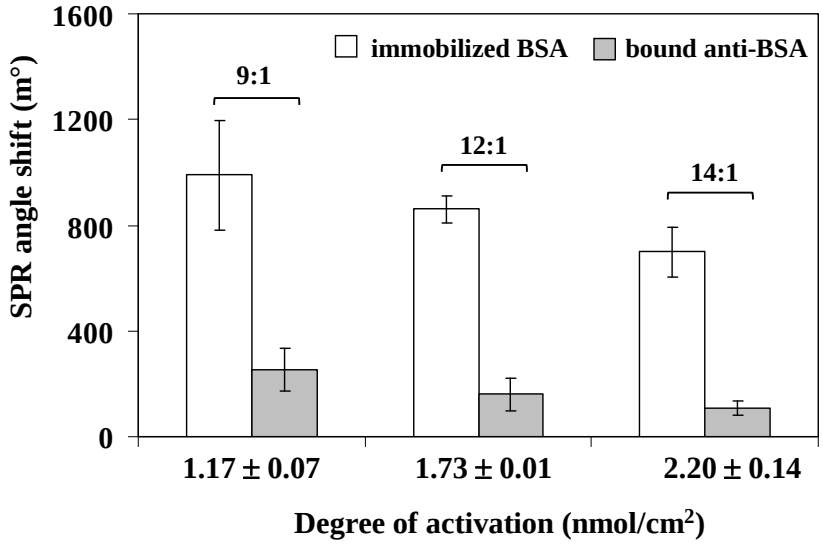

Figure 4.31 SPR angle shift corresponding to the BSA immobilization and subsequent anti-BSA (10 μg/mL) binding capacity of the PAA brushes having 100% graft density and $\overline{M}_n$ of 30 kD as a function of degree of COOH activation.

4.1.7.2.2 Effect of graft density

In order to demonstrate the effect of graft density on the analyte detectability, the BSA immobilized PAA brushes having varied graft density were used to investigate the anti-BSA binding capacity as a funtion of graft density. As shown in Figure 4.32, the amount of both immobilized BSA and anti-BSA binding capacity, which is a large

protein, was limited at high graft density of the polymer brushes. Again, this may be caused by steric hindrance of large protein and inter-chain crosslinking effect in densely packed polymer brushes resulting in the diffusion of large molecule into the inner of polymer film being prohibited. The steric hindrance can also be suppressed by reducing the grafting density of the grafted polymer brushes.

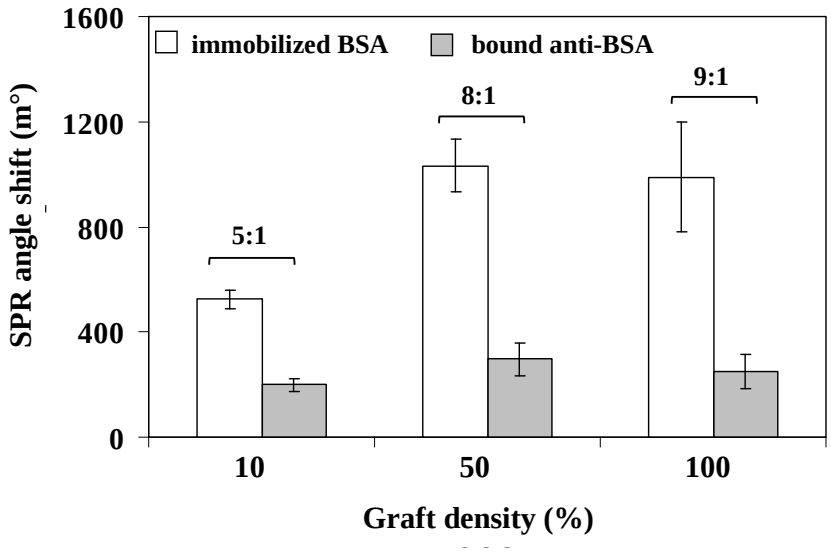

Figure 4.32 SPR angle shift corresponding to the BSA immobilization and subsequent anti-BSA (10 μg/ml) binding capacity of the PAA brushes having $\overline{M}_n$ of 30 kD as a function of graft density.

4.1.7.2.3 Specificity of BSA immobilized surface

Herein, the two model proteins, SA and FIB, were evaluated for non-specific binding of the BSA immobilized surface. The results shown in Figure 4.33 indicated that only the BSA immobilized surface obtained from PAA brushes having 50 and 100% graft density not only had excellent specific binding with anti-BSA but also preventeed the adsorption of other non-specific proteins. On the other hand, the BSA immobilized surface obtained from 10% PAA brushes and MUA surface showed a poor specificity of BSA immobilized surface. This may be caused by the hydrophobic nature of the hydrocarbon linker of the MUA and the low graft density of PAA brushes

resulting in high amount of non-specific protein adsorption. The best performance was found on the PAA brushes having 50% graft density, of which the amount of bound anti-BSA was the highest with essentially no non-specific adsorption of other proteins. These results also implied that the 3D layer of PAA brushes possessed greater binding capacity towards anti-BSA detection as compared with the 2D monolayer of MUA and subsequently should provide a high detection limit of sensor. Table 4.4 shows the *S*/*N* ratio of the BSA sensor platform. It was found that the BSA sensor platform developed from the surface-grafted PAA brushes having 50% graft density provided about 10-fold (for SA) and 9.5-fold (for FIB) enhancement of *S*/*N* ratio as compared with the biotinylated sensor platform based on MUA

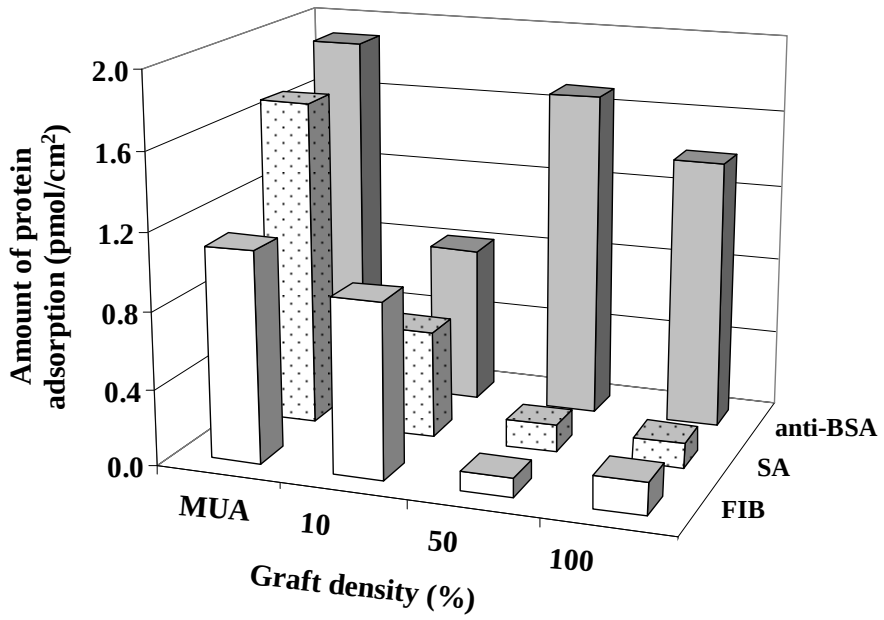

Figure 4.33 Adsorption of proteins at pH 7.4 on BSA immobilized PAA brushes having $\overline{M}_n$ of 30 kD as a function of graft density in comparison with BSA immobilized MUA.

Table 4.4 The protein adsorption amount and the signal-to-noise (*S*/*N*) ratio for anti-BSA and model protein.

	Substrate							
	MUA		10% PAA		50% PAA		100% PAA	
	pmol/cm^2	*S/N*	pmol/cm^2	*S/N*	pmol/cm^2	*S/N*	pmol/cm^2	*S/N*
anti-BSA	1.96±0.44		0.82±0.14		1.71±0.48		1.40±0.45	
SA	1.69±0.22	1.2	0.56±0.08	1.5	0.14±0.04	12.2	0.13±0.11	10.8
FIB	1.06±0.01	1.8	0.91±0.06	0.9	0.10±0.05	17.1	0.17±0.02	8.2

4.1.7.2.4 Limit of detection (LODs)

The sensor platform giving the best performance, the BSA immobilized PAA brushes having 50% graft density, was used to determine the lowest detectable concentration of anti-BSA in comparison with the BSA immobilized MUA surface. Figure 4.34 shows that the working range of BSA immobilized 50% PAA brushes was narrowed down to the lowest concentration of 0.1 μg/mL (equivalent to 0.67 nM) anti-BSA while the lowest detectable concentration of anti-BSA in the case of BSA immobilized MUA surface was 1 μg/mL (equivalent to 6.7 nM). Thus, the BSA immobilized PAA brushes provide 10-fold of magnitude lower detection limit than the BSA immobilized MUA surface. However, it should be noted that these experiments were performed with one specific component in the absence of the non-specific proteins.

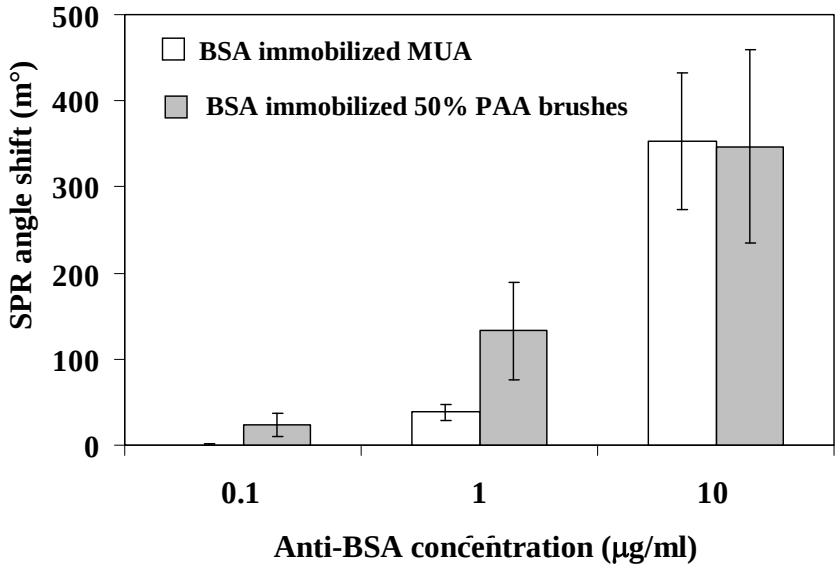

Figure 4.34 SPR angle shift corresponding to anti-BSA binding capacity of the BSA immobilized 50% PAA brushes having $\overline{M}_n$ of 30 kD and BSA immobilized MUA surface as a function of anti-BSA concentration.

4.1.7.2.5 Reusability of the BSA immobilized sensor platform

According to the success of the regeneration of the sensor platform based on immobilized BSA as presented in at the beginning of section 4.1.7.2, the stability of the sensor prepared from BSA immobilized 50% PAA brushes was evaluated by observing the specific binding with anti-BSA at the concentration of 10 μg/ml at every measurement cycles of anti-BSA detection after treatment with 10 mM NaOH until the 10^{th} cycle. Up to 5 cycles of regeneration, it was found that the SPR angle of every measurement cycles returned to the original baseline showing the completion of the regeneration. However, a progressive loss of anti-BSA binding signal (Figure 4.35) was observed after 6 cycles of measurement. This result may be caused by the denaturation of BSA by NaOH indicating that this sensor platform retained the stability and the reproducibility for at least up to 6 cycles.

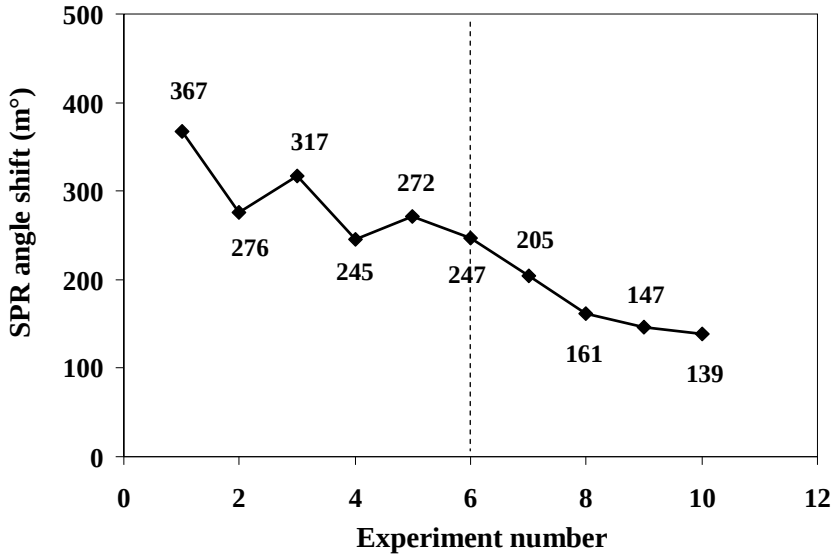

Figure 4.35 SPR angle shift obtained from the specific binding between surface-immobilized BSA with anti-BSA after 10 consecutive cycles of anti-BSA detection after regeneration by NaOH treatment.

4.2 Preparation of surface-tethered copolymer brushes of poly[(methacrylic acid)-*ran*-(2-methacryloyloxyethyl phosphorylcholine)] (PMAMPC) by "grafting to" method

4.2.1 Preparation of PMAMPC by RAFT polymerization

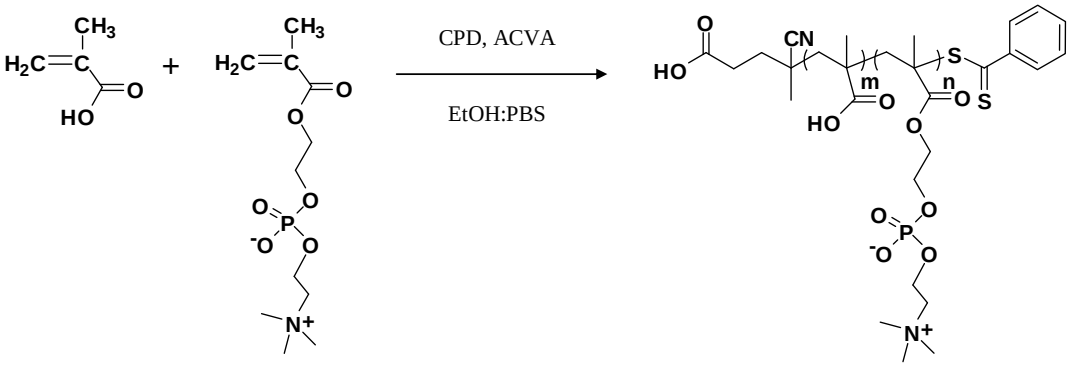

Figure 4.36 Synthetic pathway of PMAMPC by RAFT polymerization.

Reversible addition-fragmentation chain transfer (RAFT) is a controlled free radical polymerization process that should produce a well-defined co(polymer) with narrow polydispersity indices. Due to the inertness of the process to protic solvents such as water, functional (co)polymers can be prepared directly in aqueous media. The synthesis of poly[(methacrylic acid)-*ran*-poly(2-methacryloyloxyethyl phosphorylcholine)] (PMAMPC) copolymer using RAFT polymerization was carried in the presence of 4-cyanopentanoic acid dithiobenzoate (CPD) and 4,4'-azobis(4-cyanovaleric acid) (ACVA) as a chain transfer agent (CTA) and radical initiator, respectively.

Table 4.5 gives an overview of the reaction conditions and the molecular weight information of copolymers prepared by RAFT polymerizations under different conditions. A ratio of CTA/initiator or [CTA]/[I] of 4/1 was fixed, while the ratio of monomer/CTA and copolymer ratio were varied. The data in Table 4.5 shows that the copolymer composition determined by ^{1}H NMR closely resembles the copolymer ratio in the feed. In other words, the copolymer composition can be controlled by varying the mole fraction of monomer in feed. The molecular weight ($\overline{M}_n$) increased with an increase of monomer/CTA ratios and polymerization time. In addition, a controlled character of this polymerization can also be realized from the data shown in Figure 4.37 and 4.38. Figure 4.37 shows the relationship between the $\overline{M}_n$ and the conversion of PMAMPC copolymer. The $\overline{M}_n$ of the copolymer increased linearly as a function of monomer conversion for both monomer/CTA ratios of 50 and 200. The fact that the molecular weight distribution (PDI) is close to 1 indicates that the polymerization is living and can be well controlled. Figure 4.38 demonstrates the RAFT kinetics of MA and MPC. The semilogarithmic plot indicates that the polymerization is first order with respect to MA and MPC comonomer. The linearity of the first order plot of the monomer concentration implies that the concentration of polymer radical remains constant for the duration of the polymerization. The $\overline{M}_n$ increment with reaction time and the narrow PDI were also confirmed by GPC trace (Figure 4.39). The composition of MA and MPC unit in the copolymer, PMAMPC is designated as x and y, respectively. The copolymer identity is then written as PMA_xMPC_y.

Table 4.5 Summary of reaction conditions and molecular weight information of PMAMPC copolymers synthesized by RAFT polymerization.

entry	copolymer ratio in feed (%)		monomer: CTA (mole ratio)	copolymer composition (%)		time (h)	$\overline{M}_n$ (x 10^3)	$\overline{M}_w$ (x 10^3)	PDI
	MA	MPC		MA	MPC				
1	30	70	50	25	75	2	10.8	14.4	1.33
2	30	70	50	26	74	8	24.7	30.1	1.21
3	30	70	200	21	79	8	49.8	61.5	1.24
4	50	50	50	39	61	2	12.0	14.9	1.24
5	50	50	50	39	61	8	25.9	31.5	1.21
6	50	50	200	37	63	8	54.5	67.0	1.23
7	70	30	50	55	45	2	6.60	11.3	1.69
8	70	30	50	57	43	8	29.3	35.4	1.21
9	70	30	200	66	34	8	49.5	61.3	1.24

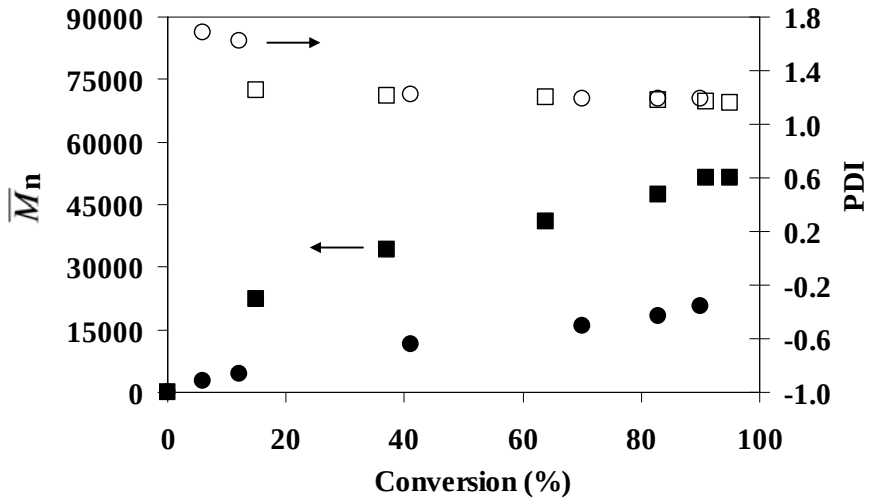

Figure 4.37 Molecular weight ($\overline{M}_n$) (●,■) and PDI (○,□) of the $PMA_{50}MPC_{50}$ determined by GPC as a function of the monomer conversion: a monomer/CTA ratio of 50 (●,○) or 200 (■,□).

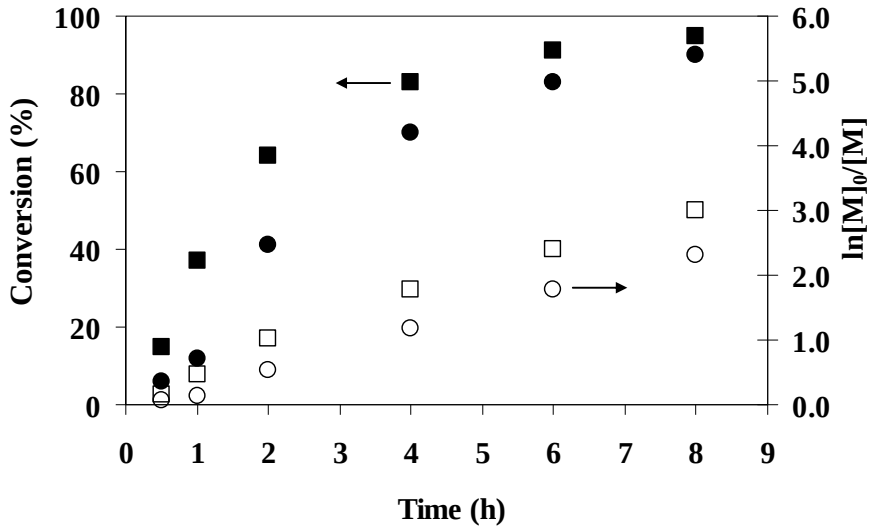

Figure 4.38 Percentage of conversion and semi-logarithmic plots of monomer conversion as a function of time: a monomer/CTA ratio of 50 (●,○) or 200 (■, □).

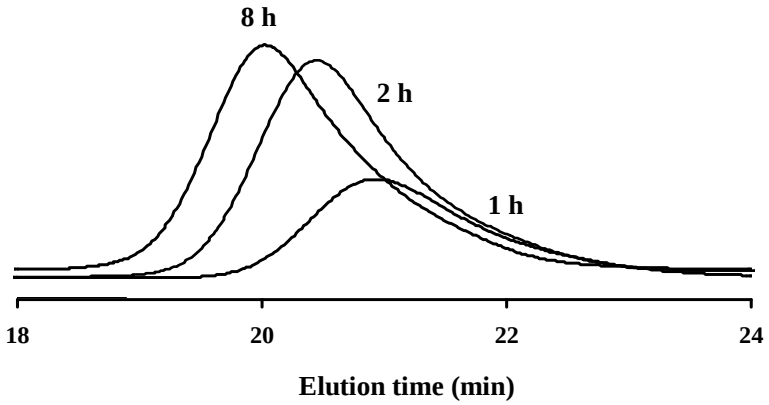

Figure 4.39 GPC traces of $PMA_{50}MPC_{50}$ prepared from a monomer/CTA ratio of 50 as a function of polymerization time.

The success of PMAMPC synthesis was also confirmed by ^{1}H NMR and FT-IR analyses as shown in Figure 4.40 and 4.41, respectively. The characteristic ^{1}H NMR peak of the MPC unit (-N($C\underline{H}_3$)$_3$ = 3.15 ppm, -$C\underline{H}_2$N =3.53ppm, and -POC$\underline{H}_2C\underline{H}_2$N – COOC$\underline{H}_2$ –$CH_2C\underline{H}_2$OP = 4.0-4.3 ppm) was clearly observed. The peak intensity at 3.15 ppm attributed to the –N(CH_3)$_3$ proton of the MPC unit and at 0.60-1.40 ppm attributed

to CH_3 proton of both MPC and MA units were used to calculate the copolymer composition.(Table 4.5). Moreover, the aromatic proton attributed to the dithiobenzoate group at the chain end of PMAMPC was also observed around 7.4-8.2 ppm. The characteristic absorption bands of both MPC unit (C=O (ester) = 1725 cm^{-1}, C-O = 1246 cm^{-1}, P-O = 1087 cm^{-1}, and $–N^+(CH_3)_3$ = 972 cm^{-1}) and MA unit (C=O (acid) = 1725 cm^{-1}, OH = 2500-3500 cm^{-1}, and C-O = 1184 cm^{-1}) appeared clearly in the FT-IR spectrum of the PMAMPC copolymer (Figure 4.41).

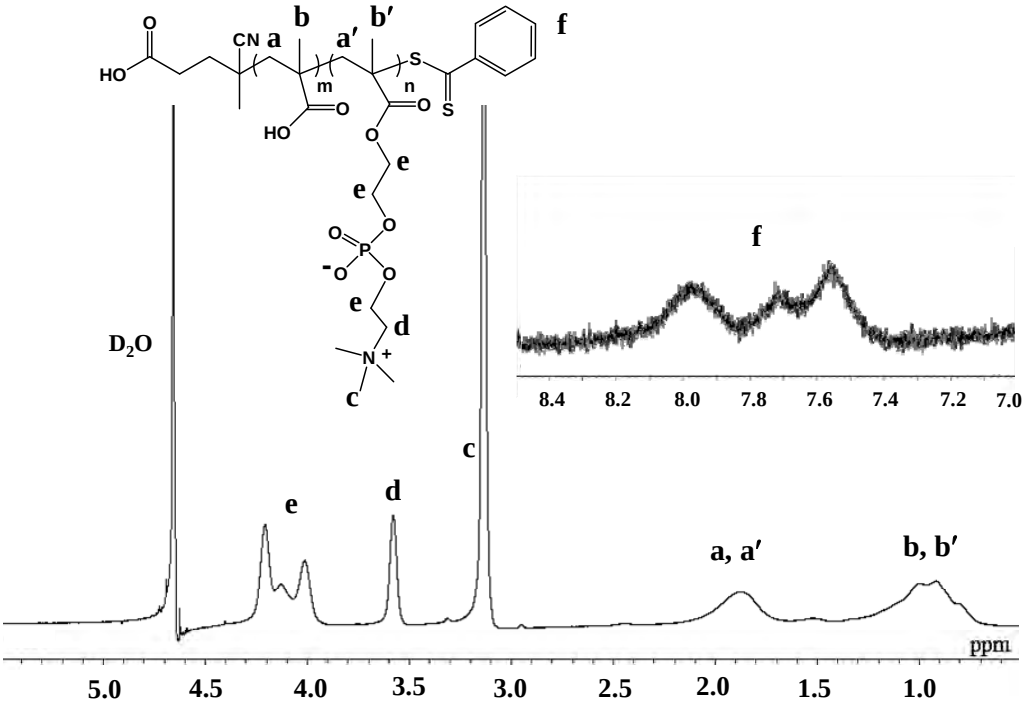

Figure 4.40 ^{1}H NMR spectrum of $PMA_{39}MPC_{61}$ having $\overline{M}_n$ of 25.9 kD.

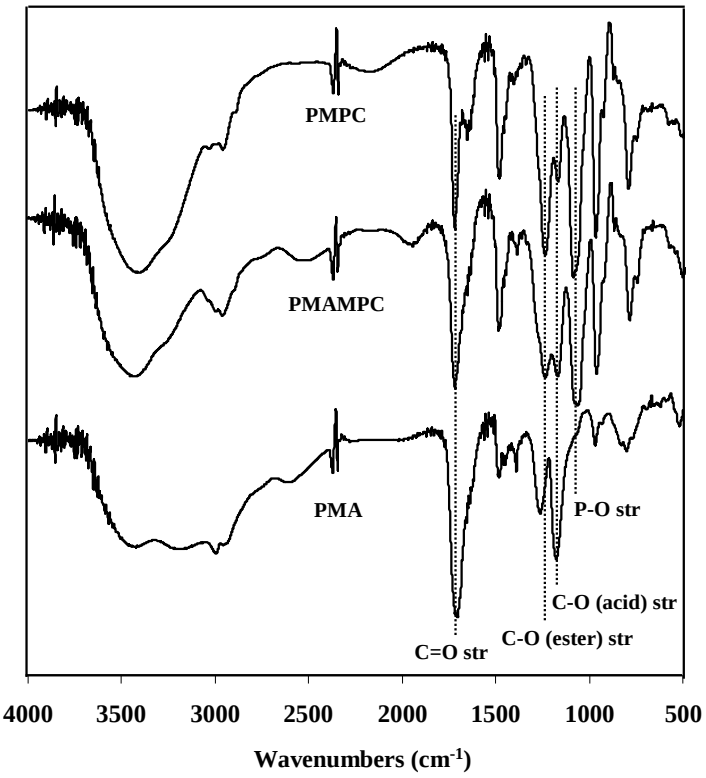

Figure 4.41 FT-IR spectra of PMPC (5.45 kDa), $PMA_{39}MPC_{61}$ (25.9 kDa), and PMA (21.3 kDa).

4.2.2 Preparation of thiol-terminated PMAMPC (PMAMPC-SH)

The dithiobenzoate group at the chain end of PMAMPA prepared by RAFT polymerization can be converted to a thiol group by aminolysis using either primary or secondary amine [29-32]. The success of thiol-terminated PMAMPC (PMAMPC-SH) preparation was confirmed by ^{1}H NMR (Figure 4.42) and UV-vis (Figure 4.43) analysis. As shown in Figure 4.42, the disappearance of aromatic proton peaks around 7.4 - 8.2 ppm after aminolysis indicated that the dithiobenzoate group at the chain end of PMAMPC was removed by aminolysis yielding PMAMPC-SH having terminal thiol group. The UV absorption data also confirmed the disappearance of dithiobenzoate group at 305 nm. The GPC trace of $PMA_{39}MPC_{61}$ before and after hydrolysis shown in Figure 4.44 has demonstrated that the molecular weight characteristic remained almost unchanged with a unimodal distribution. No bimodal distribution was observed implying that PMAMPC-S-S-PMAMPC which may occur as a result of disulfide

coupling did not form. The data shown in Table 4.6 indicate that the molecular weight characteristics of all copolymers were not changed suggesting that hydrolysis did not cause any degradation and/or coupling. The $PMA_{39}MPC_{61}$, before and after hydrolysis, was also characterized by FT-IR. As illustrated in Figure 4.45, the chemical structure of $PMA_{39}MPC_{61}$ polymer backbone was not changed after aminolysis.

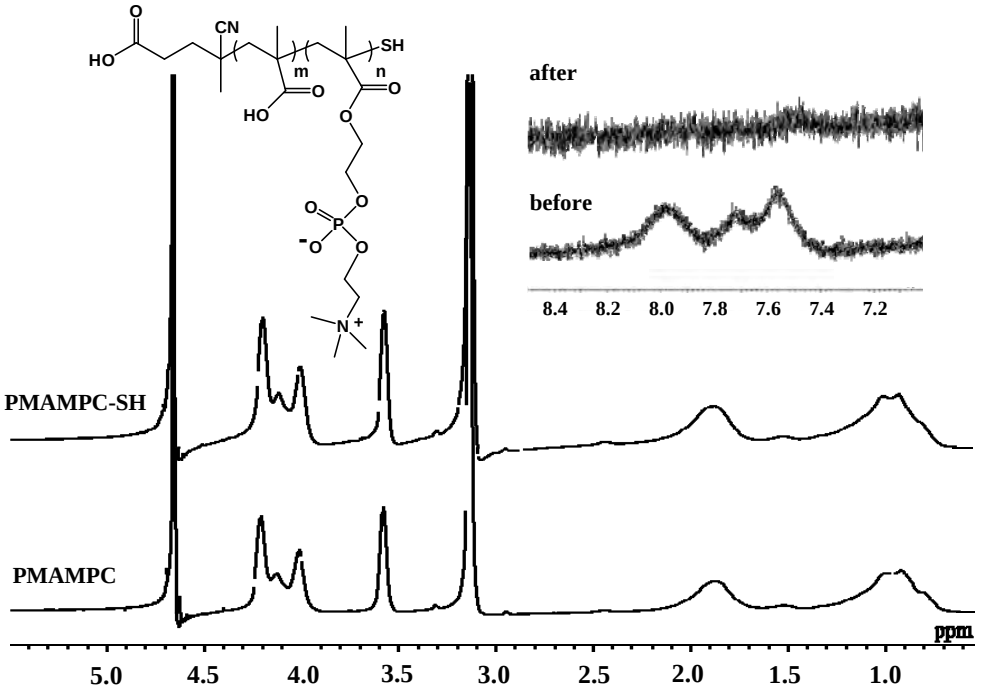

Figure 4.42 ^{1}H NMR spectrum for $PMA_{39}MPC_{61}$ (25.9 kDa) copolymer before and after aminolysis.

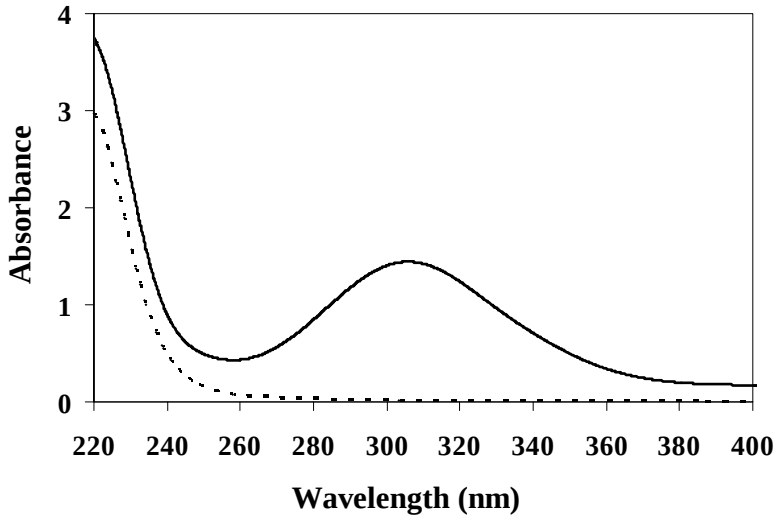

Figure 4.43 UV-vis absorption spectra for $PMA_{39}MPC_{61}$ (25.9 kDa) before (—) and after (---) aminolysis.

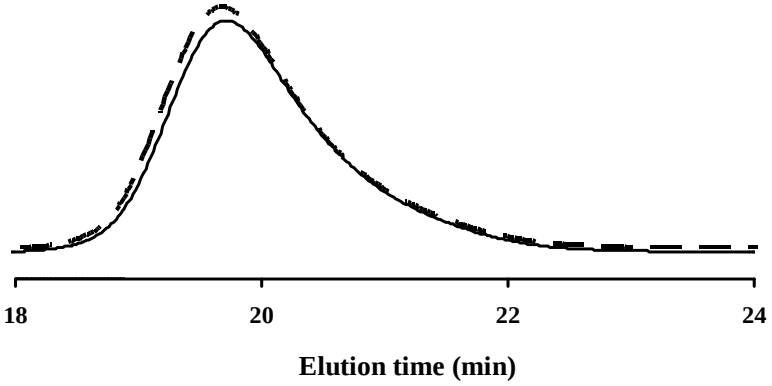

Figure 4.44 GPC trace for $PMA_{39}MPC_{61}$ (25.9 kDa) before (—) and after (---) aminolysis.

Table 4.6 Molecular weight and PDI of PMAMPC copolymer before and after aminolysis.

entry	sample	$\overline{M}_n$ (x 10^3)		$\overline{M}_w$ (x 10^3)		PDI	
		before	after	before	after	before	after
1	$PMA_{25}MPC_{75}$	10.8	12.1	14.4	15.6	1.33	1.28
2	$PMA_{26}MPC_{74}$	24.7	25.1	30.1	30.5	1.21	1.21
3	$PMA_{21}MPC_{79}$	49.8	49.3	61.5	61.4	1.24	1.24
6	$PMA_{37}MPC_{63}$	54.5	53.7	67.0	66.1	1.23	1.22
9	$PMA_{66}MPC_{34}$	49.5	49.1	61.3	60.9	1.24	1.24

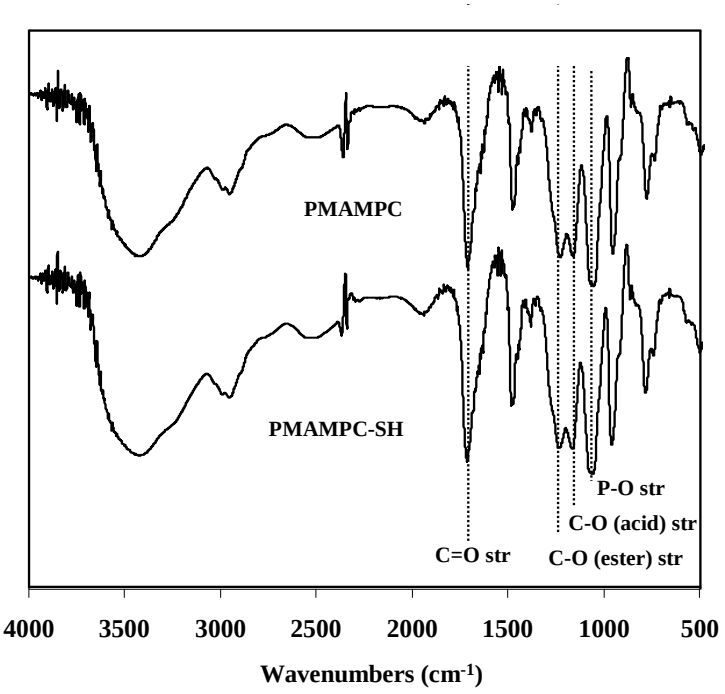

Figure 4.45 FT-IR spectra of $PMA_{39}MPC_{61}$ and $PMA_{39}MPC_{61}$-SH.

4.2.3 Preparation of PMAMPC brushes on gold-coated SPR disk

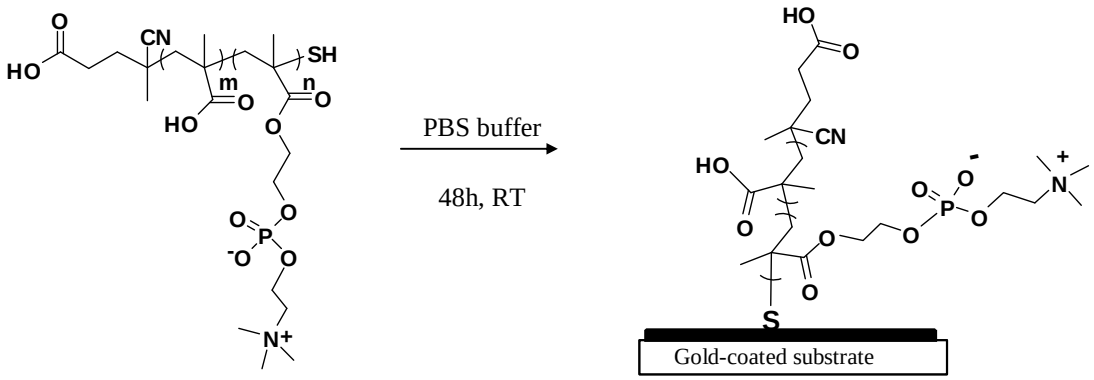

Figure 4.46 Self-assembly of PMAMPC-SH on gold-coated SPR disk.

The thiol-terminated polymer chain promotes the rapid covalent attachment on gold surface by the gold-sulfur bonds (Au-S) with a high affinity. This process, a so-called grafting-to method, provides the formation of polymer brushes on the gold surface [30,36,38]. In this research, a freshly cleaned gold-coated SPR disk was immersed in the PMAMPC-SH solution and the physically adsorbed copolymer was removed by rinsing with copious amount of surfactant. The presence of PMAMPC brushes on the gold-coated SPR disk was verified by XPS and water contact angle measurements. Figure 4.47 shows the XPS spectra of the gold-coated SPR disk that was adsorbed with $PMA_{21}MPC_{79}$ (49.8KDa) and $PMA_{21}MPC_{79}$-SH (49.3KDa) as compared with the substrate before adsorption (bare gold). Determined at a take-off angle of 15^{o}, phosphorus (P_{2p}) and nitrogen (N_{1s}) signals attributed to the phosphorylcholine group of the MPC units were only observed on the disk adsorbed with the thiol-terminated copolymer ($PMA_{21}MPC_{79}$-SH) indicating that the copolymer itself cannot be strongly bound to the gold-coated SPR disk unless being modified with the thiol group. Should there be weakly physical binding of the copolymer on the gold surface, it would be removed upon rinsing with the surfactant. The signal from S_{2p} at a binding energy of 161 eV was strongest on the substrate adsorbed with $PMA_{21}MPC_{79}$-SH. The fact that there were peaks corresponding to S_{2p} appearing on the unmodified disk and that was adsorbed with $PMA_{21}MPC_{79}$ implied that there may be trace amount of sulfur-

containing small molecule contaminant that cannot be completely removed after polymerization and aminolysis.

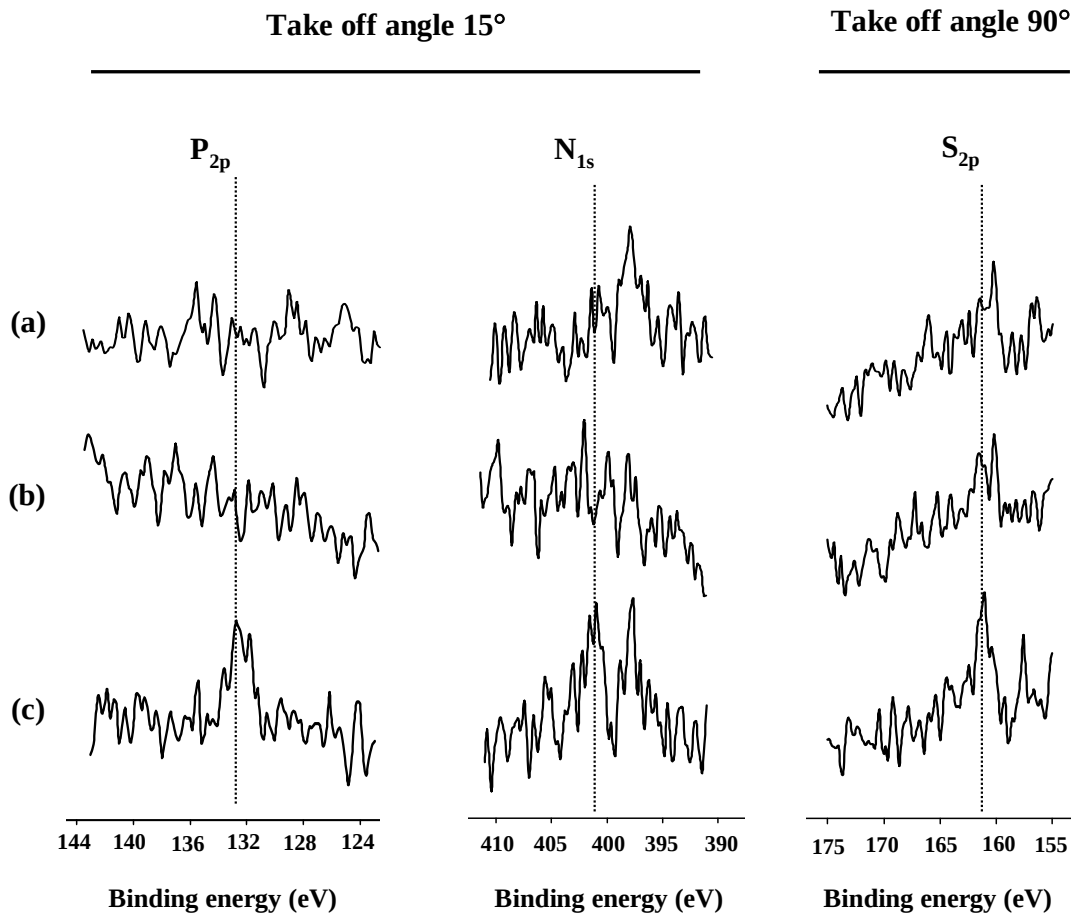

Figure 4.47 XPS spectra of the gold-coated SPR disks: (a) bare gold, and after adsorbed with (b) $PMA_{21}MPC_{79}$ (49.8 kDa) and (c) $PMA_{21}MPC_{79}$-SH (49.3 kDa).

The wettability of the gold-coated SPR disks after being adsorbed with the copolymer, PMAMPC-SH and the homopolymer counterparts, PMA-SH and PMPC-SH was determined by water contact angle analysis. The data shown in Table 4.7 evidently indicates that the thiol-terminated copolymer and homopolymers can successfully be grafted on the surface of SPR disks via grafting-to method. Extremely hydrophilic characteristic of the surface-grafted PMPC can be realized from its low θ_A/θ_R. The high composition of PMPC (79%) in the copolymer, thus made the surface-grafted PMAMPC very hydrophilic as well especially when compared with the surface-

grafted PMA. This should be desirable feature for biosensing applications in term of the ability to prevent non-specific interactions. The lower water contact angle of the gold-coated SPR disk after exposure to the non-thiolated $PMA_{21}MPC_{79}$ suggested that there may be non-specific adsorption. This observation is in accordance with the XPS data previously shown.

Table 4.7 Water contact angle of surface-modified and gold-coated SPR disk.

Sample	$\overline{M}_n$ (x 10^3)	θ_A (deg)	θ_R (deg)
Bare gold		100 ± 5.3	80 ± 7.1
$PMA_{21}MPC_{79}$	49.8	70 ± 4.8	30 ± 5.7
$PMA_{21}MPC_{79}$-SH	49.3	26 ± 2.1	13 ± 2.7
PMPC-SH	5.45	22 ± 4.4	10 ± 2.3
PMA-SH	21.3	66 ± 5.3	27 ± 8.5

Additional evidence of the success in surface grafting of PMAMPC brushes on the gold-coated SPR disk can also be seen from AFM image. To prepare a sample for AFM analysis, half of the disk was covered by a mask before being immersed in the copolymer solution. The presence of the surface-grafted copolymer can be seen from the AFM images shown in Figure 4.48. The height image and the cross sectional view of the surface grafted $PMA_{21}MPC_{79}$ (49.3K) are shown on the left and right side, respectively The thickness of the polymer film can be obtained from the section analysis and used for the calculation of graft density (σ) using eq 4.2 and mass density of 1.3 g/cm^3 for PMAMPC. Although the thickness of the PMAMPC brushes increased with increasing $\overline{M}_n$, the graft density was inversely proportional to $\overline{M}_n$. This is not surprising considering that the grafting-to method usually suffers the entropic barrier due to the crowding of the initial grafting polymer chains that prevent further insertion of the polymer. And such limitation becomes even more problematic for polymer having high molecular weight. Nonetheless, the graft density of surface-grafted

PMAMPC brushes ranged from 0.13 ± 0.02 to 0.27 ± 0.07 chains/nm^2 for $\overline{M}_n$ from 49.3KDa to 12.1KDa, respectively (Figure 4.49). These values still fall within an extended brush regime (graft density > 0.08 chains/nm^2) [47] suggesting that the PMAMPC brushes with reasonable graft density can be formed despite the fact that the preparation was based on grafting-to method. In the case of PMAMPC brushes having different copolymer composition, the graft density was assumed to be the same considering that their $\overline{M}_n$ are comparable.

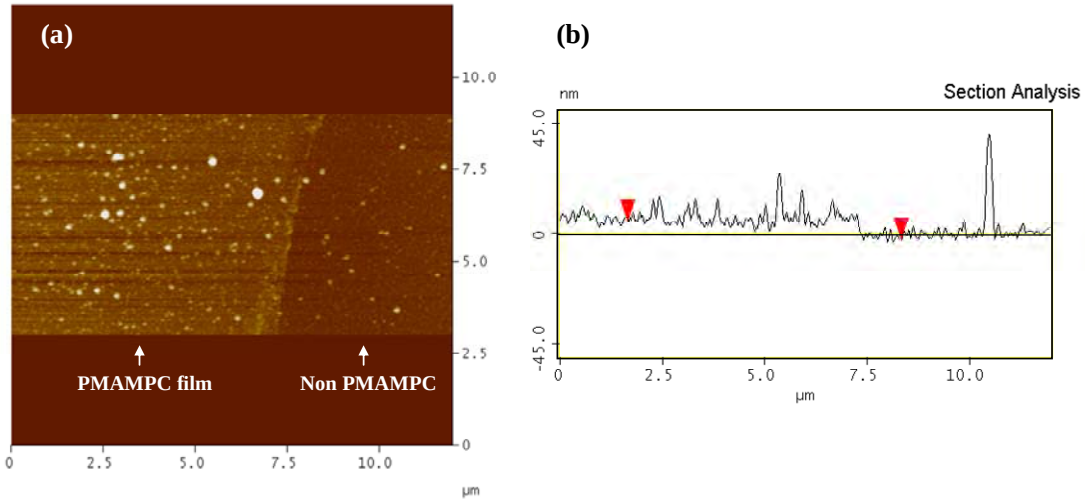

Figure 4.48 AFM images of PMAMPC brushes grafted on gold-coated SPR disk: (a) height image and (b) cross section profile.

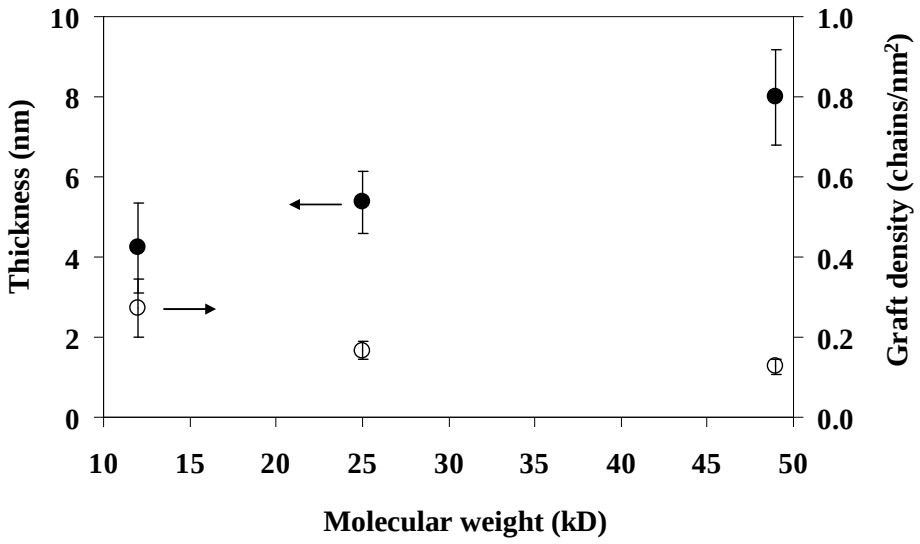

Figure 4.49 Thickness and graft density of the surface-grafted PMAMPC-brushes having varied molecular weight.

The graft density values can be used for calculating the number of MA and MPC units on the surface which is assigned as N (unit/nm^2) using the following equations:

$$N = repeat\ unit\ \times\ \sigma \tag{4.3}$$

$$repeat\ unit\ of\ MA = a\left[\ \frac{Mn}{a(F_{W\,MA}) + b(F_{W\,MPC})}\ \right] \tag{4.4}$$

$$repeat\ unit\ of\ MPC = b\left[\ \frac{Mn}{a(F_{W\,MA}) + b(F_{W\,MPC})}\ \right] \tag{4.5}$$

Where σ is the graft density of PMAMPC brushes, a is the percentage of MA units in copolymer, b is the percentage of MPC units in copolymer, $F_{W\,MA}$ is the molecular weight of MA monomer (81.6 g/mol), and $F_{W\,MPC}$ is the molecular weight of MPC monomer (295.3 g/mol). Table 4.8 lists the number of MA and MPC units on the

surface that was grafted with PMAMPC brushes. It is obvious that the number of MA and MPC unit on the surface increased with increasing $\overline{M}_n$ despite the lower graft density. Moreover, it was found that the number of MA and MPC units on surface can be controlled by varying copolymer composition of the PMAMPC brushes.

Table 4.8 Calculated graft density, repeat unit, and number of MA and MPC units of the surface-grafted PMAMPC brushes.

sample	σ (chains/nm^2)	Repeat unit		N (unit/nm^2)	
		MA	MPC	MA	MPC
$PMA_{25}MPC_{75}$ 12.1K	0.27 ± 0.07	12	38	3.24	10.26
$PMA_{26}MPC_{74}$ 25.1K	0.17 ± 0.02	27	77	4.59	13.09
$PMA_{21}MPC_{79}$ 49.3K	0.13 ± 0.02	41	156	5.33	20.28
$PMA_{37}MPC_{63}$ 53.7K	0.13 ± 0.02	103	156	13.39	20.28
$PMA_{66}MPC_{34}$ 49.1K	0.13 ± 0.02	210	105	27.3	13.65

Figure 4.50 and 4.51 show the water contact angles of the surface-grafted PMAMPC brushes with different $\overline{M}_n$ and copolymer composition, respectively. The fact that water contact angles (both θ_A and θ_R) decreased with increasing $\overline{M}_n$ agrees with the data shown in Table 4.8 that the copolymer with high $\overline{M}_n$ contained greater number of hydrophilic MPC units. A similar explanation can also be applied in the case where the water contact angles were lower as the greater content of MPC units were incorporated in the copolymers (Figure 4.51).

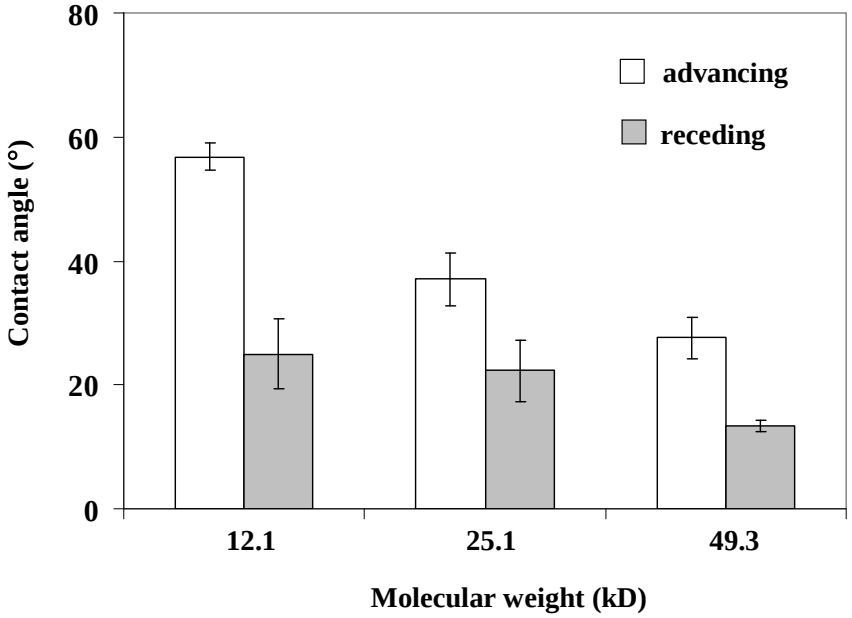

Figure 4.50 Water contact angle data of the surface grafted PMAMPC having different $\overline{M}_n$ on gold-coated SPR disk.

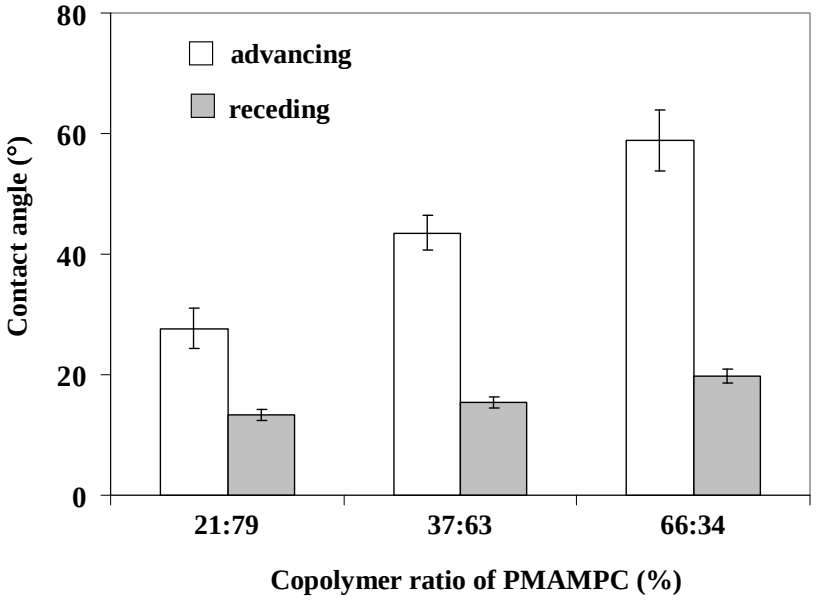

Figure 4.51 Water contact angle data of the surface grafted PMAMPC having different copolymer composition expressed in term of MA:MPC unit on gold-coated SPR disk.

4.2.4 Protein adsorption of the PMAMPC brushes grafted on gold-coated SPR disk

Selectivity of sensor or measurement platforms for target molecules plays an important role for successful biosensor development. In order to achieve specific recognition for target molecules, the covalent attachment of active biomolecules, a so-called sensing probe, such as protein, antibody, enzyme, and DNA has been immobilized to sensor surface [1-3]. However, the resistance of non-specific adsorption of sensor surface is also important. Non-specific adsorption leads to undesirable features such as high background noise or low signal-to-noise ratio (*S/N*) [4-5]. Thus, a good sensor platform should not only allow for covalent immobilization of sensing probe but also resist non-specific adsorption especially in the complex matrices such as blood plasma and clinical sample. In this study, the efficiency of PMAMPC brushes to act as a sensor platform for biosensing applications in term of *S/N* ratio was demonstrated by using surface plasmon resonance (SPR) technique.

The ability to resist the non-specific adsorption of proteins is an important aspect of sensor platform for detecting the specific protein interactions in complex samples. Firstly, the non-specific protein adsorption of PMAMPC was investigated against BSA (60 kDa), AVD (66 kDa), and human blood plasma as compared with the substrates of bare gold and MUA. The pI of BSA and AVD is 4.8 and 10.5, respectively. This implies that BSA has negative charges in PBS solution having pH 7.4, while AVD has positive charges. Blood plasma representing a complex matrix is a yellow liquid component of blood containing hundreds of dissolved proteins such as albumin, fibrinogen, and globulin for about 7% (70 mg of proteins per milliliter of plasma) and other component such as water, inorganic ion, and organic substances.

The results illustrated in Figure 4.52 indicate that the surface-grafted PMPC and PMAMPC brushes on gold-coated SPR disk can completely resist non-specific adsorption of BSA (negatively charged protein), AVD (positively charged protein) as well as the multi-component proteins in blood plasma as opposed to that of the bare gold and MUA surface. On the other hand, the surface-grafted PMA brushes could only prevent the adsorption of negatively charged protein, BSA, but was extensively suffered from the non-specific adsorption of positively charged protein, AVD and the multi-

component proteins in blood plasma. The electrostatic binding with the positively charged protein was similar to what has been previously observed on the system of the surface-grafted PAA brushes. The pKa of the PMA is reported to be 6.9-7.0 [69]. These results strongly indicated that the MPC units in the PMAMPC copolymer brushes play an important role in preventing the non-specific protein adsorption. This is in excellent agreement with many reports previously published on the fact that PMPC exhibits an excellent resistance to non-specific interactions with plasma protein and cells [72-73]. In particular, the random copolymer brushes of MPC and GMA (glycidyl methacrylate) also showed that the introduction of MPC units in the polymer brushes is effective in reducing the non-specific adsorption of proteins [74].

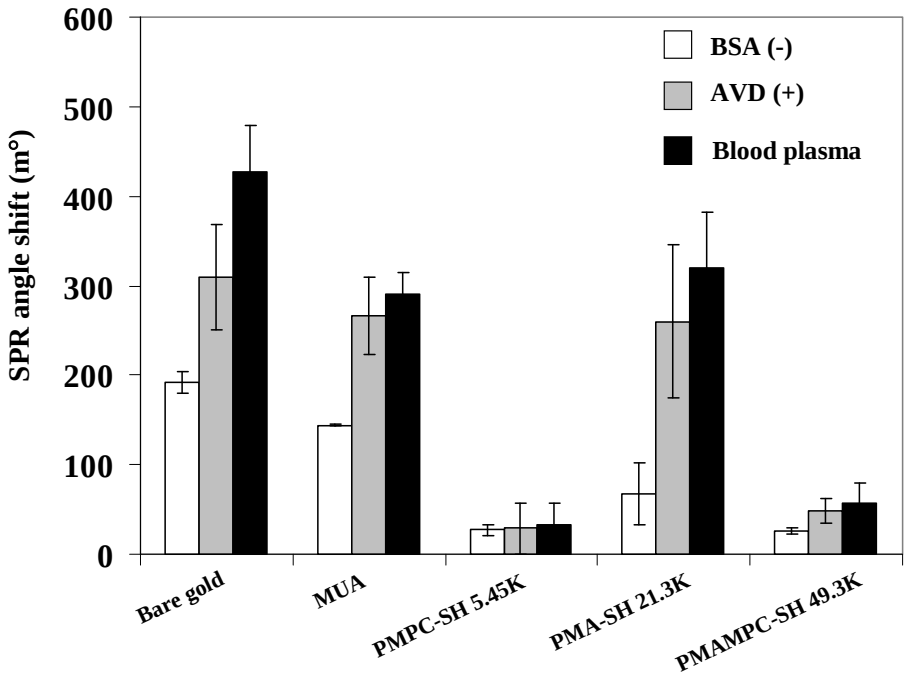

Figure 4.52 SPR angle shift corresponding to the amount of adsorbed proteins: BSA and avidin (0.1 mg/mL) in PBS solution (10 mM, pH 7.4) and 0.14% blood plasma in PBS (0.1 mg/mL) on the surface-modified SPR disk.

4.2.4.1 Effect of polymer chain length

As mentioned above, the copolymer brushes of PMAMPC show the high performance in preventing the non-specific adsorption of proteins even in blood plasma. In this subsection, the effect of polymer chain length on the amount of protein adsorption was investigated. The copolymer brushes of PMAMPC with different $\overline{M}_n$ were used. Figure 4.53 shows that the adsorbed amount of all proteins tested was reduced by the increase in $\overline{M}_n$ or polymer thickness. This can be explained based on the content of MPC units which is the highest for the copolymer having $\overline{M}_n$ of 49.3 kDa. This agrees well with work reported by Yoshimoto and coworkers that the amount of MPC units on the gold surface plays an important factor for an excellent resistance to protein adsorption [38]. Therefore, the decrease of protein adsorption as a function of $\overline{M}_n$ could be explained by the increase in thickness and the amount of MPC units on the surface.

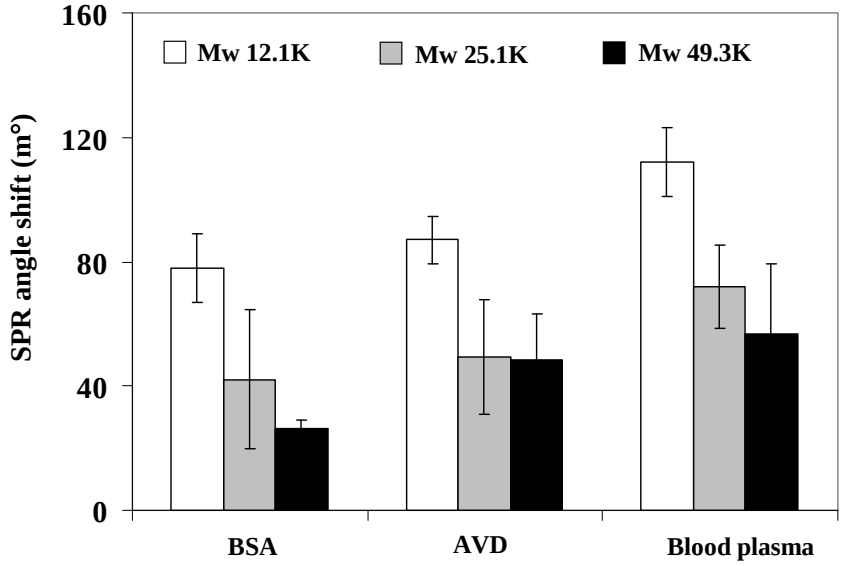

Figure 4.53 SPR angle shift corresponding to the amount of adsorbed proteins: BSA and avidin (0.1 mg/mL) in PBS solution (10 mM, pH 7.4) and 0.14% blood plasma in PBS (0.1 mg/mL) on the surface-grafted PMAMPC brushes having different $\overline{M}_n$.

4.2.4.2 Effect of copolymer composition

To achieve both functionalization and non-specific binding resistance properties of the PMAMPC brushes, the optimal balance between MA and MPC units in copolymer should be considered. Therefore, the effect of copolymer composition of PMAMPC brushes on the amount of non-specific protein adsorption was firstly investigated. The copolymer brushes of PMAMPC obtained from $\overline{M}_n$ of about 50 kD having different copolymer composition were used. Evidently in Figure 4.54, the amount of non-specific adsorption of BSA and blood plasma increased with decreasing the amount of MPC units or increasing the amount of MA units in the copolymer brushes. In the case of AVD which is positively charged, the adsorbed amount increased as the content of MA units increased. This can be explained by favorable electrostatic interactions between the negatively charged MA units and the positively charged AVD in PBS buffer pH 7.4. Alternatively, MPC units exhibit excellent protein resistance. Therefore, the ability to prevent protein adsorption of the PMAMPC brushes was deteriorated when the amount of MPC units in the copolymer was reduced. Once again, these results strongly supported that MPC units in the PMAMPC copolymer brushes play an important role in reducing the non-specific protein adsorption. In this particular studies, the best performance in suppressing the non-spectific adsorption was found on the PMAMPC copolymer having approximately 80% PMPC composition and relatively high molecular weight ($PMA_{21}MPC_{79}$, 49.3kDa).

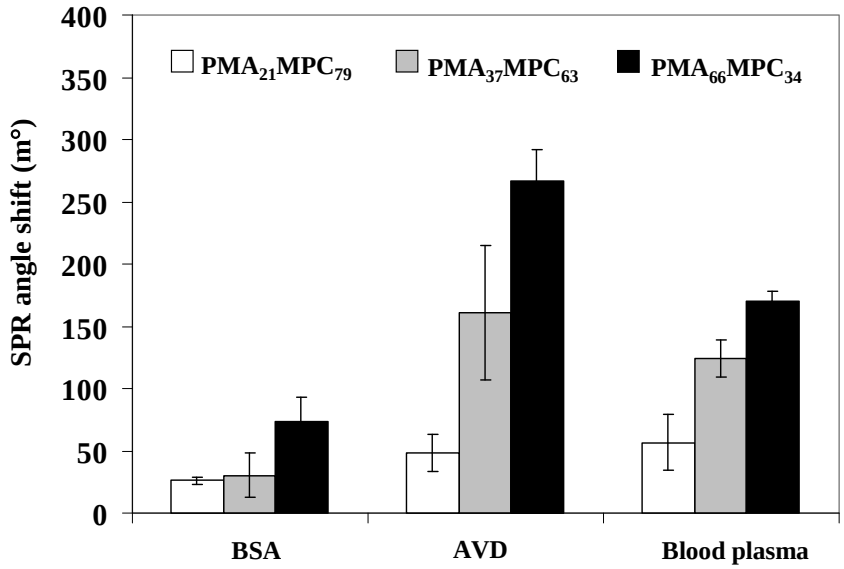

Figure 4.54 SPR angle shift corresponding to the amount of adsorbed proteins: BSA and avidin (0.1 mg/mL) in PBS solution (10 mM, pH 7.4) and 0.14% blood plasma in PBS (0.1 mg/mL) on the surface-grafted PMAMPC brushes having different copolymer composition expressed in term of MA:MPC unit.

4.2.4.3 Effect of blood plasma concentration

The whole blood plasma (70 mg of proteins per milliliter of plasma) was diluted by PBS buffer to obtain a concentration in a range of 0.14 to 100% (equivalent to 0.1 mg/mL to 70 mg/mL), and the amount of non-specific adsorption at different concentration of blood plasma was measured. Figure 4.55 showed that non-specific adsorption of blood plasma increased with the increase in blood plasma concentration and reached saturation at the concentration higher than 20%. The amount of blood plasma adsorbed on PMAMPC brushes ranged from 0.10 ± 0.01 μg/cm^2 to 0.77 ± 0.1 μg/cm^2 for a concentration of blood plasma from 0.14 to 100%. The adsorption of 100% blood plasma (undiluted blood plasma) obtained in this study is still considered relatively high compared to the value less than 10 ng/cm^2 obtained by others [20,75-77]. However, all of those reports are based on the polymer brushes prepared by "grafting from" method of which graft density and thickness should be high so the resistivity to the non-specific adsorption of protein should be more effective than our system based on the PMAMPC brushes that was prepared by "grafting to" method.

Also, blood plasma samples are from different sources with different storage times, their properties and reactivity may be different. In addition, the results have demonstrated that the adsorption of proteins in blood plasma on the PMAMPC brushes was favored by MA units so the adsorption of blood plasma should be somewhat suppressed after the MA units of the PMAMPC brushes are bound with sensing probe. The blood plasma concentration of 0.14% was selected for further study in order to reduce the interference of the non-specific adsorption of proteins in blood plasma as well as the effects of blood plasma viscosity and prevent the formation of small bubbles in the SPR system.

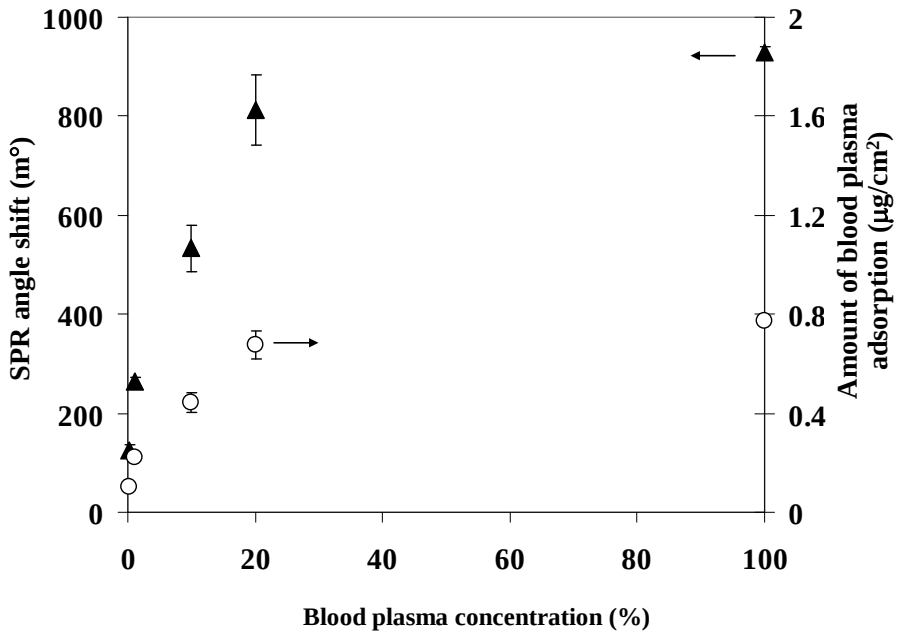

Figure 4.55 SPR angle shift and the corresponding amount of adsorbed proteins from blood plasma in PBS solution (10 mM, pH 7.4) having varied concentration on the surface-grafted PMAMPC brushes.

4.2.5 Specific interactions of biotin immobilized on the gold-coated SPR disks bearing PMAMPC brushes with avidin in complex sample

In this section, biotin molecules were chosen as a sensing probe that can bind with AVD with a high specificity and affinity, $K_D \approx 10^{-15}$ M. The biotin was immobilized on the carboxyl group of MA unit in the PMAMPC copolymer brushes by covalent attachment. The immobilization was done outside the SPR instrument. In order to investigate the possibility of using this sensor platform for detecting the target molecules in the complex sample, a AVD solution of 0.15 μM (equivalent to 10 μg/mL) in diluted blood plasma (0.14%) onto immobilized biotin on the PMAMPC brushes was examined. The non-specific binding or the detection in the absence of AVD in blood plasma was also determined in order to quantify the specific binding of sensor in term of the signal-to-noise (*S/N*) ratio.

Figure 4.56 shows the SPR response of specific and non-specific binding on various sensing platform. The non-specific binding was measured in the absence of AVD in blood plasma solution. The biotin-immobilized MUA and PMA (21.3 kDa) brushes showed a larger binding amount of AVD in blood plasma as compared with $PMA_{21}MPC_{79}$ (49.3 kDa) brushes. However, the non-specific binding response (binding in the absence of AVD in blood plasma) was also extremely high. Although the sensor platform based on $PMA_{21}MPC_{79}$ (49.3K) brushes gave the lowest amount of AVD binding response, the non-specific binding response was greatly suppressed. To quantify the specific binding of AVD in blood plasma onto biotin probe, the signal-to-noise (*S/N*) ratio was calculated and shown in Figure 4.57. It is clear that the sensor platform based on $PMA_{21}MPC_{79}$ (49.3 kDa) brushes afforded the highest *S/N* ratio of AVD binding in blood plasma and the lowest percent non-specific binding. From these results, it can be concluded that the sensor platform of based on $PMA_{21}MPC_{79}$ (49.3 kDa) brushes promoted the specific binding over the non-specific binding, showing the enhancement of *S*/*N* ratio about 8.1-fold and 4.1-fold as compared with MUA and PMA brushes, respectively.

In addition, another point that should be mentioned from this result is the decrease (about 73%) of blood plasma adsorption on the PMAMPC brushes after

immobilizing the sensing probe. This result can encourage the assumption that the adsorption of proteins in blood plasma on PMAMPC brushes was induced by MA units.

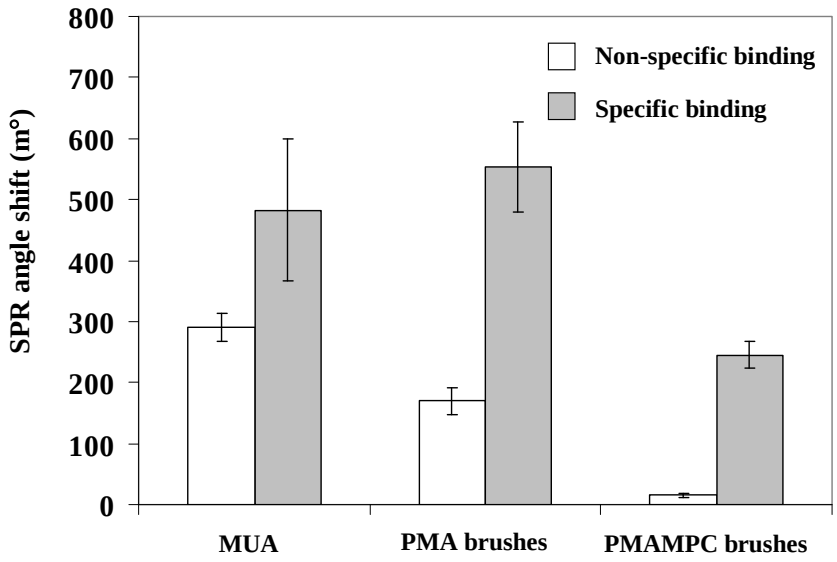

Figure 4.56 SPR angle shift corresponding to the specific and non-specific binding of 0.15 μM AVD in 0.14 % blood plasma on various sensor platforms.

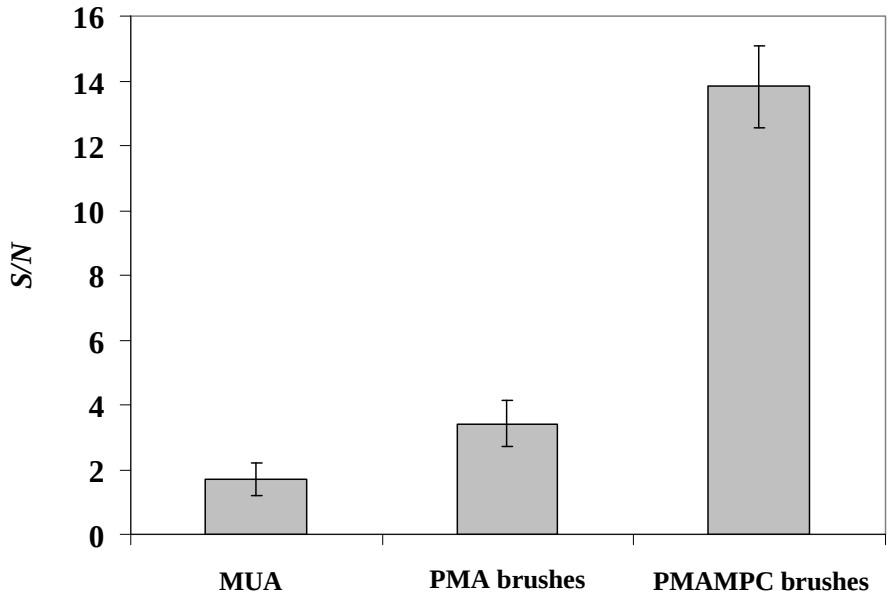

Figure 4.57 Signal-to-noise (*S/N*) ratio of AVD binding in blood plasma on various sensor platforms.

4.2.5.1 Effect of polymer chain length

Figure 4.58 and 4.59 show the specific and non-specific binding and the *S*/*N* ratio of PMAMPC brushes havinf varied $\overline{M}_n$, respectively. Figure 4.56 shows that the signal of specific binding increased with an increase in $\overline{M}_n$ or thickness, supposedly due to the increase of sensing probe, while the amount of non-specific binding decreased. However, in the case of PMAMPC (12.1 kDa), the strong influence of non-specific adsorption was observed, showing a large amount of both specific and non-specific adsorption. Evidently, the PMAMPC brushes with $\overline{M}_n$ of 49.3 kDa provided the highest *S*/*N* ratio followed by 25.1 kDa and then 12.1 kDa. These results indicate that longer polymer chain not only promoted higher specific binding but also suppressed non-specific binding.

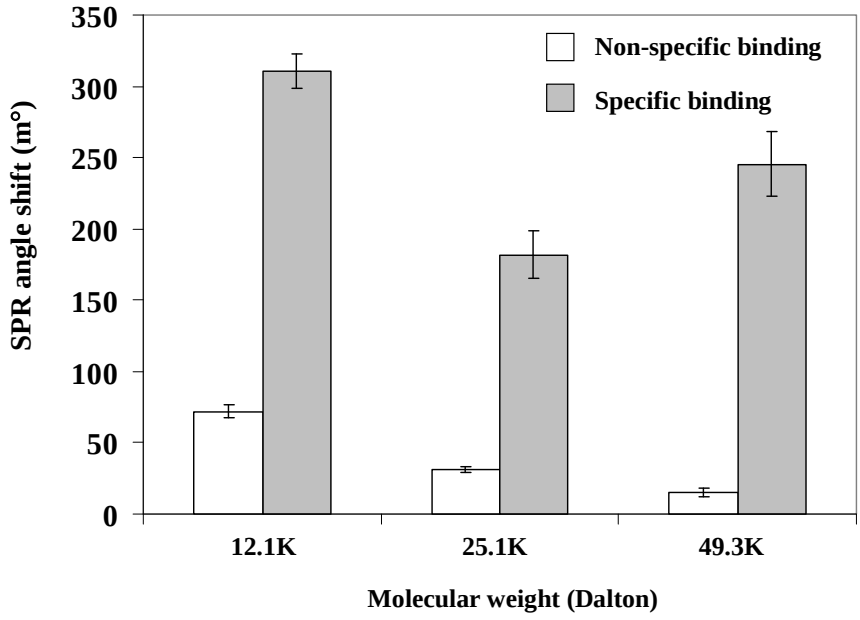

Figure 4.58 SPR angle shift corresponding to specific and non-specific binding of AVD (0.15 μM) in blood plasma (0.14 %) on the surface-attached PMAMPC brushes having varied $\overline{M}_n$.

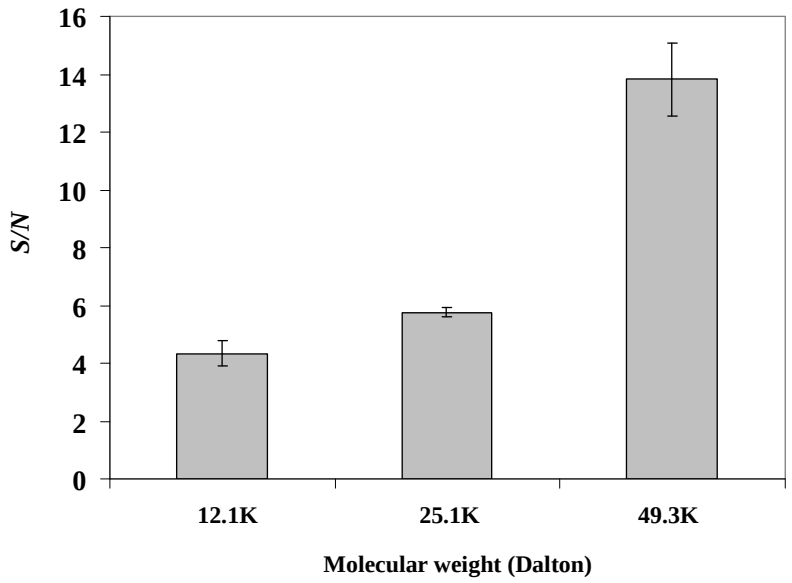

Figure 4.59 Signal-to-noise (*S/N*) ratio of AVD binding on the surface-attached PMAMPC brushes having varied $\overline{M}_n$.

4.2.5.2 Effect of copolymer composition

As mentioned above, the proper balance between MA units and MPC units is considerably important to achieve the high performance of PMAMPC brushes as a sensor platform in term of specific binding. Figure 4.60 and 4.61 show the specific and non-specific binding and the *S*/*N* ratio of the surface-attached PMAMPC brushes having varied copolymer composition, respectively. The amount of AVD binding appeared to be increased by increasing amount of MA units; however, the non-specific binding of blood plasma was also increased. Particularly, at high concentration of MA units in PMAMPC brushes, that were prepared from $PMA_{66}MPC_{34}$, did not induce the specific binding of AVD presumably due to steric hindrance of densely packed sensing probe resulting in low *S*/*N* ratio (Figure 4.61). This leads to the requirement to effectively tailor the density of sensing probe controlled by varying copolymer composition in order to improve the binding efficiency of the sensor platform. These results suggested that the amount of MA units in PMAMPC brushes of only about 20% was effective enough to provide a high efficiency of sensor platform for detecting AVD in blood plasma solution.

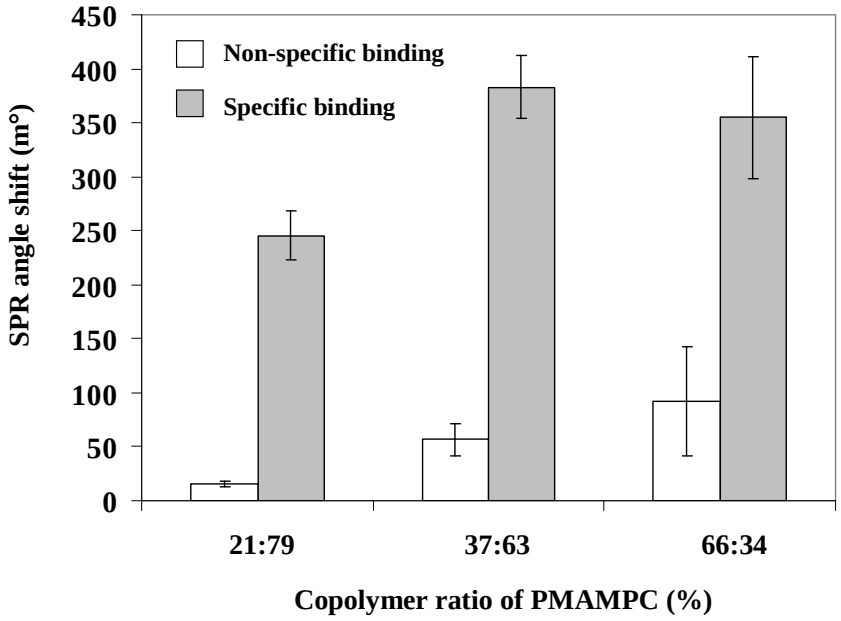

Figure 4.60 SPR response of specific and non-specific binding of AVD (0.15 μM) in blood plasma (0.14 %) on the surface-attached PMAMPC brushes having varied copolymer composition.

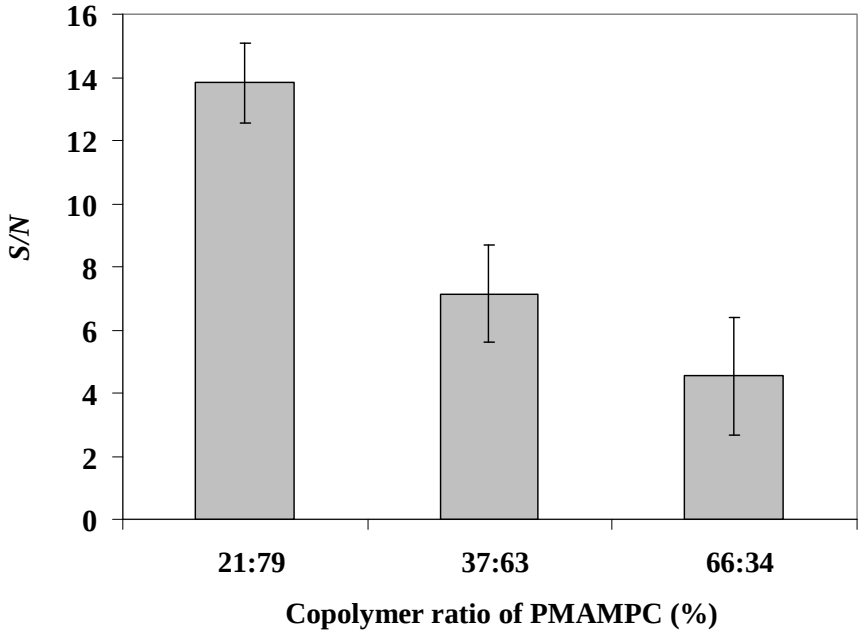

Figure 4.61 Signal-to-noise (*S/N*) ratio of AVD binding on the surface-attached PMAMPC brushes having varied copolymer composition.

4.2.5.3 Limit of detection (LODs)

To determine the lowest detectable concentration of AVD in blood plasma, the surface-attached $PMA_{21}MPC_{79}$ (49.3 kDa) brushes, the sensor platform that gave the best performance, was used to detect AVD at different concentrations ranging from 0.15 nM to 150 nM in 0.14% blood plasma solution. Figure 4.62 shows that binding signal increased as a function of AVD concentrations, and the binding did not saturate even at a high AVD concentration of 150 nM. The *S/N* was equal to 1 meaning that no discrimination of SPR response signal between specific and non-specific binding of AVD in blood plasms. Therefore, the lowest concentration of the AVD in 0.14% blood plasma or the detection limit of this sensor platform that provided a difference between the signal of specific and non-specific binding ($S/N \geq 2$) was 1.5 nM (equivalent to 100 ng/mL) while the detection limit of the sensor platform obtained from MUA, a conventional sensor platform, was 150 nM (Figure A-5 in Appendix A). In medical diagnostics application, the development of SPR sensors for detecting several analytes such as cancer markers (LODs < 1-100 ng/mL) and antibodies (LODs < 1-100 ng/mL) has been reported [78]. However, most of the detection matrixes were performed in buffers rather than in complex matrices. The results have demonstrated a potential of using the surface-attached PMAMPC brushes as a sensor platform for detecting the target molecules in complex matrices such as blood plasma and clinical samples.

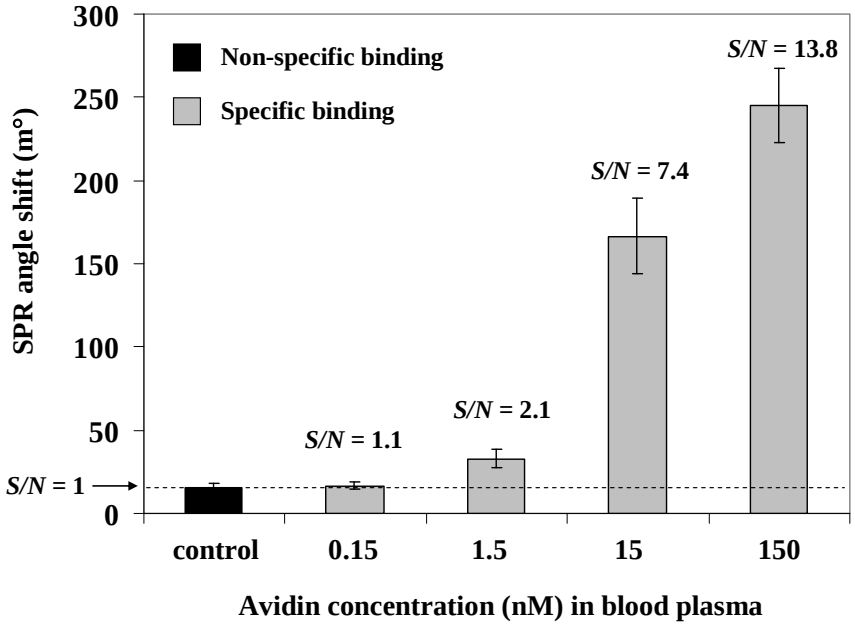

Figure 4.62 SPR angle shift corresponding to the specific and non-specific binding of AVD having different concentration in 0.14 % blood plasma on the surface attached PMAMPC.

CHAPTER V

CONCLUSION

In this research, the 3D precursor layers, carboxyl-containing polymer brushes, were prepared on gold-coated SPR disk by two approaches, “grafting to” and “grafting from”. The biosensing application of the prepared polymer brushes was demonstrated by using surface plasmon resonance (SPR) technique in comparison with the 2D monolayer of MUA.

The homopolymer brushes of PAA were synthesized by SI-ATRP and characterized by water contact angle measurements and FT-IR spectroscopy and AFM. It has been demonstrated that the graft density of PAA brushes can be controlled by the graft density of the surface initiator. As determined by TBO assay, the carboxyl group density can be varied as a function of the graft density of the PAA brushes. The carboxyl groups of PAA brushes are readily available for the covalent attachment of biotin-NH_2 and BSA, two models of sensing probe. The surface-tethered PAA brushes film simultaneously increased the biospecific interactions of both biotin/streptavidin and BSA/anti-BSA systems and decreased the non-specific adsorption of non-target proteins as compared with the MUA. Moreover, it was found that the limited accessibility of the SA and anti-BSA to the immobilized biotin and BSA, respectively, can be greatly suppressed by reducing the extent of the COOH group activation and the grafting density of the PAA brushes. The best performance for both biotin/streptavidin and BSA/anti-BSA systems was found on the sensor platform developed from the surface-grafted PAA brushes having 50% graft density.

The attachment of the homopolymer brushes of PMA and PMPC and the copolymer brushes of PMAMPC were performed by grafting to approach via self-assemble formation of thiol-terminated (co)polymers. The thiol-terminated polymers were synthesized by aminolysis reaction of dithioester end-capped polymers obtained from RAFT polymerization. The polymer chain length and copolymer composition of

the (co)polymer brushes can be well controlled using designated monomer/CTA ratio and comonomer in the feed as determined by GPC, NMR and FT-IR spectroscopy. The success of the thiol-terminated (co)polymers was verified by XPS, AFM and water contact angle measurements. The results have demonstrated a potential of using PMAMPC brushes as a sensor platform for detecting the target molecules in complex sample. The biotin-NH_2 was immobilized on the carboxyl groups of the MA units in the PMAMPC copolymer brushes by covalent attachment and then the specific binding of AVD in blood plasma to the immobilized biotin probe was evaluated. It was found that the sensor platform of PMAMPC brushes with appropriate polymer chain length (49.7 kDa) and copolymer composition (21:79) showed the enhancement of *S*/*N* ratio of about 8.1-fold and 4.1-fold as compared with MUA and PMA brushes, respectively. In addition, the detection limit for detecting AVD in blood plasma solution was found to be 1.5 nM (equivalent to 100 ng/mL). The summary of conditions and efficiencies of sensors platform prepared from carboxyl-containing polymer brushes for different bio-recognition systems is shown in Table 5.1.

Table 5.1 The summary of conditions and efficiencies of sensor platform prepared from carboxyl-containing polymer brushes.

Sensor platform	Preparation method	Sensing probe	Analyte	Detection matrix	*S/N*	Detection limit	Reproducibility
MUA	SAM	Biotin BSA Biotin	SA anti-BSA AVD	PBS PBS 0.14% human plasma in PBS	3.2-5.1 1.2-1.8 1.7	N/A 6.7 nM 150 nM	× ✓ ×
PAA brushes	"Grafting from" (SI-ATRP)	Biotin BSA	SA anti-BSA	PBS PBS	103.9-145.5 12.2-17.1	N/A 0.67 nM	× ✓
PMA brushes	"Grafting to" (PMA-SH)	Biotin	AVD	0.14% human plasma in PBS	3.4	N/A	×
PMAMPC brushes	"Grafting to" (PMAMPC-SH)	Biotin	AVD	0.14% human plasma in PBS	13.8	1.5 nM	×

REFERENCES

[1] Rusmini, F.; Zhong, Z., and Feijen, J. Protein immobilization strategies for protein biochips. *Biomacromolecules* 8(6) (2007): 1775-1789.

[2] Senaratne, W.; Andruzzi, L., and Ober, C. K. Self-assembled monolayers and polymer brushes in biotechnology: Current applications and future perspectives. *Biomacromolecules* 6(5) (2005): 2427-2448.

[3] Xu, F. J.; Neoh, K. G., and Kang, E. T. Bioactive surfaces and biomaterials via atom transfer radical polymerization. *Progress in Polymer Science* 34(8) (2009): 719-761.

[4] Masson, J.-F., et al. Preparation of analyte-sensitive polymeric supports for biochemical sensors. *Talanta* 64(3) (2004): 716-725.

[5] Masson, J.-F., et al. Biocompatible polymers for antibody support on gold surfaces. *Talanta* 67(5) (2005): 918-925.

[6] Su, X.-L., and Li, Y. A self-assembled monolayer-based piezoelectric immunosensor for rapid detection of Escherichia coli O157:H7. *Biosensors and Bioelectronics* 19(6) (2004): 563-574.

[7] Nakamura, F.; Ito, E.; Hayashi, T., and Hara, M. Fabrication of COOH-terminated self-assembled monolayers for DNA sensors. *Colloids and Surfaces A: Physicochemical and Engineering Aspects* 284-285 (2006**)**: 495-498.

[8] Nelson, K. E., et al. Surface characterization of mixed self-assembled monolayers designed for streptavidin immobilization. *Langmuir* 17(9) (2001): 2807-2816.

[9] Skoda, M. W. A., et al. Protein density profile at the interface of water with oligo(ethylene glycol) self-assembled monolayers. *Langmuir* 25(7) (2009**)**: 4056-4064.

[10] Walker, M. L.; Vanderah, D. J., and Rubinson, K. A. In-situ characterization of self-assembled monolayers of water-soluble oligo(ethylene oxide) compounds. *Colloids and Surfaces B: Biointerfaces* 82(2) **(**2011): 450-455.

[11] Tegoulia, V. A.; Rao, W.; Kalambur, A. T.; Rabolt, J. F., and Cooper, S. L. Surface properties, fibrinogen adsorption, and cellular interactions of a novel phosphorylcholine-containing self-assembled monolayer on gold. *Langmuir* 17(14) (2001**)**: 4396-4404.

[12] Herrwerth, S.; Eck, W.; Reinhardt, S., and Grunze, M. Factors that determine the protein resistance of oligoether self-assembled monolayers-internal hydrophilicity, terminal hydrophilicity, and lateral packing density. *Journal of the American Chemical Society* 125(31) (2003): 9359-9366.

[13] Wang, R. L. C.; Kreuzer, H. J., and Grunze, M. Molecular conformation and solvation of oligo(ethylene glycol)-terminated self-assembled monolayers and their resistance to protein adsorption. *The Journal of Physical Chemistry B* 101(47) (1997): 9767-9773.

[14] Lee, B. S., et al. Surface-initiated, atom transfer radical polymerization of oligo(ethylene glycol) methyl ether methacrylate and subsequent click chemistry for bioconjugation. *Biomacromolecules* 8(2) (2007): 744-749.

[15] Lee, B. S.; Chi, Y. S.; Lee, K.-B.; Kim, Y.-G., and Choi, I. S. Functionalization of poly(oligo(ethylene glycol) methacrylate) films on gold and Si/SiO2 for immobilization of proteins and cells: SPR and QCM studies. *Biomacromolecules* 8(12) (2007**)**: 3922-3929.

[16] Yang, N.; Su, X.; Tjong, V., and Knoll, W. Evaluation of two- and three-dimensional streptavidin binding platforms for surface plasmon resonance spectroscopy studies of DNA hybridization and protein-DNA binding. *Biosensors and Bioelectronics* 22(11) (2009): 2700-2706.

[17] Feng, C. L., et al. Reactive thin polymer films as platforms for the immobilization of biomolecules. *Biomacromolecules* 6(6) (2005): 3243-3251.

[18] Kurosawa, S.; Aizawa, H.; Talib, Z. A.; Atthoff, B. r., and Hilborn, J. n. Synthesis of tethered-polymer brush by atom transfer radical polymerization from a plasma-polymerized-film-coated quartz crystal microbalance and its application for immunosensors. *Biosensors and Bioelectronics* 20(6) (2004): 1165-1176.

[19] Zhang, S. G. Hydrogels - wet or let die. *Nature Material* 3(1) (2004): 7-8.

[20] Zhang, Z., et al. Blood compatibility of surfaces with superlow protein adsorption. *Biomaterials* 29(32) (2009): 4285-4291.

[21] Iwata, R.; Satoh, R.; Iwasaki, Y., and Akiyoshi, K. Covalent immobilization of antibody fragments on well-defined polymer brushes via site-directed method. *Colloids and Surfaces B: Biointerfaces* 62(2) (2009): 288-298.

[22] Zhang, Z.; Chen, S., and Jiang, S. Dual-functional biomimetic materials: Nonfouling poly(carboxybetaine) with active functional groups for protein immobilization. *Biomacromolecules* 7(12) (2006): 3311-3315.

[23] Dong, R.; Krishnan, S.; Baird, B. A.; Lindau, M., and Ober, C. K. Patterned biofunctional poly(acrylic acid) brushes on silicon surfaces. *Biomacromolecules* 8(10) (2007): 3082-3092.

[24] Dai, J., et al. High-capacity binding of proteins by poly(acrylic acid) brushes and their derivatives. *Langmuir* 22(9) (2006): 4274-4281.

[25] Cullen, S. P.; Liu, X.; Mandel, I. C.; Himpsel, F. J., and Gopalan, P. Polymeric brushes as functional templates for immobilizing ribonuclease A: Study of binding kinetics and activity. *Langmuir* 24(3) (2007): 913-920.

[26] Akkahat, P., and Hoven, V. P. Introducing surface-tethered poly(acrylic acid) brushes as 3D functional thin film for biosensing application. *Colloids and Surface B: Biointerface* (2011) doi/10.1016/j.colsurfb.2011.03.042

[27] Zhao, B., and Brittain, W. J. Polymer brushes: Surface-immobilized macromolecules. *Progress in Polymer Science* 25(5) (2000): 677-710.

[28] Barbey, R., et al. Polymer brushes via surface-initiated controlled radical polymerization: Synthesis, characterization, properties, and applications. *Chemical Reviews* 109(11) (2009): 5437-5527.

[29] Lowe, A. B.; Sumerlin, B. S.; Donovan, M. S., and McCormick, C. L. Facile preparation of transition metal nanoparticles stabilized by well-defined (co)polymers synthesized via aqueous reversible addition-fragmentation chain transfer polymerization. *Journal of the American Chemical Society* 124(39) (2002): 11562-11563.

[30] Sumerlin, B. S., et al. Modification of gold surfaces with water-soluble (co)polymers prepared via aqueous reversible addition−fragmentation chain transfer (RAFT) polymerization. *Langmuir* 19(14) (2003): 5559-5562.

[31] Zhu, M.-Q.; Wang, L.-Q.; Exarhos, G. J., and Li, A. D. Q. Thermosensitive Ggold nanoparticles. *Journal of the American Chemical Society* 126(9) (2004): 2656-2657.

[32] Shan, J.; Nuopponen, M.; Jiang, H.; Kauppinen, E., and Tenhu, H. Preparation of poly(N-isopropylacrylamide)-monolayer-protected gold clusters: Synthesis methods, core size, and thickness of monolayer. *Macromolecules* 36(12) (2003): 4526-4533.

[33] Willcock, H., and O'Reilly, R. K. End group removal and modification of RAFT polymers. *Polymer Chemistry* 1(2) (2010): 149-157.

[34] Scales, C. W.; Convertine, A. J., and McCormick, C. L. Fluorescent labeling of RAFT-generated poly(N-isopropylacrylamide) via a facile maleimide-thiol coupling reaction. *Biomacromolecules* 7(5) (2006): 1389-1392.

[35] Schessler, H. M.; Karpovich, D. S., and Blanchard, G. J. Quantitating the balance between enthalpic and entropic forces in alkanethiol/gold monolayer self assembly. *Journal of the American Chemical Society* 118(40) **(**1996): 9645-9651.

[36] Yoshimoto, K.; Hirase, T.; Nemoto, S.; Hatta, T., and Nagasaki, Y. Facile construction of sulfanyl-terminated poly(ethylene glycol)-brushed layer on a gold surface for protein immobilization by the combined use of sulfanyl-ended telechelic and semitelechelic poly(ethylene glycol)s. *Langmuir* 24(17) (2008): 9623-9629.

[37] Uchida, K., et al. Creation of a mixed poly(ethylene glycol) tethered-chain surface for preventing the nonspecific adsorption of proteins and peptides. *Biointerphases* 2(4) (2007): 126-130.

[38] Yoshimoto, K.; Hirase, T.; Madsen, J.; Armes, S. P., and Nagasaki, Y. Non-fouling character of poly 2-(methacryloyloxy)ethyl phosphorylcholine -modified gold surfaces fabricated by the 'grafting to' method: Comparison of its protein resistance with poly(ethylene glycol)-modified gold surfaces. *Macromolecular Rapid Communications* 30(24) (2009): 2136-2140.

[39] Husseman, M., et al. Controlled synthesis of polymer brushes by "living" free radical polymerization techniques. *Macromolecules* 32(5) (1999): 1424-1431.

[40] Sedjo, R. A.; Mirous, B. K., and Brittain, W. J. Synthesis of polystyrene-block-poly(methyl methacrylate) brushes by reverse atom transfer radical polymerization. *Macromolecules* 33(5) (2000): 1492-1493.

[41] Edmondson, S.; Osborne, V. L., and Huck, W. T. S. Polymer brushes via surface-initiated polymerizations. *Chemical Society Reviews* 33(1) (2004): 14-22.

[42] Jones, D. M.; Brown, A. A., and Huck, W. T. S. Surface-initiated polymerizations in aqueous media: Effect of initiator density. *Langmuir* 18(4) (2002): 1265-1269.

[43] Kusumo, A., et al. High capacity, charge-selective protein uptake by polyelectrolyte brushes. *Langmuir* 23(8) (2007): 4448-4454.

[44] Wang, J.-S., and Matyjaszewski, K. Controlled/"living" radical polymerization. Atom transfer radical polymerization in the presence of transition-metal complexes. *Journal of the American Chemical Society* 117(20) (1995): 5614-5615.

[45] Matyjaszewski, K. Mechanistic and synthetic aspects of atom transfer radical polymerization. *Journal of Macromolecular Science Pure and Applied Chemistry* A34(10) (1997): 1785-1801.

[46] Chambard, G.; Klumperman, B., and German, A. L. Effect of solvent on the activation rate parameters for polystyrene and poly(butyl acrylate) macroinitiators in atom transfer radical polymerization. *Macromolecules* 33(12) (2000): 4417-4421.

[47] Wu, T., et al. Behavior of surface-anchored poly(acrylic acid) brushes with grafting density gradients on solid substrates: 1. Experiment. *Macromolecules* 40(24) (2007): 8756-8764.

[48] Bruening, M. L.; Dotzauer, D. M.; Jain, P.; Ouyang, L., and Baker, G. L. Creation of functional membranes using polyelectrolyte multilayers and polymer brushes. *Langmuir* 24(15) (2008): 7663-7673.

[49] Lindqvist, J., et al. Intelligent dual-responsive cellulose surfaces via surface-initiated ATRP. *Biomacromolecules* 9(8) (2008): 2139-2145.

[50] Xu, L. Q., et al. One-pot preparation of ferrocene-functionalized polymer brushes on gold substrates by combined surface-initiated atom transfer radical polymerization and “click chemistry”. *Langmuir* 26(19) (2010): 15376-15382.

[51] Huang, W.; Kim, J.-B.; Bruening, M. L., and Baker, G. L. Functionalization of surfaces by water-accelerated atom-transfer radical polymerization of hydroxyethyl methacrylate and subsequent derivatization. *Macromolecules* 35(4) (2002): 1175-1179.

[52] Retsch, M.; Walther, A.; Loos, K., and Müller, A. H. E. Synthesis of dense poly(acrylic acid) brushes and their interaction with amine-functional silsesquioxane nanoparticles. *Langmuir* 24(17) (2008): 9421-9429.

[53] Lego, B. A.; Skene, W. G., and Giasson, S. Swelling study of responsive polyelectrolyte brushes grafted from mica substrates: Effect of pH, salt, and grafting density. *Macromolecules* 43(9) (2010): 4384-4393.

[54] Moad, G.; Chong, Y. K.; Postma, A.; Rizzardo, E., and Thang, S. H. Advances in RAFT polymerization: The synthesis of polymers with defined end-groups. *Polymer* 46(19) (2005): 8458-8468.

[55] Weber, C.; Remzi Becer, C.; Guenther, W.; Hoogenboom, R., and Schubert, U. S. Dual responsive methacrylic acid and oligo(2-ethyl-2-oxazoline) containing graft copolymers. *Macromolecules* 43(1) (2009): 160-167.

[56] Rinaldi, D., et al. RAFT copolymerization of methacrylic acid and poly(ethylene glycol) methyl ether methacrylate in the presence of a hydrophobic chain transfer agent in organic solution and in water. *Journal of Polymer Science: Part A: Polymer Chemistry* 47(12) (2009): 3045-3055.

[57] Pelet, J. M., and Putnam, D. High molecular weight poly(methacrylic acid) with narrow polydispersity by RAFT polymerization. *Macromolecules* 42(5) (2009): 1494-1499.

[58] Queffelec, J.; Gaynor, S. G., and Matyjaszewski, K. Optimization of atom transfer radical polymerization using Cu(I)/tris(2-(dimethylamino)ethyl)amine as a catalyst. *Macromolecules* 33(23) (2000): 8629-8639.

[59] Ying, L., et al. Immobilization of galactose ligands on acrylic acid graft-copolymerized poly(ethylene terephthalate) film and its application to hepatocyte culture. *Biomacromolecules* 4(1) (2002): 157-165.

[60] Su, X.; Wu, Y.-J., and Knoll, W. Comparison of surface plasmon resonance spectroscopy and quartz crystal microbalance techniques for studying DNA assembly and hybridization. *Biosensors and Bioelectronics* 21(5) (2005): 719-726.

[61] Yang, Q.; Kaul, C., and Ulbricht, M. Anti-nonspecific protein adsorption properties of biomimetic glycocalyx-like glycopolymer layers: Effects of glycopolymer chain density and protein size. *Langmuir* 26(8) (2010): 5746-5752.

[62] Lego, B. a.; François, M.; Skene, W. G., and Giasson, S. Polymer brush covalently attached to OH-functionalized mica surface via surface-initiated ATRP: Control of grafting density and polymer chain length. *Langmuir* 25(9) (2009): 5313-5321.

[63] Dabirian, R.; Zdravkova, A. N.; Liljeroth, P.; van Walree, C. A., and Jenneskens, L. W. Mixed self-assembled monolayers of semirigid tetrahydro-4H-thiopyran end-capped oligo(cyclohexylidenes). *Langmuir* 21(23) (2005): 10497-10503.

[64] Shon, Y.-S.; Lee, S.; Perry, S. S., and Lee, T. R. The adsorption of unsymmetrical spiroalkanedithiols onto gold affords multi-component interfaces that are homogeneously mixed at the molecular level. *Journal of the American Chemical Society* 122(7) (2000): 1278-1281.

[65] Marutani, E., et al. Surface-initiated atom transfer radical polymerization of methyl methacrylate on magnetite nanoparticles. *Polymer* 45(7) (2004): 2231-2235.

[66] Nagase, K., et al. Effects of graft densities and chain lengths on separation of bioactive compounds by nanolayered thermoresponsive polymer brush surfaces. *Langmuir* 24(2) (2007): 511-517.

[67] Sarkar, D., and Somasundaran, P. Conformational dynamics of poly(acrylic acid). A study using surface plasmon resonance spectroscopy. *Langmuir* 20(11) (2004): 4657-4664.

[68] Chu, L.-Q.; Tan, W.-J.; Mao, H.-Q., and Knoll, W. Characterization of UV-induced graft polymerization of poly(acrylic acid) using optical waveguide spectroscopy. *Macromolecules* 39(25) (2006): 8742-8746.

[69] Dong, R.; Lindau, M., and Ober, C. K. Dissociation behavior of weak polyelectrolyte brushes on a planar surface. *Langmuir* 25(8) (2009): 4774-4779.

[70] Yoshikawa, C., et al. Protein repellency of well-defined, concentrated poly(2-hydroxyethyl methacrylate) brushes by the size-exclusion effect. *Macromolecules* 39(6) (2006): 2284-2290.

[71] Gautrot, J. E.; Huck, W. T. S.; Welch, M., and Ramstedt, M. Protein-resistant NTA-functionalized polymer brushes for selective and stable immobilization of histidine-tagged proteins. *ACS Applied Materials & Interfaces* 2(1) (2009): 193-202.

[72] Ishihara, K., et al. Hemocompatibility of human whole blood on polymers with a phospholipid polar group and its mechanism. *Journal of Biomedical Materials Research* 26(12) (1992): 1543-1552.

[73] Ishihara, K., et al. Why do phospholipid polymers reduce protein adsorption? *Journal of Biomedical Materials Research* 39(2) (1998): 323-330.

[74] Iwasaki, Y.; Omichi, Y., and Iwata, R. Site-specific dense immobilization of antibody fragments on polymer brushes supported by silicone nanofilaments. *Langmuir* 24(16) (2008): 8427-8430.

[75] Vaisocherová, H., et al. Functionalizable surface platform with reduced nonspecific protein adsorption from full blood plasma--Material selection and protein immobilization optimization. *Biosensors and Bioelectronics* 24(7) (2009): 1924-1930.

[76] Yang, W.; Xue, H.; Li, W.; Zhang, J., and Jiang, S. Pursuing “zero” protein adsorption of poly(carboxybetaine) from undiluted blood serum and plasma. *Langmuir* 25(19) (2009): 11911-11916.

[77] Yang, W., et al. Film thickness dependence of protein adsorption from blood serum and plasma onto poly(sulfobetaine)-grafted surfaces. *Langmuir* 24(17) (2008): 9211-9214.

[78] Homola, J. Surface plasmon resonance sensors for detection of chemical and biological species. *Chemical Reviews* 108(2) (2008): 462-493.

APPENDICES

APPENDIX A

Proton nuclear magnetic resonance spectroscopy (^{1}H NMR)

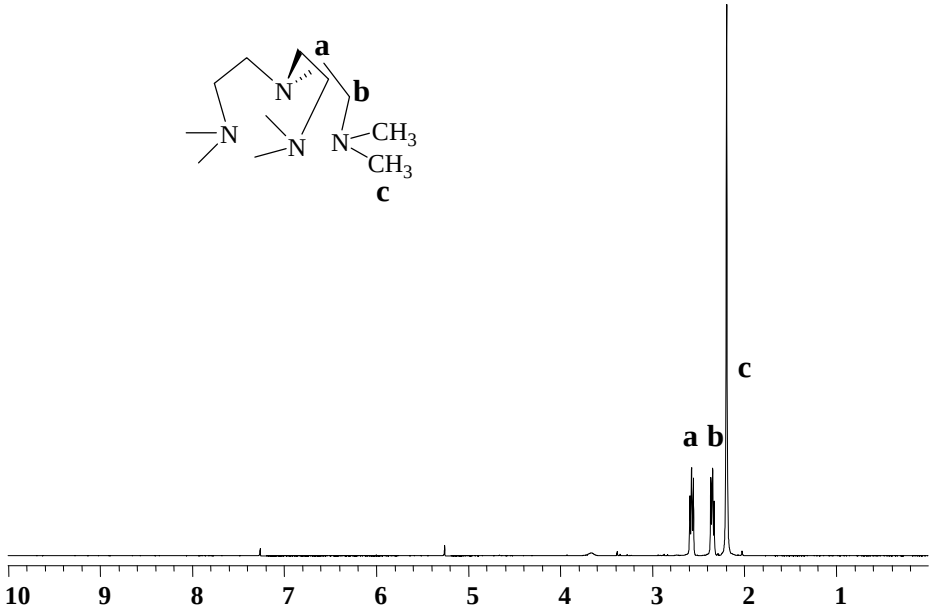

Figure A-1 ^{1}H NMR spectrum (400 MHz, $CDCl_3$) of tris (2-(dimethylamino) ethyl)amine [Me_6TREN].

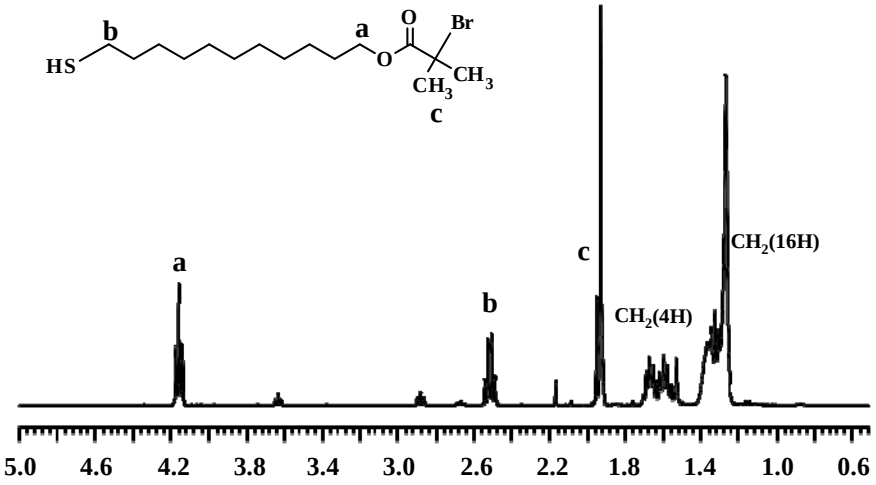

Figure A-2 ^{1}H NMR spectrum (400 MHz, $CDCl_3$) of tris (2-(dimethylamino) ethyl)amine [Me_6TREN].

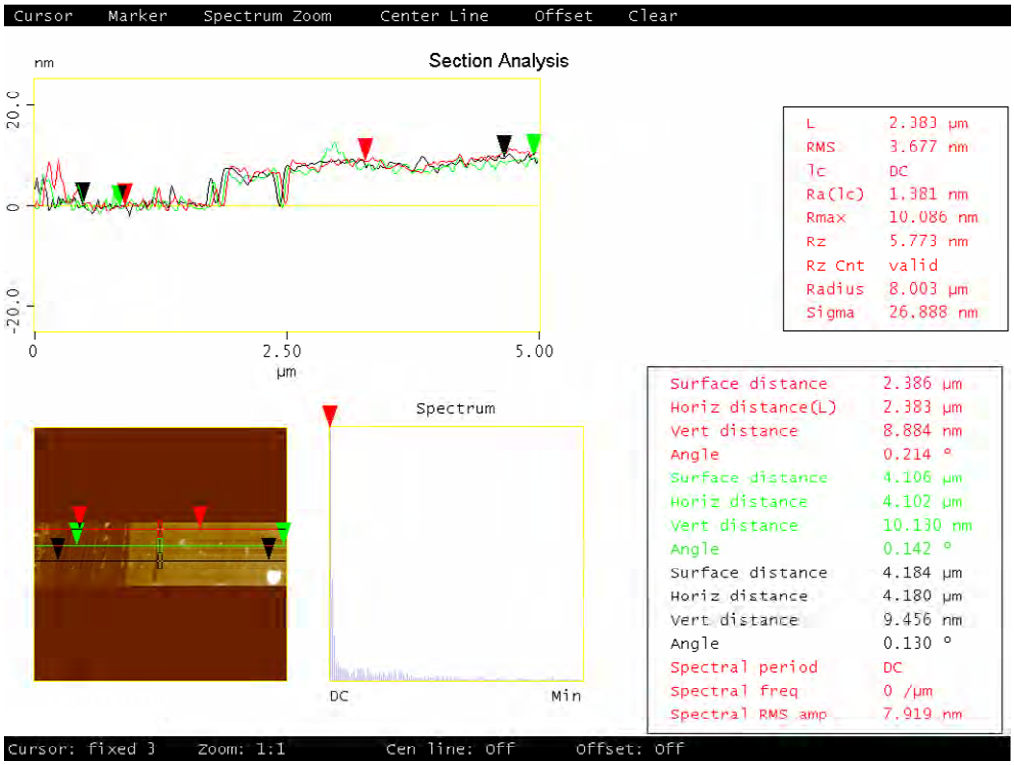

Figure A-3 AFM image after being scraped by AFM tip show the thickness of P*t*-BA brushes (30kD).

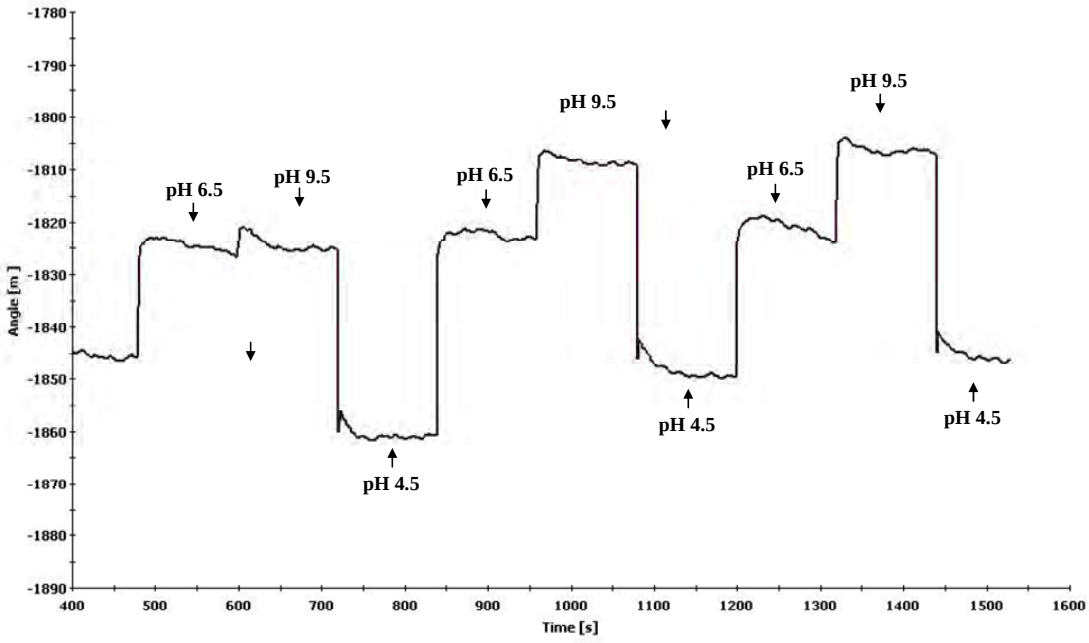

Figure A-4 SPR angle shift of MUA upon pH alternation.

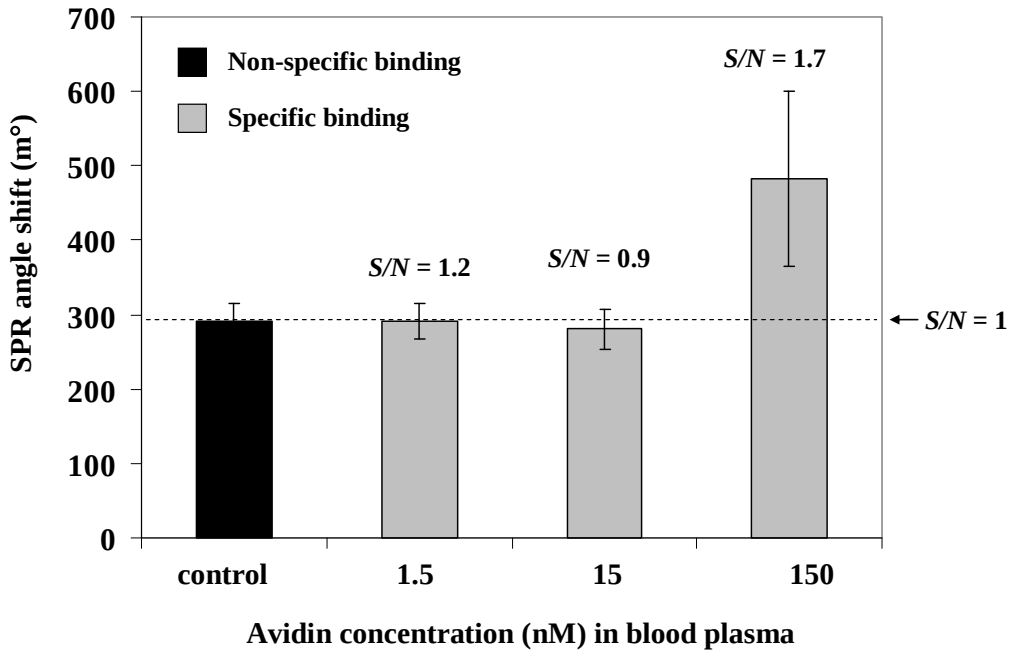

Figure A-5 SPR angle shift corresponding to the specific and non-specific binding of AVD having different concentration in 0.14 % blood plasma on the surface attached MUA.

APPENDIX B

Toluidine blue O assay

Toluidine blue O assay is a method used for determination of the amount of carboxyl groups. The carboxyl groups of PAA brushes can form a complex with toluidine blue o. The absorbance of the solution containing the desorbed complex was measured at 633 nm. The COOH content was obtained from a calibration plot of the optical density versus dye concentration which is displayed in Figure C-2.

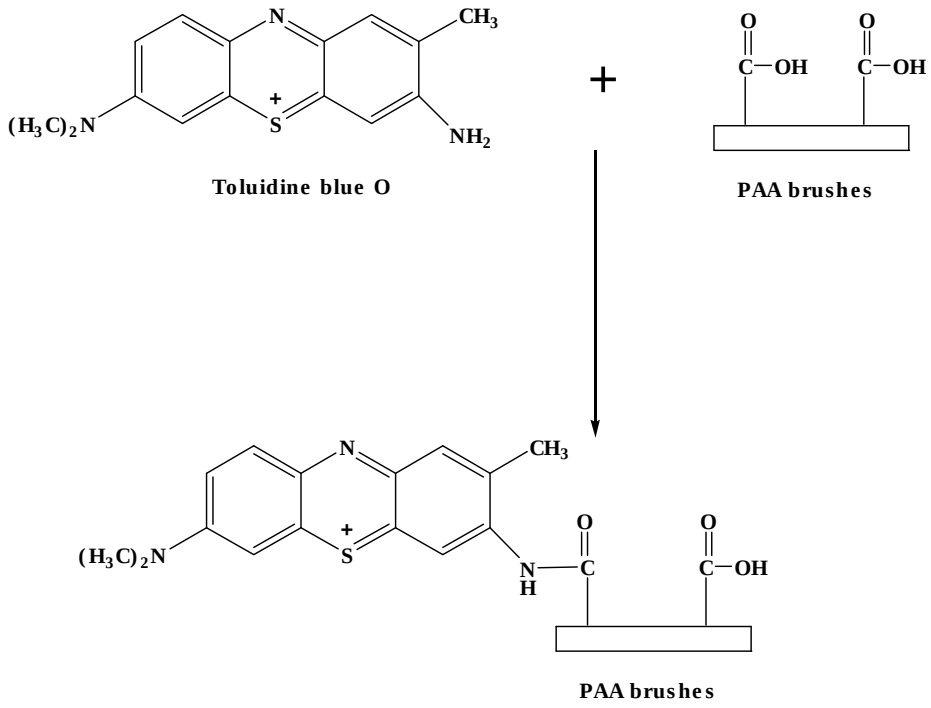

Figure B-1 Formation of toluidine blue O complex with carboxyl group.

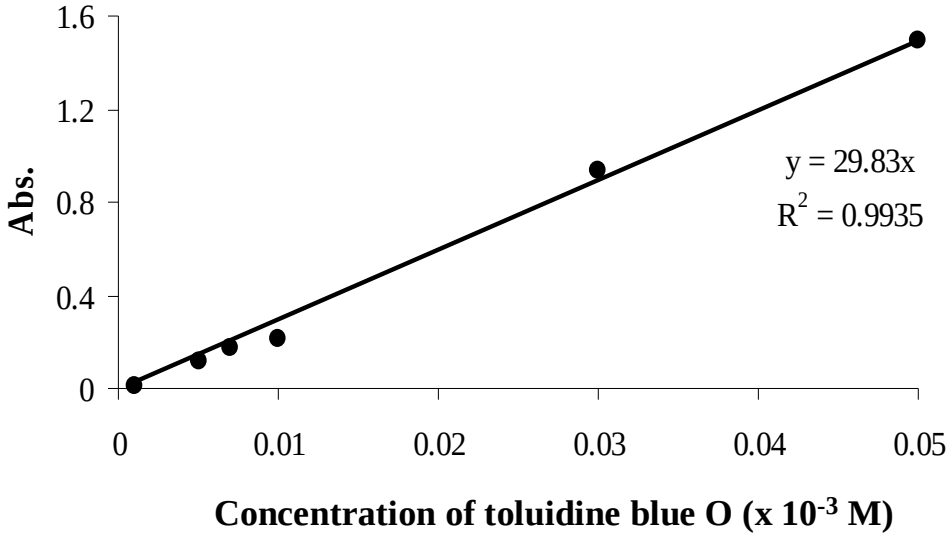

Figure B-2 Calibration curve of UV absorbance as a function of toluidine blue O concentration.

VITAE

Miss Piyaporn Akkahat was born on Feb 22nd, 1980 in Sakonnakorn, Thailand. She received the Bachelor Degree of Science, majoring in Chemistry from Burapha University in 2003 and graduated with the Master Degree of Science, majoring in Petrochemistry and Polymer Science from, Faculty of Science, Chulalongkorn University in 2006. She began her PhD study in Program of Petrochemistry, Faculty of Science, Chulalongkorn University in the academic year of 2006 and graduated in the academic year of 2010.

Awards:

June 2006	IUPAC Poster Prize from the 3rd IUPAC-sponsored International Symposium on Macro- and Supramolecular Architectures and Materials (MAM-06): Practical Nano-Chemistry and Novel Approaches
Sep 2008	Best Student Paper Presentation Award in Polymer Session, The 5th Thailand Materials Science and Technology Conference, Bangkok, Thailand

Presentation in Conference:

Sep 2010	The 59th SPSI symposium on Macromolecules, "Using Poly(acrylic acid) Brushes as SPR Precursor Layer for DNA Sensor", Sapporo, Japan, *Poster Presentation*

Publication:

1. Akkahat, P.; Hoven, V. P. "Introducing Surface-tethered Poly(acrylic acid) Brushes as 3D Functional Thin Film for Biosensing Application" *Colloids and Surface B: Biointerface, doi/10.1016/j.colsurfb.2011.03.042*)